

# Electrostatic Self-Assembly of Nanodiamond Nucleation Layers used in the production of X-Ray Refractive Lenses

---

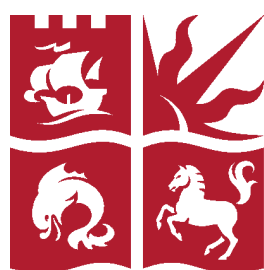
Emily R. Tofts

*A dissertation submitted to the University of Bristol in  
accordance with the requirements for the award of the  
Honours degree of Master of Science in Chemistry.*

Submission date: June 2013

Supervisor: Professor Paul May

Word count: 14,591



University of  
**BRISTOL**



# Acknowledgements

I would like to gratefully acknowledge the support and guidance given throughout the year by Professor Paul May, without whom this work would not have been possible. I would also like to thank Dr. Oliver Fox for his assistance in CVD diamond growth and day-to-day advice, his help has been immeasurable. Additionally, thanks go to Mr. Jonathan Jones who kindly provided training on both Scanning Electron Microscopes used in this project. Finally, I would like to thank the University of Bristol Diamond Group who welcomed me into their group and made my year incredibly enjoyable.

# Declaration

I declare that the work in this dissertation was carried out in accordance with the requirements of the University's Regulations and Code of Practice for Taught Postgraduate Programmes and that it has not been submitted for any other academic award. Except where indicated by specific reference in the text, this work is my own work. Work done in collaboration with, or with the assistance of others, is indicated as such. I have identified all material in this dissertation which is not my own work through appropriate referencing and acknowledgment. Where I have quoted from the work of others, I have included the source in the references/ bibliography. Any views expressed in the dissertation are those of the author.

SIGNED: ..... DATE: .....



## Table of Contents

Abstract.....	9
1. Diamond: an overview.....	12
1.1 Diamond's structure, stability and grain size.....	12
1.2. Optical properties of diamond: utilised in x-ray focusing lenses.....	13
1.2.1 Current refractive lens materials.....	14
1.2.2 Compound refractive and Kinoform lenses.....	15
1.2.3 Growth of nucleated nanodiamond substrates.....	17
2. Nucleation of nanodiamond films: techniques.....	19
2.1 Abrasion (mechanical and ultrasonic).....	19
2.2 Electrospray nucleation.....	19
2.3 Nucleation through plasma chemical vapour deposition.....	20
2.4 Self-assembly of ND nucleation layers – an overview.....	21
3. Electrostatic interactions of nanodiamond particles.....	23
3.1 Agglomeration of dispersed nanodiamond particulates.....	23
3.2 Dispersed nanodiamond agglomerate size.....	24
4. Effect of substrate on nanodiamond growth.....	26
4.1 Surface pre- treatment.....	26
4.1.1 Wet-chemistry substrate cleaning methods.....	26
4.1.2 Plasma substrate cleaning methods.....	27
5. Self-assembly and nucleation experimental parameters.....	28
5.1 Effects of polymer.....	28
5.1.1 Identity of polymers used for coating silicon surfaces.....	28
5.1.2 Polymer molecular weight.....	29
5.2 Zeta potential and pH effects.....	30
5.2.1 Altering zeta potential, pH and surface functional groups through ND particle pre-treatment.....	31
5.2.2 Zeta potential of polymers and ND used in self-assembly.....	32
5.3 Effect of nanodiamond immersion time.....	32

6. Selected-area deposition on a silicon surface after self-assembly nucleation.....	34
6.1. Selected-area patterning using lithography.....	34
6.2 Selected-area patterning using masking.....	34
6.3 Selected-area patterning using plasma etching.....	35
6.4 Selected-area patterning using micro-contact printing.....	35
7. Aim.....	37
8. Experimental method.....	39
8.1 Description of polymers used.....	39
8.2 MWCVD reactor.....	40
8.3 Microscopy – Optical and SEM.....	41
9. Results and Discussion.....	43
9.1 Examining cleaning method of Si substrate.....	43
9.1.1 Improving solvent based cleaning methods.....	44
9.1.1.1 Repetition of solvent cleaning steps.....	44
9.1.1.2 Examining drying methods within a solvent-based clean.....	45
9.2 Investigations into cationic polymers.....	46
9.2.1 Increasing PEI immersion time.....	47
9.2.2 Examining the molecular weight of PEI.....	48
9.2.3 Comparing the effects of PDDA and PEI.....	49
9.3 Washing after exposure to cationic polymer.....	50
9.4 Optimising the anionic polymer in nanodiamond particle nucleation.....	51
9.4.1 Immersion time in PSS.....	51
9.4.2 Effects of PSS pH on nanodiamond nucleation density.....	53
9.4.3 Changing nanodiamond particle concentration within the PSS-ND dispersion.....	55
9.5 Investigations into washing methods after PSS-ND nucleation step.....	55
9.6 Drying after both polymer immersions.....	56
9.7 Recommendation of a standard operating procedure.....	58
9.7.2 Diameter of diamond nanoparticles deposited after $t = 5$ min.....	59

9.7.3 Thickness of continuous film deposited for $t = 5$ min .....	60
9.8 Alterations to the SOP when a resist coating is used for selected-area deposition .....	61
10. Future work.....	63
11. Conclusion .....	65



# Abstract

This investigation was conducted in order to produce diamond refractive lens structures capable of focusing x-ray beams to widths of  $< 300$  nm. Hard x-ray beams are frequently used to image substances in biomedical and material processes; by decreasing the focal spot size of the incident beam, it is possible to image samples with greater resolution.

Commonly, x-rays are focused at synchrotron sources using silicon reflective and refractive optics. However, silicon has a high atomic number (relative to carbon) and so absorbs more x-ray radiation, decreasing the intensity of the focused beam. Also silicon optics are expensive to produce, due to the large quantity of high-quality material required, and difficult to produce free of aberrations. For these reasons, investigations are being conducted into creating diamond refractive optics capable of focusing hard x-rays. Diamond is a suitable alternative material choice due to its lower atomic number, high melting point and low x-ray absorption.

Diamond refractive optics can be produced in two main designs – compound refractive lenses or kinoform lenses. Compound refractive lenses (CRLs) consist of a series of concave lenses which act to reduce the focal point sequentially as the x-ray beam passes through the material. However, successful focusing depends on each lens refracting the x-ray beam to the same degree. As such, slight aberrations in lens structures can result in x-ray scattering and a decrease in the focal point clarity. For this reason, kinoform lenses are currently seen as a preferential option. Diamond kinoform lenses consist of a curved structure which possesses a smooth elliptical surface on one side and a stepped surface on the other. X-rays are refracted as they pass between the air-diamond interface. This technique requires less diamond material than CRLs for production of the same focal point. As x-ray radiation is passing through less diamond material, less energy is absorbed or scattered resulting in a greater transmitted intensity.

One way of producing diamond refractive lenses is by using a silicon mould nucleated with diamond nanoparticles. The nanodiamond nuclei are then grown into continuous films using Microwave Chemical Vapour Deposition (MWCVD), prior to the mould being etched away. In order for high-quality lens structures to be produced, it is imperative that the silicon mould contains a high density of nanodiamond nucleation sites. Therefore, the aim of this project was to produce a reproducible method for seeding silicon substrates with a high density of nanodiamond nucleated particles. The developed method can then be used to fabricate diamond refractive lenses.

Self-assembly of nanodiamond particles was encouraged through optimising electrostatic interactions present between the silicon substrate and layers of complimentary polymer. Silicon substrates were immersed in 10 w/v % poly (diallyldimethylammonium chloride), prior to immersion

in 10 w/v% poly (styrene sulfonate) containing dispersed nanodiamond. This method of layering complimentary polymers successfully resulted in nanodiamond self-assembling onto a silicon wafer. Where 10 wt. % nanodiamond concentration in poly (styrene sulfonate) was used, this resulted in a density of  $190 \times 10^{+7} \pm 5 \times 10^{+7}$  particles  $\text{cm}^{-2}$  being produced.



# 1. Diamond: an overview

Diamonds for centuries have attracted wide-spread interest for a variety of reasons. Traceable as far back as 6,000 years ago to India,<sup>1</sup> this mineral has an impressive array of properties which has led to its use in aesthetic decoration, religious superstition<sup>2</sup> and industrial processes.<sup>3</sup>

Diamond gets its name from the Greek *adámas* meaning ‘unbreakable’<sup>4</sup> due to its resistance to both abrasion and corrosion.<sup>5</sup> As well as being the most durable material known,<sup>6</sup> diamond has the highest room temperature thermal conductivity,<sup>7</sup> a low thermal expansion coefficient<sup>8</sup> and the widest optical transparency band.<sup>9</sup> The wide band gap of pure diamond means it is a good electrical insulator<sup>10</sup> but it can also be easily doped to become a semiconductor.<sup>11</sup>

These properties have led to the scientific and industrial value of diamonds rising far above that of decorative gemstones. Diamond is now used widely in technologies such as electronics, cutting, drilling, grinding and polishing.<sup>12,13</sup> However, in order for diamond to be used for industrial applications, it is necessary to source the mineral in large enough and pure enough quantities. Naturally occurring diamond, as well as being expensive to source and mine, often contains structural defects or impurities which impact its intrinsic properties.<sup>14</sup> Research has therefore been conducted to find cost-effective methods of producing defect-free diamond on an industrial scale.

## 1.1 Diamond’s structure, stability and grain size

Diamond consists of  $sp^3$ -hybridised carbon atoms arranged in a tetrahedral lattice. Connected solely with covalent bonds, the carbon atoms in diamond can be arranged either in a cubic or hexagonal structure. Other than diamond, the most common allotrope of carbon is graphite. This contains  $sp^2$ -hybridised carbon atoms which bond in a planar, layered structure. Each carbon covalently bonds to three neighbouring atoms in a trigonal planar manner, leaving a single electron free to form pi-bonds with the adjacent layer.

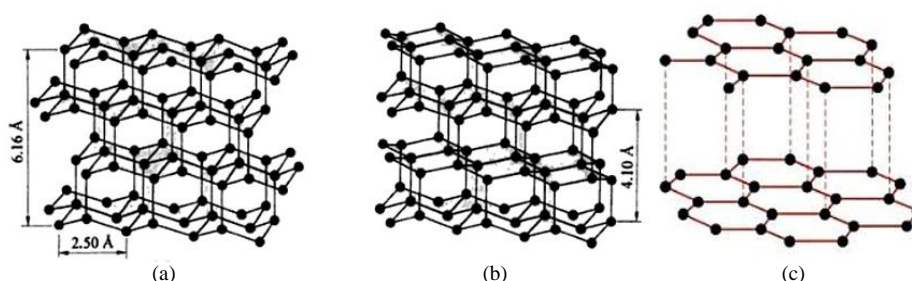


**Figure 1:** The crystal structure of diamond: (a) cubic diamond structure, (b) hexagonal diamond, (images reproduced from reference 15) and (c) the crystal structure of graphite (image reproduced from reference 16).

Graphite is the thermodynamically stable allotrope at standard conditions, whereas diamond is metastable (kinetically stable but thermodynamically unstable). In order to industrially produce

diamond it is therefore necessary to create conditions which thermodynamically favour diamond over graphite. As these two materials are separated by a large activation barrier, diamond will not spontaneously convert to graphite after it is formed and so will remain stable.<sup>17</sup>

During the production of diamond the orientation of the facets can be controlled with experimental conditions. It is possible to form three types of primary diamond facets:  $\langle 111 \rangle$ ,  $\langle 110 \rangle$  and  $\langle 100 \rangle$ . Miller indices describe a  $\langle 111 \rangle$  dominated morphology as being a pyramidal structure with triangular facets, a  $\langle 100 \rangle$  structure as having square facets and a  $\langle 110 \rangle$  structure as having a stepped-face appearance.

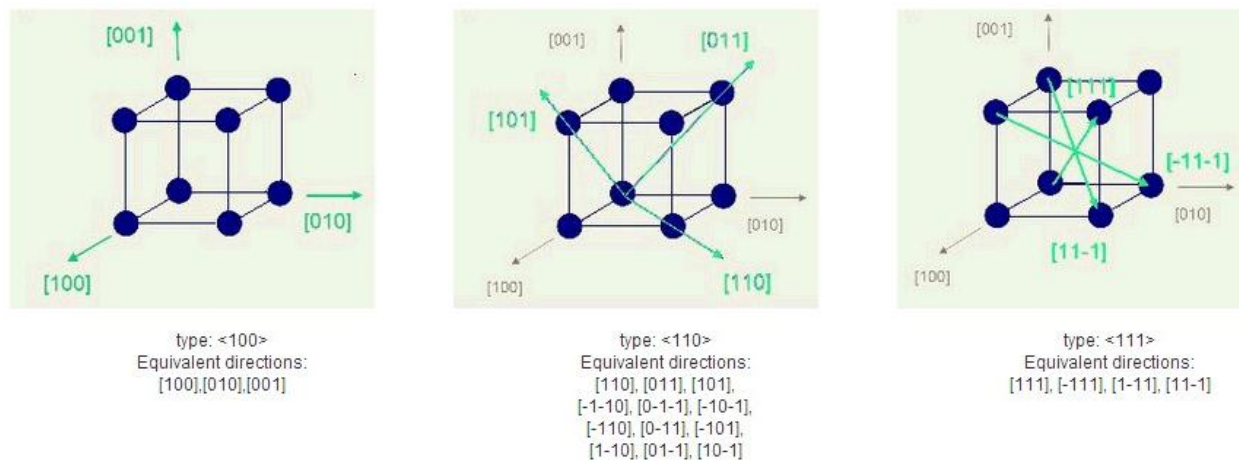


**Figure 2:** Miller indices described orientations of a diamond crystal structure:  $\langle 100 \rangle$ ,  $\langle 110 \rangle$  and  $\langle 111 \rangle$ . Image reproduced from reference 18.

As well as the crystalline morphology, the grain size of produced diamond can also be controlled. Microcrystalline diamond corresponds to a grain size of 100 - 1,000 nm<sup>19</sup>, resulting in a rougher surface than structures with smaller grains. Materials where grains are < 100 nm are termed nanocrystalline diamond,<sup>20</sup> resulting in a smooth surface with each crystallite having a termination layer of  $sp^2$ -bonded carbon.<sup>21</sup> Finally, ultrananocrystalline diamond grains can be produced which are smaller than nanocrystalline grains (2 - 5 nm)<sup>20</sup> and therefore form ultra-smooth structures. The smoothness of a diamond crystal can have important implications in industries which utilise its optical properties. Optical properties are affected by surface roughness and minimising the surface defects and aberrations acting to minimise surface refraction.

## 1.2. Optical properties of diamond: utilised in x-ray focusing lenses

X-rays are high energy radiation and have many scientific uses. One common use is in the imaging of structures through the use of hard x-rays ( $E > 4$  keV).<sup>22</sup> X-ray imaging is currently used for probing biological cells,<sup>23</sup> nanocrystalline materials,<sup>24</sup> non-crystalline materials<sup>25</sup> and many other substances of interest.<sup>26</sup> In order to use hard x-rays as a scientific probe with high resolution, it is necessary to

generate an x-ray beam that is intense and diametrically small. One method for achieving this is through the use of a focused synchrotron source.

A synchrotron source is a cyclical particle accelerator used for producing high intensity electromagnetic radiation, such as hard x-rays. Electrons are fired from an electron gun within the synchrotron, produced via thermionic emission. The electron beam is then accelerated under vacuum to  $\sim 3$  GeV on passing through a linear accelerator (linac), booster synchrotron and finally a large storage ring.

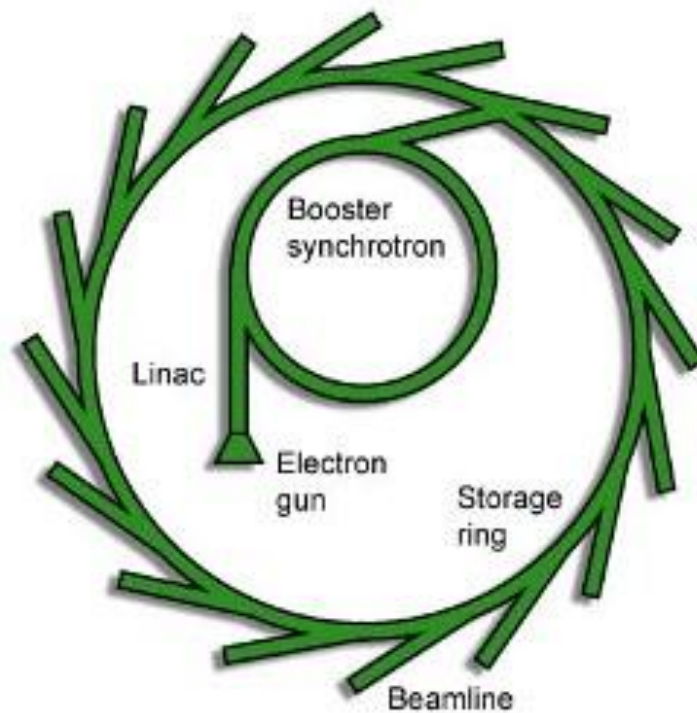


**Figure 3:** Schematic of a synchrotron with particle accelerators and experimental beamlines labelled. ([www.diamond.ac.uk](http://www.diamond.ac.uk)).

Electrons are guided around the storage ring with a series of bending magnets. At each bending magnet electromagnetic radiation is produced. This is channelled from the large storage ring into experimental beamlines. These experimental beamlines are then collimated, focused and made monochromatic in an optics hutch before being used as an experimental probe.

### 1.2.1 Current refractive lens materials

Currently silicon and beryllium are used to create compound refractive lenses and kinoform lenses. However, there are a number of issues with both of these materials which could be circumvented through the use of diamond.

Although silicon is easy to shape into lens structures (through etching), it is not an ideal material for focusing hard x-ray beams. Silicon has a relatively large atomic number ( $Z = 14$ ) compared to carbon. When x-ray radiation passes through this material, the light interacts with the

electrons in the silicon via the photoelectron effect. This leads to a decrease in intensity of x-ray radiation transmitted after the focusing optic.

Beryllium has a lower atomic number ( $Z = 4$ ) and smaller interaction volume<sup>27</sup> so should create superior refractive lenses. However, beryllium is present on Earth in relatively low abundance<sup>28</sup> and so it can be costly to create refractive lenses on an industrial scale. For these reasons, diamond is a substance of interest for producing refractive lenses.

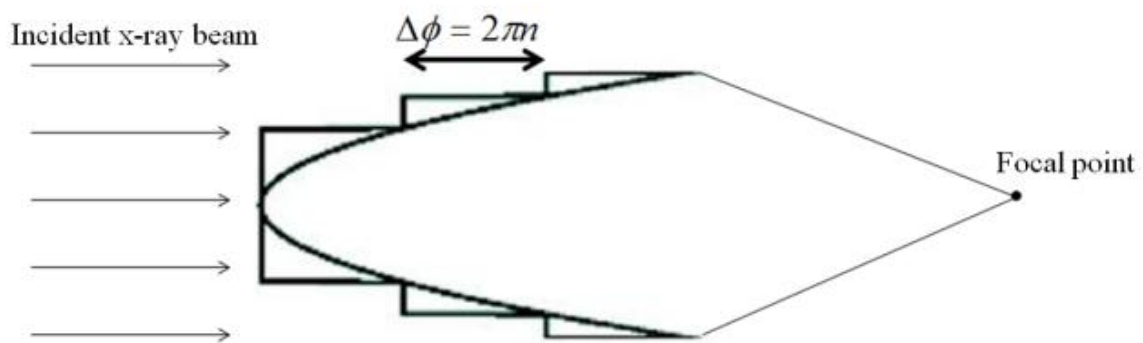
Diamond is seen to be a good choice of material for refractive lenses due to its low atomic number ( $Z = 6$ ) and high thermal stability. As focal widths decrease in size, the energy of the resulting x-ray beam will increase. The high thermal stability of diamond indicates it is less likely to deteriorate when exposed to the increased energy of hard x-rays of new light sources.

### 1.2.2 Compound refractive and Kinoform lenses

It is possible to decrease the focal point of x-ray beams by using two types of lens structure – compound refractive lenses and kinoform lenses. Both of these techniques utilise refractive properties to decrease an incident x-ray beam to a smaller focal point.



(a)



(b)

**Figure 4:** Schematic diagrams showing a compound refractive lens (a) and kinoform lens (b), both used for focusing incident x-ray beams.

The refractive index,  $n$ , of x-rays in most materials is almost unity, and therefore focusing x-ray beams with refractive optics can be problematic. The focal length,  $f$ , required is dependent on the

radius of lens curvature,  $R$ , the x-ray refractive index and the refractive index decrement  $\delta$  (typically  $10^{-6}$  for hard x-rays).

$$f = \frac{R}{2n\delta}$$

**Equation 1**

Due to a refractive index of  $\sim 1$ , the focal length required for refracting x-ray beams using a single concave lens is large. Therefore, compound refractive lenses consisting of a sequence of individual concave lenses arranged linearly have been developed. As x-rays pass through each convex lens they are refracted sequentially. However, in order to focus x-rays over a reasonable focal length it is often necessary that a large number of concave lenses,  $N$ , are used.

$$f_{CRL} = \frac{f}{N}$$

**Equation 2**

Unfortunately, increasing the number of concave lenses used also increases the path length of x-ray within the lens. This increases the amount of x-ray radiation absorbed during transmission through the refractive lens. Therefore, in order to decrease x-ray absorption, kinoform structures offer a favourable alternative lens model.

In a kinoform lens, x-ray radiation passes through a smaller amount of diamond material prior to production of the same focal width. Therefore, the use of a kinoform lens results in less absorption and scattering of the x-ray beam. This leads to an increased in the focal spot intensity.

Kinoform lenses consist of an elliptical structure which is responsible for focusing the incident x-ray beam. However, in order to decrease interaction between x-ray radiation and lens material, it is possible to remove passive material. As x-rays travel through the material of length,  $x$ , a phase difference occurs.

$$phase\ difference = \frac{2\pi\delta x}{\lambda}$$

**Equation 3**

It is possible to remove material responsible causing a  $2\pi$  phase shift whilst maintain the elliptical surface shape. This passive material corresponds to the step-shaped segments pictured in **Figure 4**. By removing this passive material it is possible to decrease the absorption of radiation within the lens structure and thus increase the intensity of emitted x-ray radiation.

CRL and Kinoform refractive optics can be produced from synthetic diamond by using a pre-designed mould which is selectively nucleated to produce precise diamond structures. This method has the advantage of being reproducible in producing well-defined diamond structures. As refractive optics rely on surface smoothness, minimising surface aberrations is important. This can be achieved

through increasing the density of nanodiamond particles nucleating the mould, ensuring all edges of the mould are fully filled.

Currently, heteroepitaxial, polycrystalline diamond films are created by nucleating a non-diamond substrate with methods such as abrasion (mechanical<sup>29</sup> and ultrasonic<sup>30</sup>), chemical vapour deposition,<sup>31</sup> electrospraying<sup>32</sup> or self-assembly.<sup>76</sup> The advantages and disadvantages of these various methods, the ways of increasing nucleation density and the methods for producing selective nucleation are discussed in greater detail later.

### 1.2.3 Growth of nucleated nanodiamond substrates

After a substrate has been nucleated successfully, it is then possible to deposit a diamond film. While diamond film deposition is not the subject of this investigation, it is important that diamond nucleation sites are grown to an extent where they can be observed and measured. Deposition of diamond normally requires that the substrate is exposed to a plasma containing around 1% CH<sub>4</sub>, in excess H<sub>2</sub>, at a temperature of above 700 °C.<sup>55</sup> (In this investigation a plasma of 6% CH<sub>4</sub> was used.) The expected deposition occurs due to the following mechanism.

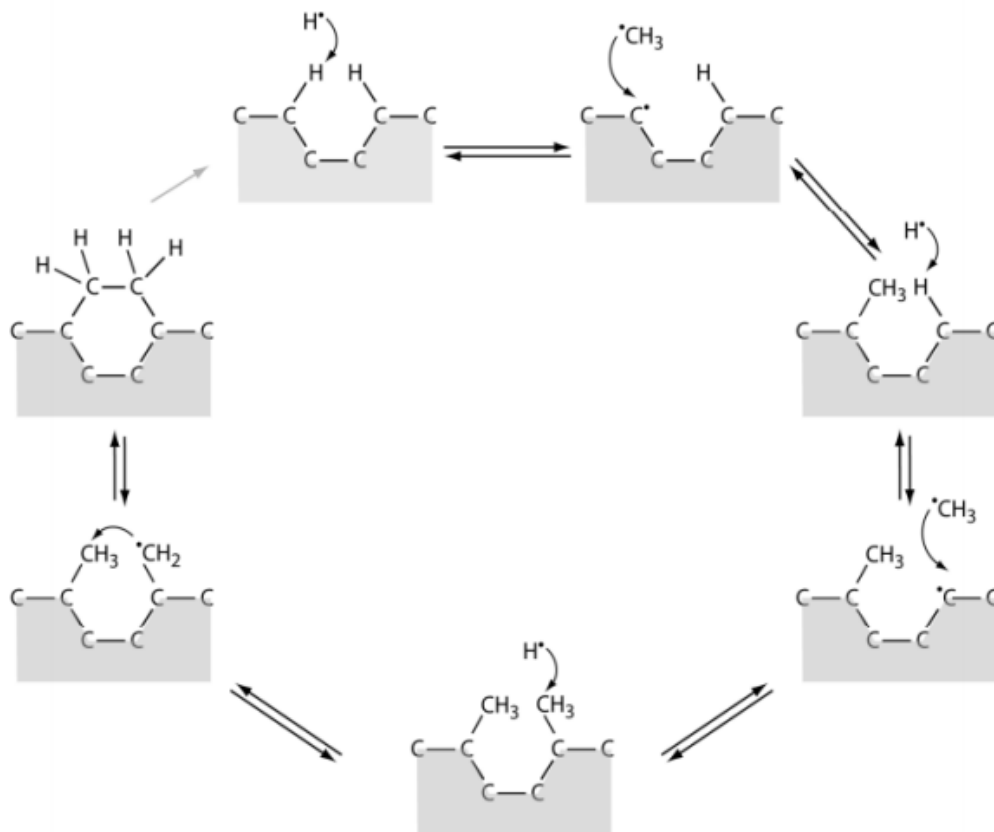


**Figure 5:** An illustration of the standard CVD diamond growth model. Reference 46.

The diamond deposition mechanism occurs in a step-wise process. Exposed carbon on the growing diamond surface is in a  $sp^3$  structure. Gaseous methyl radicals, which have been activated in the plasma, then add to vacant carbon sites extending the  $sp^3$  structure. This process continues until a large diamond structure has been grown.

In order for this process to occur methyl radicals must be created. Two ways of activating methane into methyl radicals for deposition onto the surface are by the use of a hot filament reactor (in HFCVD) or a microwave plasma-assisted reactor (in MWCVD). While both of these methods are reproducible and reliable, there is a key difference in the method used for activating the gas mixture. A HF reactor contains a filament which is heated to high temperatures in order to activate a  $CH_4/H_2$  mix, while a MWCVD system uses microwave radiation to increase the energy of gas phase molecules and produce a reactive plasma.

In both of these processes there is an increase in the quantity of activated carbon molecules available to react at the substrate surface. However, as mentioned in **Section 1.1**, an increase in carbon deposition does not necessarily mean the formation of diamond. The process must therefore work to encourage the formation of  $sp^3$ -bonded carbons (diamond) and minimise  $sp^2$ -bonded structures (graphite). This is done through the presence of atomic hydrogen.

Atomic hydrogen works in four ways to encourage the formation of  $sp^3$ -bonded carbon, and aid the formation of diamond. Firstly, in order to maintain a  $sp^3$  arrangement, the spare bond is terminated with atomic hydrogen. This is necessary to prevent the bond structure changing to a  $sp^2$  conformation and graphite being favoured. Secondly, atomic hydrogen reacts with methane in the gas phase, creating methyl radicals capable of attaching to nucleated carbon sites. Thirdly, atomic hydrogen etches  $sp^2$ -bonded carbon at a faster rate than  $sp^3$ -bonded carbon and thus will remove any graphitic structures formed, returning them to the gas-phase. Finally, atomic hydrogen etches large hydrocarbon molecules that could deposit instead of  $sp^3$ -bonded diamond, re-exposing carbon sites and increasing the likelihood of a defect-free diamond layer forming.

## 2. Nucleation of nanodiamond films: techniques

### 2.1 Abrasion (mechanical and ultrasonic)

In order for diamond layers to successfully deposit onto the surface of a substrate during CVD (such as a mould), it is necessary for there to be nucleation sites on the surface. One method for creating nucleation sites is by the use of mechanical abrasion – using a powder made from hard particles, such as diamond,<sup>33,34</sup> to physically scratch and damage the surface to be coated, thereby increasing surface roughness. It has been suggested that mechanical abrasion results in diamond shaped scratches, as well as residual diamond particulates embedded in the surface after abrasion<sup>35</sup> both of which may help to encourage nucleation during CVD. However, this method can be too destructive to the surface and so is unsuitable for delicate processes.

Another technique for introducing surface roughness and nucleation sites is the use of ultrasonic abrasion. Unlike mechanical abrasion this technique enhances diamond nucleation by agitating the substrates in diamond or diamond-metal slurries.<sup>30</sup> By incorporating other materials with the abrasive diamond particles, both surface abrasion and chemical modification can occur, thus increasing the number of nucleation sites.<sup>36</sup> In this method the substrate is agitated ultrasonically in a slurry containing diamond powder and sometimes another species, such as  $\text{Al}_2\text{O}_3$ <sup>37</sup> or Ti.<sup>38</sup> This encourages non-diamond nanoparticles to embed in the substrate surface and increase its roughness. However, the choice of additional species is important in this process, because some metals may dissolve into diamond under the CVD conditions hindering film growth and contaminating the diamond film.<sup>39,40</sup>

While both of these processes are relatively simple to implement, they are both relatively destructive to the surface of the substrate. Therefore, in applications such as micro- and nano-electronics, a more delicate, non-destructive nucleation method is required – such techniques include electrospaying, plasma chemical vapour deposition, spin coating and electrostatic self-assembly.

### 2.2 Electropray nucleation

Unlike the methods above, where techniques are used to seed diamond particles onto substrates with some unwanted, destructive surface effects, electrostatic spray (electropray) methods can achieve high nucleation densities<sup>32,41</sup> with little influence on the substrate surface. Nanodiamond particles suspended in a carrier liquid (either water<sup>42</sup> or another liquid<sup>43</sup>) are nebulised into ionised droplets which are then accelerated towards a grounded substrate in the form of a spray. Charged diamond

particulates, following electric field paths;<sup>44,45</sup> adhere to the substrate providing a site for further diamond deposition. However, studies<sup>43</sup> have shown that where suspensions of particulates are used, droplets containing particles tend to reside on the extremities of the spray often resulting in a non-uniform coverage of the substrate.

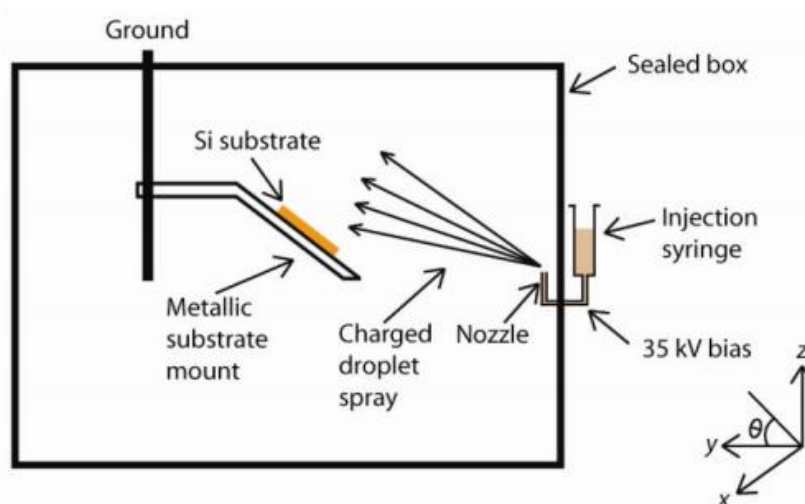


**Figure 6:** Schematic diagram of the electrospray deposition technique. Co-ordinates shown are used to define the angle of orientation of the substrate relative to the syringe nozzle ( $\theta$ ). Reference 46.

To improve uniformity the dispersion medium used in the nanodiamond suspension must be a volatile liquid which can completely evaporate before reaching the substrate. This method can produce a uniform and dense coating of diamond particles,<sup>46</sup> not influenced by the solvent droplets.

## 2.3 Nucleation through plasma chemical vapour deposition

Another method which is used for nucleating substrates is chemical vapour deposition (CVD). In this technique, nucleation sites are created by exposing the substrate to a plasma with a high methane fraction in  $H_2/Ar$ .<sup>47</sup> A high methane concentration is used to form a carbide layer and remove any oxide present on the surface of the substrate, so that successful nucleation can occur.<sup>48</sup> The substrate is treated in a hydrogen plasma for 10 min and 3.0% methane is fed into the  $H_2/Ar$  plasma for 45 min. The substrate is kept at a temperature of 850 °C.<sup>48</sup>

Similar to the conditions used during diamond growth, a stable plasma is formed in the centre of a microwave chemical vapour deposition (MWCVD) reactor and the substrate left to undergo nucleation. Substrates as diverse as silicon carbide,<sup>49</sup> silicon,<sup>50</sup> boron nitride,<sup>51</sup> iridium<sup>52</sup> and molybdenum<sup>31</sup> have been used to successfully form diamond nucleating layers. This method has an advantage over abrasive methods in that it is non-destructive to the substrate and it allows nucleation

and growth to occur without removing the substrate from the reactor. It is also possible to improve this technique and increase the resultant density by applying a negative bias voltage to the substrate.<sup>48</sup>

Another possible nucleation method is to electrically bias the substrate in the deposition reactor in order to increase the likelihood of diamond nucleation in a technique known as bias-enhanced nucleation (BEN).<sup>50,53,54</sup> A negative potential difference (100-200 V)<sup>55</sup> is applied to the substrate during MWCVD causing carbon-containing ions to accelerate towards the substrate and implant into the surface. This results in a carbon rich layer in the top few layers of the substrate and increases the initial nucleation rate. This nucleation method also allows the orientation of diamond films to be chosen.<sup>56,57</sup> Where Si substrates are used, diamond crystals align with the electrically biased substrate in a heteroepitaxial fashion so that the [001] planes of the growing diamond crystal are parallel to silicon (001) and the <110> directions are parallel to silicon <110>. Although this method is often preferential for nucleating diamond in a particular orientation, BEN only allows oriented nucleation over small areas (usually several square centimetres) and so large-scale oriented nucleation is difficult to achieve.<sup>58</sup>

In a similar approach to BEN, a negative bias relative to the filament (0 to 400 V) is applied to the substrate in a H<sub>2</sub>/CH<sub>4</sub> gas mixture to improve nucleation during HFCVD. It has been found<sup>48</sup> that without the bias process nucleation density was less than 10<sup>5</sup> cm<sup>-2</sup> but can be increased to 10<sup>10</sup> cm<sup>2</sup>.

As with the electro spraying method, this negative bias step can be too destructive for processes where surfaces are coated for electronics applications. In order to nucleate a substrate without damaging the surface or placing it under high temperature or bias voltage, and to ensure suitability for large scale nucleation, electrostatic self-assembly of ND nanoparticles is the preferential choice and will be discussed below.

## 2.4 Self-assembly of ND nucleation layers – an overview.

Self-assembly of polymer solutions containing nanodiamond (ND) particles is a topic of much research<sup>59</sup> due to its potential application as a non-destructive nucleation process used in the deposition of nanodiamond films by CVD. It has been used in a wide variety of industrial<sup>60,61</sup> and technological procedures<sup>62,63,64</sup> as a result of such research. Self-assembly is a process whereby a disordered system undergoes internal interactions<sup>65</sup> resulting in the formation of a larger, ordered structure.<sup>66</sup> In the case of CRL and Kinoform optic production, if nanodiamond particles can be encouraged to self-assemble onto a mould via electrostatic attractions then these seeded nanoparticles

can be grown into larger diamond structures by CVD and the mould etched away. If it is possible to optimise this procedure so a high density of nucleated nanoparticles is achieved within the mould, a well-defined optical lens could be produced.

However, as nanodiamond particles are not naturally attracted towards common CVD substrates (such as Si) these interactions need to be engineered. One method for encouraging nanodiamond particles to self-assemble onto a substrate is through the use of complementary polymer coatings. Nanodiamond particles will then experience weak attractive forces towards the substrate resulting in a seed layer which can then be thermodynamically stabilised. Through lowering the Gibbs energy of the system, self-assembled, defect-free structures can be successfully formed.<sup>67</sup>

While self-assembly occurs entirely as a result of attractive and repulsive forces of a system, the success and extent of the interaction can be controlled by altering certain external factors.<sup>68,69</sup> This results in either a change in the interactive force or a change in the thermodynamic stability of the system. The electrostatic interactions which lead to successful nanocrystalline diamond self-assembly will be described in the following discussion. Research into strengthening and controlling these interactions in order to improve self-assembly will be examined.

### 3. Electrostatic interactions of nanodiamond particles

In general, for spontaneous self-assembly to occur the atoms or molecules present in a system must experience long-range repulsive forces and short-range attractive forces.<sup>70</sup> These interactions, when optimised, can lead to strong superstructures being formed.

However, this predisposition to self-assemble is not always desired. In some cases, it is even necessary to prevent molecules from experiencing strong short-range attraction so that self-assembly cannot occur. For example, nanodiamond particles in solution, if not in a stable dispersion, will self-assemble and form agglomerates. This is undesirable as a stable and uniform dispersion of nanodiamond particles is required to seed a substrate.

#### 3.1 Agglomeration of dispersed nanodiamond particulates.

It has been found that some nanodiamond particulates (*e.g.* from detonation synthesis) naturally agglomerate when in solution, to form a structure with strongly repulsive core.<sup>71</sup> While this needs to be addressed in order to produce an even colloidal dispersion (in which a substrate can be placed for nucleation), the same mechanism is responsible for the formation of self-assembled super-crystalline structures and so it is crucial that it is properly understood.

Until recently it was believed that agglomeration of diamond particles was due to random attractions mediated through Van der Waal forces. However, Barnard *et al.*<sup>72</sup> have established that nanodiamond particles will self-assemble into agglutinates through much stronger Coulombic interactions to form structures of 100-200 nm diameter. It was found that separate diamond particles will collide and agglomerate at 2.7 Å, with the likelihood of that collision being successful, and forming an ionic bond, varying according to the combination of diamond orientations.

This work was extended by Chang *et al.*<sup>73</sup> who examined both aggregation and agglomeration in colloidal 5 nm diamond nanoparticle suspensions with electron microscopy and computer simulations. They found that the preferred orientation of agglutinates is in the  $\langle 100 \rangle^+ \langle 111 \rangle^0$  or  $\langle 111 \rangle^- \langle 111 \rangle^0$  facing surface facet arrangement.

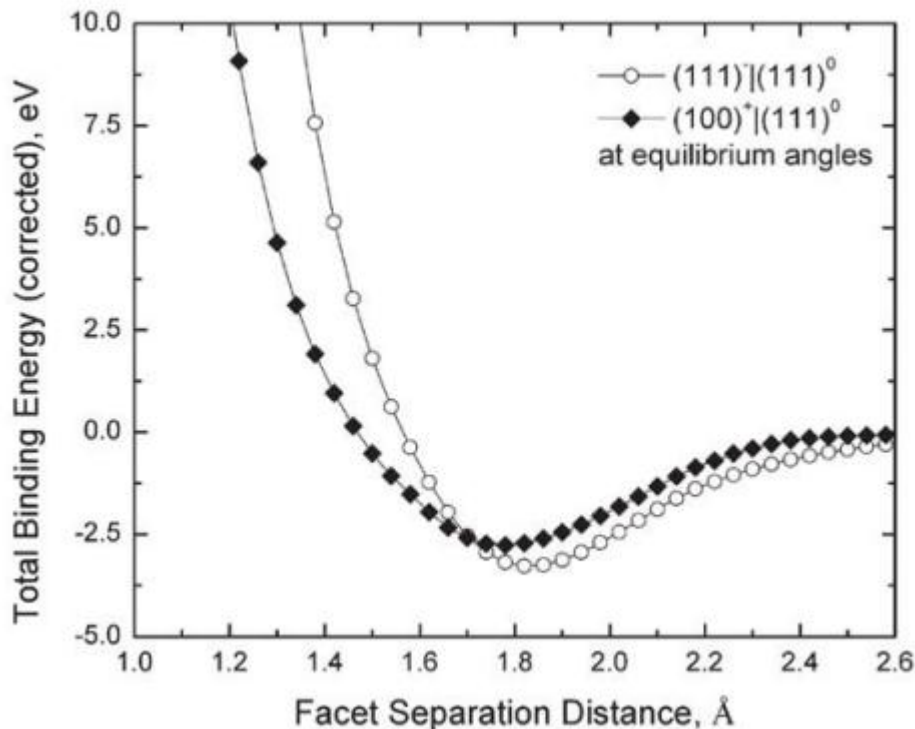


**Figure 7:** Potential energy well due to coherent interfacial Coulombic interactions (CICI) between nanodiamond particles, calculated using density-functional based tight binding (DFTB) simulations. Reproduced from reference 73.

It is interesting to note that both types of interactions require the presence of one neutral and one charged facet. The presence of these types of interactions can be referred to as coherent-interfacial Coulombic interactions (CICI) and will result in an ordered structure. However, when incoherent interactions predominately occur, diamond particles will aggregate in an IICI structure – a disordered configuration. It is therefore important that the type, as well as strength, of internal interactions is considered when discussing self-assembly of nanodiamond particles.

## 3.2 Dispersed nanodiamond agglomerate size

Research has been carried out to examine the influence of dispersed diamond agglomeration size in solution on the resulting self-assembled diamond layer present on a solid substrate. Lee *et al.*<sup>74</sup> dispersed nanodiamond (ND) particles in an anionic dispersant (polysodium-4-styrene sulphonate, PSS) and found that the thickness and roughness of nanocrystalline diamond films deposited by CVD on substrates nucleated using this solution can be controlled by altering the nanodiamond particle aggregate size and density.

The process involved attritionally milling 0.5 g of nanodiamond (ND) with 200 ml deionised water and 10 vol% PSS for 6 h at 1000 rpm. They found this caused a decrease in the size of naturally forming ND aggregates in the polymer solution and entirely prevented ND precipitating out through self-aggregation. The stability, and thus effectiveness of dispersion, can be examined using

the zeta potential of the colloidal suspension. A zeta potential of larger than -25 mV is indicative of an electrostatically stable system.<sup>75</sup> After dispersion for 6 h the zeta-potential of the PSS-ND solution used was found to be -60.5 mV with an average particle size of 15 nm.

A Si substrate with a SiO<sub>2</sub> mask was then dipped in 10 w/v% poly ethylenimine (PEI) (the cationic polymer) for 10 min prior to being immersed in the PSS-ND solution (the anionic polymer) for 12 h. This formed a monolayer of nanodiamond particles with an average nucleation density of  $3.8 \pm 0.4 \times 10^{11} \text{ cm}^{-2}$ , due to the strong complementary electrostatic interactions. It was concluded that the smaller aggregates of dispersed ND particles resulted in higher density nanodiamond seeds being present on the substrate.

This research was confirmed in a number of reports<sup>76,77</sup> which looked at the influence of the pre-crushing processes on aggregated diamond particulates. In an experimental setting, it is possible to measure the ND aggregate size in a polymer dispersion by using a light-scattering particle-sizer. It is also important to note that aggregates may form over time, and so the age of the ND-PSS dispersion may affect the resultant density of film seeding.

Whilst Coulombic interactions are important in the formation of self-assembled nanodiamond nucleation layers, they are not the only parameter which will affect the efficacy of nanodiamond seeding. Both the substrate on which the diamond layer will be grown and the properties of the polymers used to promote self-assembly will affect the strength of interactions between diamond particles.<sup>78</sup>

## 4. Effect of substrate on nanodiamond growth

The choice of surface on which nanodiamond particles are seeded by electrostatic self-assembly is also important. As the aim is to grow a diamond film, the surface chosen must be chemically compatible with diamond. Common choices include  $\text{Si}_3\text{N}_4$ , Si or  $\text{SiO}_2$ .<sup>55</sup> They are a good choice for diamond deposition as carbon will not dissolve into the body of substrate but will instead nucleate at the surface; they can withstand the high temperatures required for diamond deposition; and they possess a similar thermal expansion coefficient to diamond, so on cooling will minimise the possibility of cracking and give an improved adhesion between film and substrate.

Once a suitable substrate for seeding has been chosen, the treatment it undergoes can encourage or prevent nucleation, or influence the nucleation density.

### 4.1 Surface pre- treatment

Self-assembly of nanodiamond particles onto a substrate such as silicon is due to electrostatic interactions. Therefore, it is important that the substrate is absolutely clean so that the interactions between Si-polymer-polymer-nanodiamond layers are not weakened by contaminants. The substrate must be sufficiently cleaned in a manner which removes all organic and inorganic contaminants, but which does not damage the surface. Several methods exist and can be categorized into wet-chemistry and plasma cleaning methods.

#### 4.1.1 Wet-chemistry substrate cleaning methods.

Liu *et al.*<sup>79</sup> have demonstrated self-assembly of functionalised nanodiamond particles onto an oxidised silicon wafer. The silicon wafer was cleaned with an ultrasonic bath containing acetone, isopropyl, alcohol and DI water, respectively, for 5 min. This is a relatively fast, simple method of cleaning.

A more intensive method for cleaning Si substrates is often referred to as the RCA process – developed at the RCA laboratories. A series of chemical steps are followed in order to selectively remove contaminants without attacking the surface.<sup>80</sup> The process takes approximately 1 h to complete and requires the use of mixtures such as sulphuric acid and hydrogen peroxide – which can be experimentally dangerous and generate heat.<sup>80</sup>

Tremsin *et al.*<sup>81</sup> have cleaned Si wafers using immersion in hydrofluoric acid diluted in DI water (25:1). They found this eliminated all possible contaminants on the substrate, without causing damage to the surface.

## 4.1.2 Plasma substrate cleaning methods

All three of the cleaning methods described in the previous section involve wet-chemistry and require lengthy solvent/acid immersion and drying steps. An alternative method to wet-chemistry cleaning is through the use of a plasma. Plasma cleaning has the advantage of decreasing the use of hazardous chemicals and so making the process safer.<sup>82</sup> There is also concern whether wet-chemistry cleaning will clean the surface down to the atomic level.<sup>83</sup>

Plasma cleaning works by generating electrons, ions and radicals which remove contaminants by sputtering, etching and heating. Sputtering is a slow process which removes all contaminants by bombarding the surface of the substrate with ions and radicals. After extended periods of time this can result in implantation and damage to the surface. Therefore, it is time, energy and temperature dependent. Etching is a more selective, faster process which is non-destructive if the appropriate plasma and substrate is used. The heating of the substrate also acts to remove lightly bonded contaminants by giving them enough energy to adsorb from the surface. This can be a slow, non-destructive process and is effective over a relatively limited range of temperatures before surface deformation occurs.

One example is the O<sub>2</sub> plasma which is used to effectively remove contaminants from silicon substrates. This is a fast process which has the advantage of not requiring removal from the reactor between cleaning, nucleation and growth if using an *in-situ* plasma seeding technique. However, an oxygen-based plasma can oxidise the surface if left for too long.<sup>82</sup>

Alternatively, a H<sub>2</sub>/Ar-plasma can be used<sup>84</sup> to chemically clean at low energies (less than 30 V) and low substrate temperatures. Typical etch rates during cleaning are 1 nm min<sup>-1</sup> for both silicon and silicon oxide substrates.<sup>84</sup> After 10 min, native oxide and contaminants are successfully removed from the silicon surface to below 0.1 monolayers (the detection limit of the equipment used). This type of plasma is preferential to oxygen-based-plasmas as there is no risk of oxidation, and the low voltage used decreases ion bombardment by decreasing the ion energy and preventing surface damage from occurring.

In summary, appropriate wet-chemistry cleaning methods have been shown to cosmetically clean silicon substrates although there are doubts as to its effectiveness below the top few atomic layers. Wet-chemistry methods also increase the experimental use of hazardous chemicals. However, plasma cleaning can lead to oxidation of the surface and/or damage through ion bombardment if not conducted under the correct conditions.

## 5. Self-assembly and nucleation experimental parameters

Once a substrate has been sufficiently cleaned and all organic and inorganic contaminants removed, the surface can then be nucleated using diamond particles. When nucleating a substrate using self-assembly techniques there are many experimental variables that can affect the extent and success of diamond seeding.

### 5.1 Effects of polymer

Polymers are used in the self-assembly nucleation process to increase the electrostatic attraction between the silicon surface and the ND particles. Through increasing this interaction, ND particulates are more likely to attach to the substrate surface and remain there, acting as nucleation sites for subsequent film growth. Kim<sup>85</sup> has stated that the morphology of polymer coating layers - and thus the strength of self-assembly interactions - can be controlled by manipulation of the electrostatic forces present on side-chains of the polymer. These can be altered by controlling the polymer solution concentration, ionic strength and pH of an aqueous polymer solution.

#### 5.1.1 Identity of polymers used for coating silicon surfaces

It is well established that for both SiO<sub>2</sub> and Si substrates to be effectively coated, due to their surface negative charge, a cationic polymer is needed – commonly used examples are poly (diallyldimethylammonium) chloride (PDDA)<sup>86,87</sup> and poly (ethyleneimine) (PEI)<sup>88,89</sup>

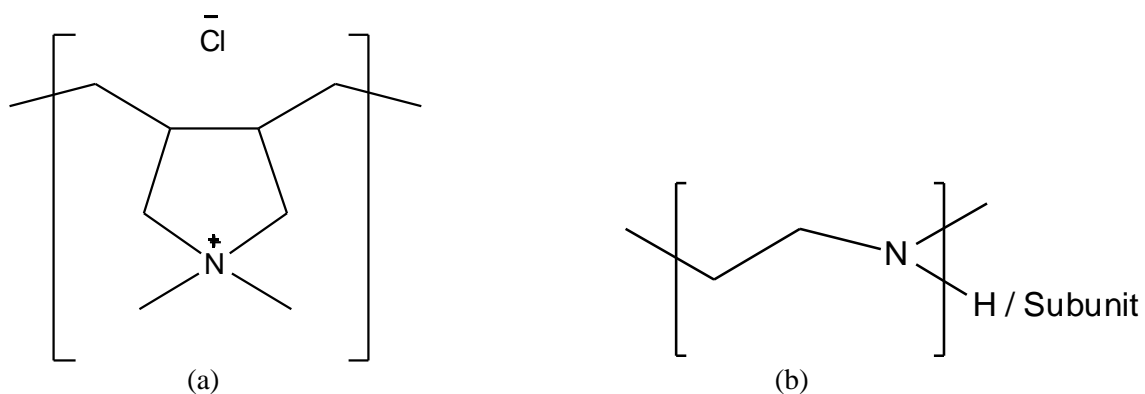


**Figure 8:** Schematic drawing of two cationic polymer sub-units: PDDA (a) and PEI (b). PEI can be branched or linear depending on if bonded to a hydrogen atom or another sub-unit.

Cationic PEI (PE<sup>+</sup>) bonds to the negatively charged Si surface due to the strong interaction between the ionic side-groups of the PEI backbone and the oppositely charged surface of the

substrate.<sup>90</sup> During a typical self-assembly process, the cationic polymer is applied to the surface of the substrate through immersion in an aqueous solution. The substrate is then washed to remove excess polymer leaving behind molecules that are electrostatically attached to the substrate.<sup>76</sup> After washing, the cationic-polymer-coated substrate is dried and dipped into an anionic polymer-ND dispersion - such as poly (sodium-4-styrenesulfonate) (PSS)<sup>91</sup>.

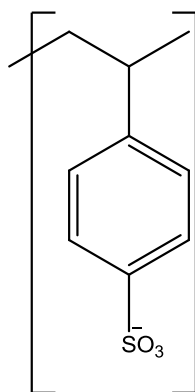


**Figure 9:** Schematic drawing of a subunit of the anionic polymer PSS.

The anionic polymer-coated-ND particles are electrostatically attracted toward the cationic-polymer-coated substrate and so electrostatic self-assembly will occur. The seeded substrate (ND/anionic polymer/cationic polymer/substrate) can then be placed in a CVD reactor where it is exposed to a methane containing plasma for further diamond deposition to occur.

### 5.1.2 Polymer molecular weight

While it is necessary that two polymers with opposite charge in solution are used for electrostatic seeding (cationic attached to substrate, anionic attached to diamond), the molecular weight of both polymers can be varied to improve the electrostatic attraction between layers.

Where high-molecular-weight polymers are used to coat the substrate, the overall charge of the adsorbed polymer layer is larger than that of the surface (the charge reversal effect).<sup>92</sup> As the polymer film is stabilised by short-range hydrophobic interactions, high-molecular-weight polymers (resulting in thicker films) will experience more electrostatic repulsion between the firmly attached polymers at the surface of the substrate and loosely attached polymers further away. This means that electrostatically attracted macromolecules (either oppositely charged polymers or inorganic particles) can detach from the polymer layer before they reach the substrate surface – resulting in agglomerates of polymer and a cationic-polymer layer which is uneven.<sup>93</sup> This can lead to a non-uniform self-assembled layer which is undesirable.

However, where a low-molecular-weight polymer is used to coat the substrate surface, better ordered layers can be obtained due to the increased occurrence of cross-links and the low chance of

adsorbed segments of the polymer being detached.<sup>93</sup> This improves the packing of the polymer onto the substrate and thus increases the electrostatic attraction between complementary polymers.

Berret *et al.*<sup>94</sup> have discussed the importance of molecular weight on electrostatic self-assembly in a recent review paper. It was found that surfactants with low molecular weight act to decrease their contact area with oppositely charged molecules (*e.g.* water) by clumping together into tightly linked, dense layers. The same principle can be applied to a system where electrostatic interactions are dominant, where low molecular weight polymers would also be favourable in successfully coating a silicon substrate.

In the case of PSS-coated nanodiamond particulates, it has been shown that as the molecular weight of the polymer increases, the overall size of the coated diamond particle increases.<sup>95</sup> When self-assembling nanodiamond onto a silicon substrate this effect may decrease the overall density of the resulting film due to the increasing distance between nucleation centres with increasing polymer molecular weight. When increasing the nucleation density and strengthening cross-linking within the self-assembled coating, low-molecular-weight polymers are preferential.

## 5.2 Zeta potential and pH effects

A zeta potential is used to describe the electrostatic potential near the surface of a particle within a system.<sup>96</sup> A value of 25 mV (whether positive or negative)<sup>75</sup> is taken as the point where a system is stable and will resist aggregation. As the zeta potential tends away from zero, the stability of a system can be said to increase. Maximising the zeta potential of a particular dispersion, indicates increased repulsion between particles,<sup>97</sup> and is therefore important in preventing agglomeration in solution.

As well as being dependent on the stability of dispersion, self-assembly processes are also dependent on the electrostatic interactions between layers of polymers and particulates. It is therefore important that the relative zeta potentials of neighbouring layers interchange between negative and positive values in order to induce net attraction.

Where a silicon substrate is used with a SiO<sub>2</sub> mask it is important that the ND particles are dispersed in a strongly anionic suspension to prevent electrostatic bonding with the negatively charged SiO<sub>2</sub> mask. There are a number of ways of altering the zeta potentials and therefore the electrostatic interactions including nanoparticle pre-treatment, pH adjustment and choice of dispersing solvents.

## 5.2.1 Altering zeta potential, pH and surface functional groups through ND particle pre-treatment

The largest influence on the zeta potential is the pH<sup>75</sup> of the solution due to its impact on surface groups and thus stability. It has been found that the zeta potential generally becomes more positive with decreasing pH and positive with increasing pH.<sup>98,99</sup> Ali *et al.*<sup>100</sup> found that the pH controls the linear charge density of an adsorbing polymer and thus even small changes in pH will affect the likelihood of self-assembly. A range of pH, from 2.5 – 9.0, was examined for solutions of PSS and it was found that the polymer chains adsorb as a thin layer with a flat conformation at high pH and a thicker conformation at a lower pH. The most cross-linked multilayer structures were obtained when the PSS solution was at a pH of between 4.5 and 6.5. This was due to PSS forming a thick, loopy conformation at acidic pH, resulting in an increased adsorption on the surface.<sup>100,101</sup>

As well as altering the polymers surrounding ND particles, the nanodiamond properties can also be altered through pre-treatment – for example with hydrogen gas annealing and air annealing.<sup>102</sup> These pre-treatment methods give rise to nanodiamond particles with slightly different surface functional groups, zeta potentials and pH, thus altering the likelihood of self-assembly.

Hees *et al.*<sup>102</sup> dispersed both hydrogen-annealed and air-annealed diamond powders in DI water in order to measure the electrostatic attraction between the diamond particles and a silicon surface. The substrate was immersed in both nanodiamond colloids for 10 min and it was found that H-annealed particles produced a lower mean particle size and a more monodispersed seed layer.<sup>102</sup> Using Fourier transform infrared spectroscopy it was shown that air-annealed nanoparticles in solution possess oxygen-containing surface functional groups (such as carboxyl, carbonyl and hydroxyl), whereas hydrogen-annealed nanoparticles had less oxygen related groups. As the presence of differing functional groups has been shown to affect the zeta potential<sup>103</sup> this will also affect the electrostatic attractions and be pH dependent.<sup>102</sup>

Air-annealed nanoparticles in solution were found to have a negative zeta potential which became more negative with increasing pH due to the deprotonation of carboxyl and hydroxyl groups. This colloidal dispersion was stable above pH = 4. However, hydrogen-annealed nanoparticles had a positive zeta potential over most of the pH range due to electrons in the diamond nanoparticles interacting with H<sub>3</sub>O<sup>+</sup> ions in the water. As the pH increases, the zeta potential decreases until the colloids are no longer stable above pH = 4. Therefore, depending on which substrate the nanodiamond particles are to be seeded on, the type of annealing pre-treatment the particles undergo can be important.

Both Si and SiO<sub>2</sub> have negative zeta potentials over most of the pH range<sup>104</sup> and, therefore, will repel air-annealed ND particles and attract H-annealed ones.

**Table 1:** Dependence of zeta potential on nanodiamond solution pH. pH adjusted using HF/H<sub>2</sub>O<sub>2</sub> and NH<sub>4</sub>OH/H<sub>2</sub>O<sub>2</sub> solutions. Reproduced in part from reference 104.

	HF/H <sub>2</sub> O <sub>2</sub> solution	NH <sub>4</sub> OH/H <sub>2</sub> O <sub>2</sub> solution
pH	3	8.8
Si surface zeta potential	-20mV	-50mV
SiO <sub>2</sub> surface zeta potential	+10mV	-60mV

Where SiO<sub>2</sub> is used as a substrate (and not a mask) it was found<sup>102</sup> that it will form the strongest interactions with H-annealed diamond particles at pH = 8.5, due to the largest difference in zeta potential. Using a high pH results in a high nucleation density of  $8 \times 10^{11} \text{ cm}^{-2}$ . However, above pH = 8.5 H-annealed nanoparticles were noted to aggregate and not give full coverage of the SiO<sub>2</sub> substrate, due to the decreasing difference in zeta potential. Air-annealed particles do not change in zeta potential to the same extent as H-annealed ND material but instead have a similar zeta potential to SiO<sub>2</sub> throughout the pH range, resulting in a lower density of  $1 \times 10^9 \text{ cm}^{-2}$ .

Therefore, the type of pre-treatment the nanodiamond particles receive must be tailored to the substrate and mask material requiring nucleation. It is also important to measure the pH and zeta potential of any polymer dispersions used in the self-assembly nucleation process due to the effect on the stability of the colloidal dispersion and likelihood of aggregation.

### 5.2.2 Zeta potential of polymers and ND used in self-assembly

Lee *et al.*<sup>74</sup> measured the zeta potential of the ND-PSS solution used to electrostatically attach nanodiamond to PEI-coated silicon and silicon oxide substrates. Prior to dispersion in PSS, the ND in water had a zeta potential of 29.6 mV. However, when the ND is dispersed in a 10 wt. % PSS solution, the system has a high negative zeta potential of -60.5 mV and so could form strong electrostatic bonds with the cationic PEI-coated substrate.<sup>74</sup> The zeta potential of PEI has been shown to alter with concentration, with a zeta potential of around 12 mV at  $10 \text{ mg ml}^{-1}$ .<sup>105</sup> As large zeta potentials of opposing signs maximise the electrostatic attractive force experienced between polymers in solution,<sup>106</sup> altering zeta potential through polymer choice, pH and ND pre-treatment will affect the likelihood of self-assembly.

### 5.3 Effect of nanodiamond immersion time

Once a stable polymer-ND dispersion has been formulated for a self-assembly process, the silicon substrate (coated in a cationic polymer) is immersed in it in order for self-assembly to occur.

Hahner *et al.*<sup>107</sup> examined the effect of immersion time for the self-assembly process of *n*-alkanethiols on gold and silver surfaces. The immersion times were varied from a few seconds to 43 h. It was found that self-assembly was not instantaneous, but rather that after 10 minutes 80% of the monolayer present at 43 h had self-assembled.

In the case of nanodiamond self-assembly, there is much variation within past research for immersion times. Lee *et al.*<sup>74</sup> used a dipping time of 12 h with ND-PSS on PEI-Si and observed a nucleation density of  $4.4 \times 10^{11} \text{ cm}^{-2}$ . However, Campos *et al.*<sup>108</sup> used a dipping time of 30 min with ND-PSS on PDDA-Si and observed a nucleation density of about  $1 \times 10^{11} \text{ cm}^{-2}$ . This indicates that whilst self-assembly of ND-polymer systems may not be instantaneous, 30 min immersion appears to be sufficient.

As well as immersion time, the extent of exposure should also be considered. Suzuki *et al.*<sup>109</sup> examined the self-assembly of acid-treated carbon nanotubes (forming COOH-CNT) onto amine-terminated diamond grains. They immersed surface-functionalised diamond grains into a dispersion of  $1.25 \text{ g l}^{-1}$  COOH-CNT in dimethylformamide solution five times, rinsing with ethanol and heating at  $110 \text{ }^\circ\text{C}$  for 10 min in air between immersions. It was found that this process resulted in an almost complete coverage of diamond by CNT. However, these results were not compared to an experiment with a single immersion.

To conclude, both the immersion time and number of immersions can affect nucleation density, particularly if the immersion time is too short to reach close to maximum coverage (<30 min).

## 6. Selected-area deposition on a silicon surface after self-assembly nucleation

Once a substrate, such as silicon, has been sufficiently cleaned and undergone high-density nucleation outlined above, it can then be used to deposit a diamond film. However, in some applications, such as electronics,<sup>110</sup> complete coverage of a substrate is not required and techniques for achieving selected-area nucleation and deposition have been developed.

Patterning of a substrate for selected-area deposition of diamond can be controlled in three common ways, although more techniques are still being developed. First, patterning with lithography, where a resist is mixed with diamond particles in order to seed selectively. Alternatively, the substrate can be covered with an appropriate mask and then nucleated.<sup>110</sup> The stencil mask can then be removed prior to deposition resulting in selected-area nucleation, or post-growth removing diamond that has grown on top of the mask. Finally, patterning can be encouraged by selectively etching nucleated/deposited diamond in an  $O_2$ <sup>111</sup> or  $O_2/CF_4$ <sup>112,113</sup> plasma.

### 6.1. Selected-area patterning using lithography

Masood *et al.*<sup>114</sup> have achieved selective nucleation by mixing a positive photoresist with fine diamond powder (0.1-0.2  $\mu\text{m}$ ). The photoresist thickness was controlled by altering the spinning time and speed, and patterned using a standard photolithographic process. However, it was found that after resist development, scattered diamond particles from the resist were present on the substrate, resulting in undesired growth. It was therefore necessary to remove the resist with gentle etching – for a  $SiO_2$  surface using buffered hydrofluoric acid and for a Si surface using dilute KOH.<sup>114</sup> The selectivity of this process is limited by the lithography process and the grain size used in the diamond powder.

### 6.2 Selected-area patterning using masking

Ha *et al.*<sup>115</sup> have used a masked-substrate approach to selectively deposit diamond onto a silicon-based substrate in order to produce a gated, diamond array for use in electronics. A  $SiO_2$  coating was used as the mask where parts of the stencil (2-3  $\mu\text{m}$ ) were etched away using photolithography and dry etching so that regions of Si surface were exposed. The masked-substrate was then nucleated using BEN and grown for 5 h using MWCVD. After deposition the  $SiO_2$  mask layer was removed in a buffered HF solution and resulted in a substrate with selected-area diamond deposition interspersed with exposed Si surface.

Alternatively, the covering mask could be removed prior to deposition resulting in a substrate with some areas selectively nucleated. Masood *et al.*<sup>114</sup> have used a silicon substrate masked with either  $SiO_2$  or  $Si_3N_4$  which shielded certain areas from nucleation during ultrasonic bombardment of

ND solution. In a similar process to ultrasonic abrasion, the exposed surface was nucleated by implantation of diamond particles and an increase in surface roughness. The mask was then removed prior to deposition resulting in effective selective area patterning. However, in this method the masking layer can be eroded due to the ultrasonic bombardment, requiring the use of a relatively thick initial mask (0.6  $\mu\text{m}$  of  $\text{SiO}_2$  or 0.4  $\mu\text{m}$  of  $\text{Si}_3\text{N}_4$  required for 30 min treatment when 0.1  $\mu\text{m}$  powdered diamond powder is ultrasonically agitated.)

While selected-area patterning has shown to be successful when a mask is used this technique can still be improved. For instance, where a mask is removed pre-growth, blurring at the edge of the pattern has been found to occur due to the diamond growing in random directions, decreasing the resolution of the final film.<sup>110</sup> Similarly, the thickness of the patterned diamond layers formed in both methods is limited to the thickness of the  $\text{SiO}_2$  mask,<sup>115</sup> which will prevent highly intricate patterns being possible.

### 6.3 Selected-area patterning using plasma etching

The final technique for selected-area patterning is based on selective etching of diamond. Diamond oxidises readily at high temperature<sup>116</sup> and so can be removed under certain extreme conditions. In this method a diamond film is first grown across the entire surface and then a mask (such as  $\text{Si}_3\text{N}_4$ ) deposited and annealed. It is necessary that the mask used can withstand the high temperatures present in the plasma. The substrate is then exposed to an oxygen-based plasma in order to remove unmasked diamond. This results in areas of diamond coated with a mask, and patterns of exposed substrate. Finally, the mask is removed from the surface (in the case of  $\text{Si}_3\text{N}_4$  using a concentrated HF solution) resulting in selected-area patterning.

This method too has its drawbacks, for instance, where thick diamond layers are required (>10  $\mu\text{m}$ ) selective etching is time consuming and unsuitable due to the resilience of diamond,<sup>110</sup> it is also a challenge to etch away unwanted diamond, without undercutting the patterned film.<sup>114</sup>

As all three common methods of selected-area nucleation and growth can negatively affect the diamond film deposition and research is underway to produce new processes. One such method which does not require removal of a mask, etching or photolithography is micro-contact printing.<sup>117</sup>

### 6.4 Selected-area patterning using micro-contact printing

In this method nanodiamond particulates, in the form of an 'ink' are transferred onto the substrate in a highly specific manner, which results in selective nucleation of the surface without any damage.

Zhuang *et al.*<sup>117</sup> transferred a monodispersion of detonation nanodiamond (the ink) onto a silicon surface through the use of a stamp made from oxidised poly (dimethyl-siloxane) (PDMS). It was found that the density and quantity of diamond particles on the stamp was a crucial factor in the success of selected-area deposition.

Firstly, the density of adsorbed diamond particles was optimised by decreasing particle size, and minimising electrostatic repulsion. Secondly, PDMS was oxidised to increase the amount of ‘ink’ on the stamp. This lowered the zeta potential and tripled the interaction between ND and PDMS. The process worked through transferring the adsorbed ND (ink) on the ox-PDMS (stamp) onto the Si substrate. This resulted in highly selective diamond nucleation without the use of destructive techniques.

As microcontact 3D printing is still a relatively new technology, there are issues with its effectiveness making it unsuitable for wide scale use. Firstly, as the ND transfers onto the PDMS surface there is an increase in surface tension that makes it progressively more difficult for further ND to attach to the substrate. Secondly, on contact with Si, the ND can become embedded in the PDMS (as well as Si), increasing the ND-PDMS adhesion and thus decreasing ND-Si transfer. However, it is believed that these issues may be resolved by the presence of a softer layer, such as polymethylmethacrylate (PMMA), on top of the silicon surface. It is theorised<sup>117</sup> that the surface of the PMMA will be easier to coat than Si, and thus not increase DND-PDMS adhesion.

## 7. Aim

The aim of this investigation is to produce a repeatable method by which a high density of nanodiamond nucleation sites are formed on a 1 cm<sup>2</sup> silicon substrate using a self-assembly nucleation process. Once this method is fully optimised, silicon kinoform and CRL moulds were selectively nucleated through self-assembly and diamond layers were grown in a MWCVD reactor. A high density of nanodiamond particles ensures that all of the edges of the mould are filled and that the resulting nanodiamond structure is sufficiently detailed. After the CVD step, the silicon moulds are removed by etching to produce refractive lenses for use in focusing synchrotron x-ray beams.



## 8. Experimental method

For the self-assembly nucleation and selected-area deposition process to be successful it was apparent from past research, described above, that the following general steps must be followed in order: cleaning of substrate, immersion in a cationic polymer, immersion in an anionic polymer containing nanodiamond particles and finally deposition in a MWCVD reactor. In order to increase the density of self-assembled nanodiamond particles each variable was examined and where possible optimised for the eventual production of a recommended method.

### 8.1 Description of polymers used

In this study, PEI (800 Da<sup>118</sup> and 1300 Da<sup>88</sup>), PDDA (100000 Da<sup>119</sup>) and PSS (70000 Da<sup>120</sup>) obtained from Sigma-Aldrich were used. All polymers were dispersed as an aqueous solution using Millipore Milli-Q deionised (DI) water. PEI and PDDA were made up in 10 w/v % dispersions in water and mixed using a Bandelin sonoPLUS HD2070 MS72 ultrasonic mixer for 5 min at 40% power. PSS was first heated to improve dissolving and then added to DI water to create a 10 w/v % aqueous solution. The PSS dispersion had varying concentrations of ND added, prior to 10 min of ultrasonic dispersion at 40% power.

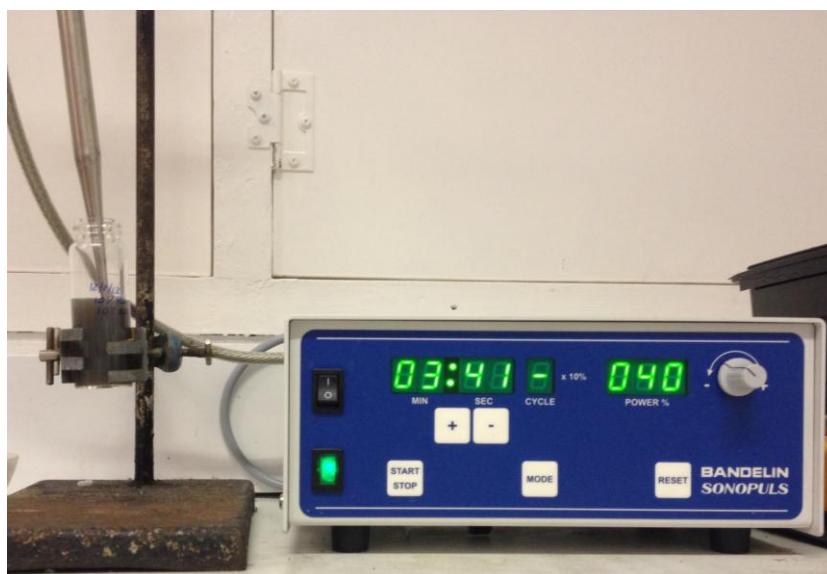


**Figure 10:** Photograph of 10 w/v% PSS, 10 w/v% ND aqueous solution being dispersed using a Bandeloin SonoPLUS ultrasonic probe.

The nanodiamond particles used were purchased from the Carbon Research Institute, Tokida, Japan, as a 50 w/v % aqueous colloid dispersion in water, with a nominal particle size of  $4.8 \pm 0.6$  nm. Nanodiamond polymer dispersions were analysed using zeta potential, z-mean and pH measurements.

These were taken at 25°C using Malvern Zetasizer Z, Malvern Zetasizer S90 and Oakton pH/CON 150 equipment respectively.

## 8.2 MWCVD reactor

In order to assess the nanodiamond nucleation step, each sample was grown for 5 min in a MWCVD reactor to increase nanoparticle size and allow quantitative analysis of the nucleation density. A detailed description of the MWCVD equipment and the operating procedure can be found in Fox,<sup>121</sup> although a brief outline is given below.

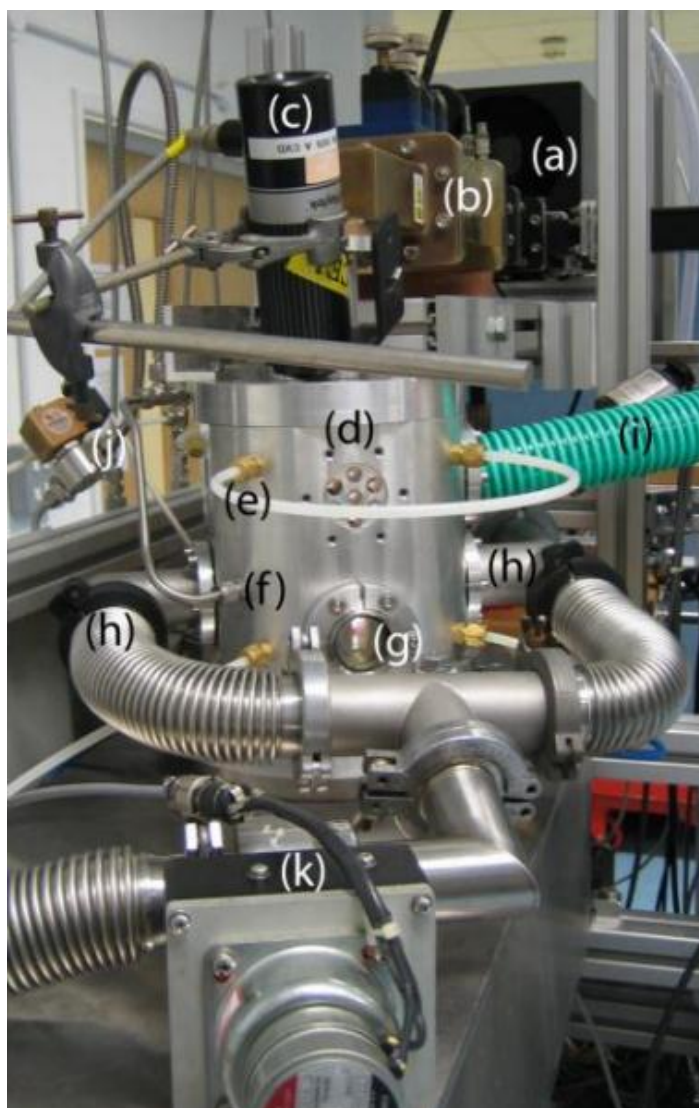


**Figure 11:** The MWCVD setup used for diamond deposition. (a) MW magnetron (b) MW waveguide (c) optical pyrometer (d) reaction chamber (e) water-cooler (f) process gas inlet (g) silica viewing window (h) gas exhaust (i) air-cooler pipe (j) solenoid valve (k) pressure regulating butterfly valve. Reproduced from reference 121.

An Astex-type 2.45 GHz MWCVD reactor (**Figure 11**) was used for growing nanocrystalline diamond from nucleated substrates described in this work. Typically, a 1 cm<sup>2</sup> ND nucleated, silicon

substrate was placed onto a molybdenum substrate holder situated in the centre of the reaction chamber on a 250  $\mu\text{m}$ -thick tungsten wire ring. The tungsten wire acts as thermal break between the water-cooled reactor base and substrate ( $\sim 1000$  K). The reactor was then vacuum-sealed and the air-cooler (i) and water-cooler (e) turned on. Premixed  $\text{CH}_4$ ,  $\text{H}_2$  and Ar gasses were fed into the reactor chamber beneath the dielectric (silica) window. The flow rate of the gases was controlled using a MKS 247 C electronic control box connected to six mass-flow controllers (MFC).

The process gases were then activated with 2.45 GHz microwave radiation, generated by a 1.5 kW magnetron (HS-1000). In the resulting plasma, active carbon species are produced and some diffuse near the Si substrate to form a polycrystalline diamond layers as they add to the ND nuclei. In all deposition runs within this investigation, plasma conditions were maintained at a total pressure,  $p = 110$  Torr and input power,  $P = 1.0$  kW. The temperature of plasma cannot be controlled independently of the pressure and power.

## 8.3 Microscopy – Optical and SEM

After the short deposition in a MWCVD reactor the diamond grains were of a sufficient size to be imaged. An optical microscope (Zeiss Axiolab) was used to image nucleated surfaces, with a magnification of up to  $\times 1000$ . This was used to provide information on the uniformity of nucleated substrates.

To assess the nanoparticle nucleation density due to experimental variations and measure the diameter of surface particles, a scanning electron microscope (SEM) was also used. High-quality images with nanometre scale resolution are produced when a beam of electrons (0.5 – 30 kV) is scanned over the sample surface. This causes the sample to emit secondary electrons and x-rays which are then analysed to provide information about the surface topography. In this project, two scanning electron microscopes were used: JEOL JSM 5600 LV and JEOL JSM 6330F. These use thermionic emission and field emission, respectively, to produce an electron beam.

As well as examining the surface topography, SEM imaging can be used to measure the thickness of the nanodiamond layer in cases where a continuous film has been produced. In the later stages of this project, production of a thin diamond layer was sought in order to prove that a high nucleation density had been achieved. In this case, an Oxford Lasers Alpha 532 laser machining system was used to cleave the lens samples, producing a cross-sectional view suitable for examination with the SEM.



## 9. Results and Discussion

The aim of this project was to increase the density of nucleated nanodiamond particles on a  $1\text{ cm}^2$  polished Si substrate. To achieve this goal, a single variable within the nucleation process was varied whilst keeping all others constant. Each sample was grown in a gaseous mixture of  $500\text{ cm}^3\text{ min}^{-1}\text{ H}_2$ ,  $35\text{ cm}^3\text{ min}^{-1}\text{ CH}_4$  and  $4\text{ cm}^3\text{ min}^{-1}\text{ N}_2$  for 5 min using a MWCVD reactor. This deposition increased the particle nucleation size to allow imaging with Scanning Electron Microscopy (SEM) and Optical Microscopy. A full record of images used in the production of a best-practice methodology is contained in the appendix.

While all experiments discussed here are conducted with one variable changed and all other variables held constant, not all experiments were conducted in the order listed here. For that reason, comparisons between investigations should not be drawn until the end best-practice method.

### 9.1 Examining cleaning method of Si substrate

In the self-assembly process, it is crucial that electrostatic interactions are optimised to achieve a high-density nucleation. As discussed in Chapter 4, one way of maximising substrate-polymer interactions is through the removal of surface contaminants. For this reason, several possible substrate cleaning methods were compared and the resulting nanoparticle density after self-assembly analysed.

All samples were rinsed in DI water, acetone, ethanol and methanol sequentially with a light drying, using Fisher brand FB13067 lens cleaning tissue, between steps. Solvents were used in order of decreasing boiling point so that solvent removal and drying became sequentially easier. This decreased the chance of uneven solvent drying occurring and the uniformity of the substrate being compromised.

In the case of Method 1, the cleaning process ended here. For Methods 2 – 4 an additional cleaning step took place. These consisted of rinsing in 0.01 M sulphuric acid (Method 2), rinsing in 1 M nitric acid (Method 3), and exposure to a  $10\text{ cm}^3\text{ min}^{-1}\text{ N}_2/500\text{ cm}^3\text{ min}^{-1}\text{ H}_2$  plasma (75 Torr, 1,000 W) for 5 min (Method 4). Finally, the samples underwent nanodiamond nucleation and short deposition prior to imaging, with all other variables kept constant.

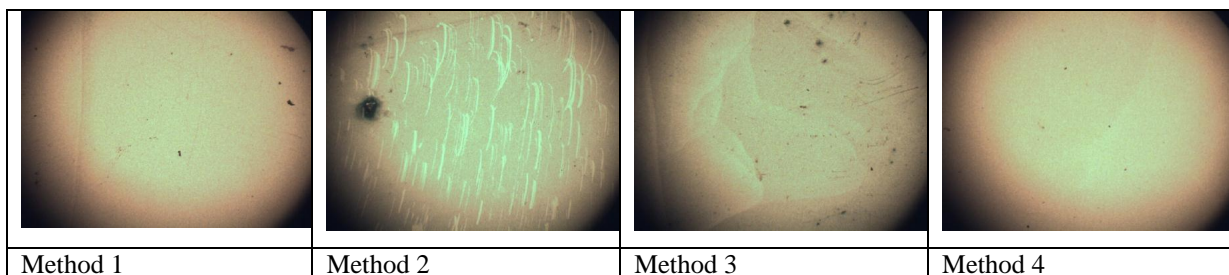


**Figure 12:** Comparison of different cleaning methods prior to diamond nucleation and growth. Images taken using optical microscopy (magnification  $\times 5$ )

As seen from the above images (and **Appendix 11.1**), Methods 1 and 4 produced largely uniform nanodiamond films. Where sulphuric acid was used prior to self-assembly (Method 2) surface damage appears to have occurred, leading to sections where no nanodiamond has nucleated. Nitric acid (Method 3) has not caused surface damage, but has produced a streaked effect visible at lower magnifications. This non-uniform finish indicates contaminants are remaining on the surface of the substrate, even after cleaning, disrupting electrostatic interactions with subsequent polymers.

It was concluded that  $H_2/N_2$  plasma cleaning (Method 4) and methanol cleaning (Method 1) are appropriate methods, as both produce uniform results with a similar density of nanoparticles. However, for experimental ease of use, methanol cleaning will be used for further samples.

### 9.1.1 Improving solvent based cleaning methods

Investigations were conducted to optimise the solvent cleaning process by increasing contaminant removal and decreasing surface abrasion. In order to achieve this, repetitions of cleaning methods and alternative methods of drying were examined.

#### 9.1.1.1 Repetition of solvent cleaning steps

Three silicon substrates were examined with differing cleaning methods. Firstly, a sample was cleaned with the same method detailed above. This was then compared to a sample which was rinsed with each solvent twice, and a third sample where the entire cleaning process was repeated twice.

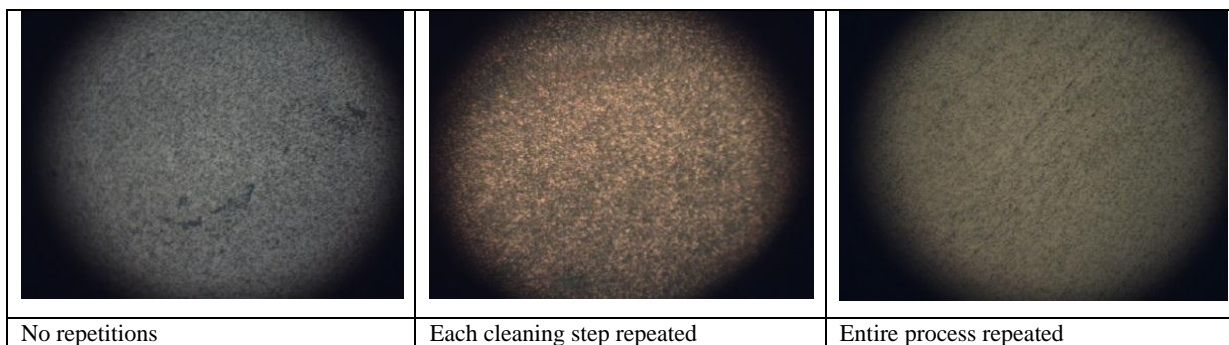


**Figure 13:** Optimising the cleaning process through repetition of solvent cleaning steps. Images taken using optical microscopy (magnification  $\times 50$ ).

No noticeable difference in diamond particle uniformity occurred with either repetition of cleaning. Therefore a single cleaning step, as described in **Section 9.1**, was determined as being acceptable in removing surface contaminants.

### 9.1.1.2 Examining drying methods within a solvent-based clean

In the above cleaning method, lens cleaning tissue was used to dry the substrate between rinses. However, this is not applicable when used in the nucleation of the Si lens moulds. Firstly, this method increases the risk of surface abrasion occurring and, secondly, drying small internal structures within the mould would be impossible. Due to these issues, an alternative drying step using a pressurised N<sub>2</sub> gas flow was examined. Nitrogen was chosen as it is an inert gas, so will not introduce new contaminants to the surface or encourage oxidation.

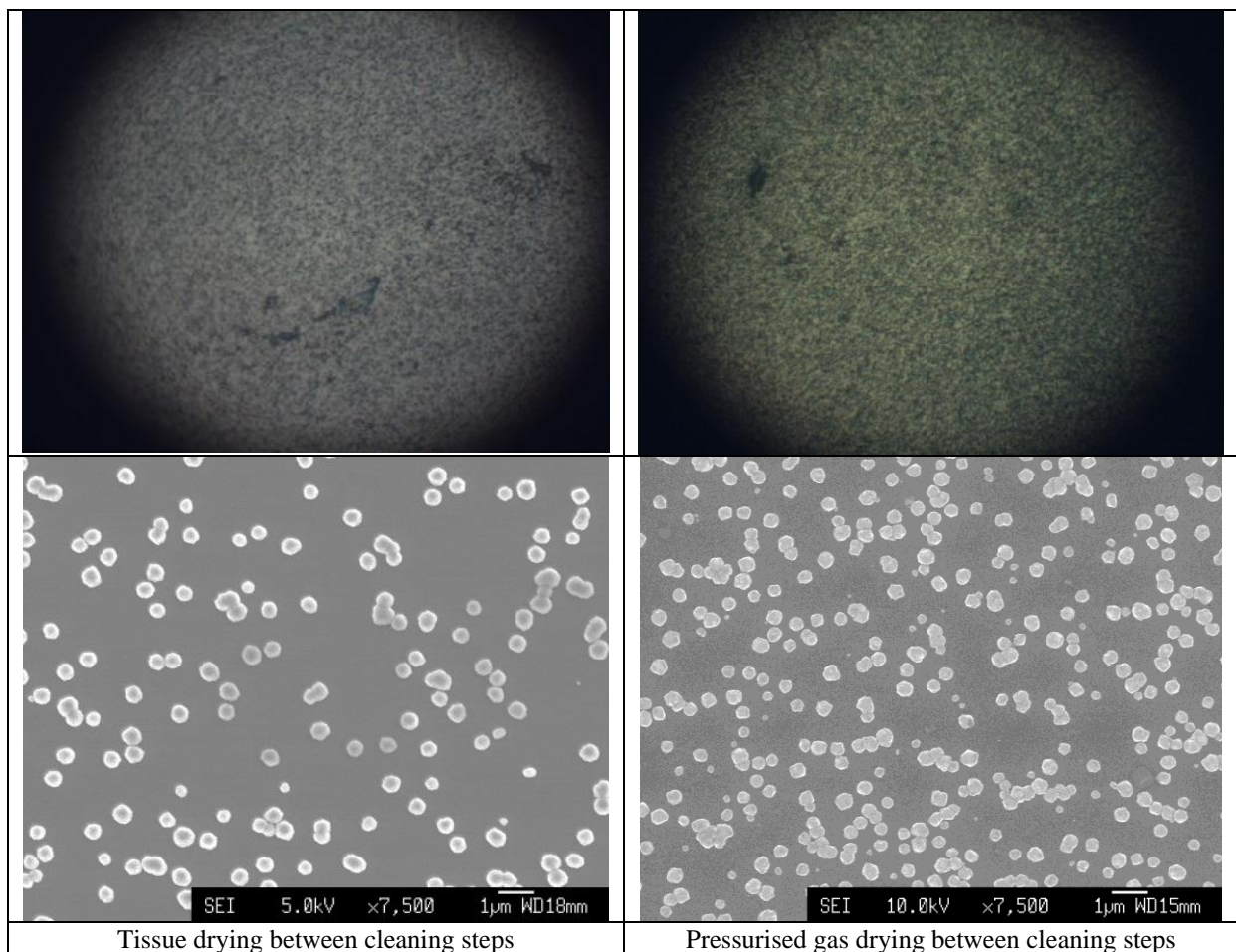


**Figure 14:** Comparison of tissue drying and nitrogen gas drying between cleaning steps. Above: Images taken using optical microscopy (magnification  $\times 50$ ). Below: Images taken using SEM (magnification  $\times 7500$ ).

No real difference in uniformity was noted when the sample was dried with lens tissue and with N<sub>2</sub>. This indicates that gaseous drying is as effective as lens tissue in removing solvent and preventing uneven drying which would be shown through the presence of drying marks.

However, it was noted that the use of lens cleaning tissue slightly decreases the end density of nanodiamond films. This may be due to surface contaminants being transferred from the tissues onto the surface which would decrease electrostatic interactions and result in a lower nanoparticle density. Therefore, to minimise the risk of both surface abrasion and contaminant introduction, a N<sub>2</sub> flow is recommended for drying during cleaning processes and contact with the substrate surface is to be avoided.

## 9.2 Investigations into cationic polymers

Immersion of the Si substrate in a cationic polymer is necessary for nanodiamond particles dispersed in an anionic polymer to be electrostatically attracted to the surface and nucleate it. However, as it is possible that nanodiamond nucleation may also occur as a result of gravitational settling, and not electrostatic attraction, nanoparticle nucleation was examined when PEI (1,300 Da) was used and when the PEI immersion step was removed from the process.

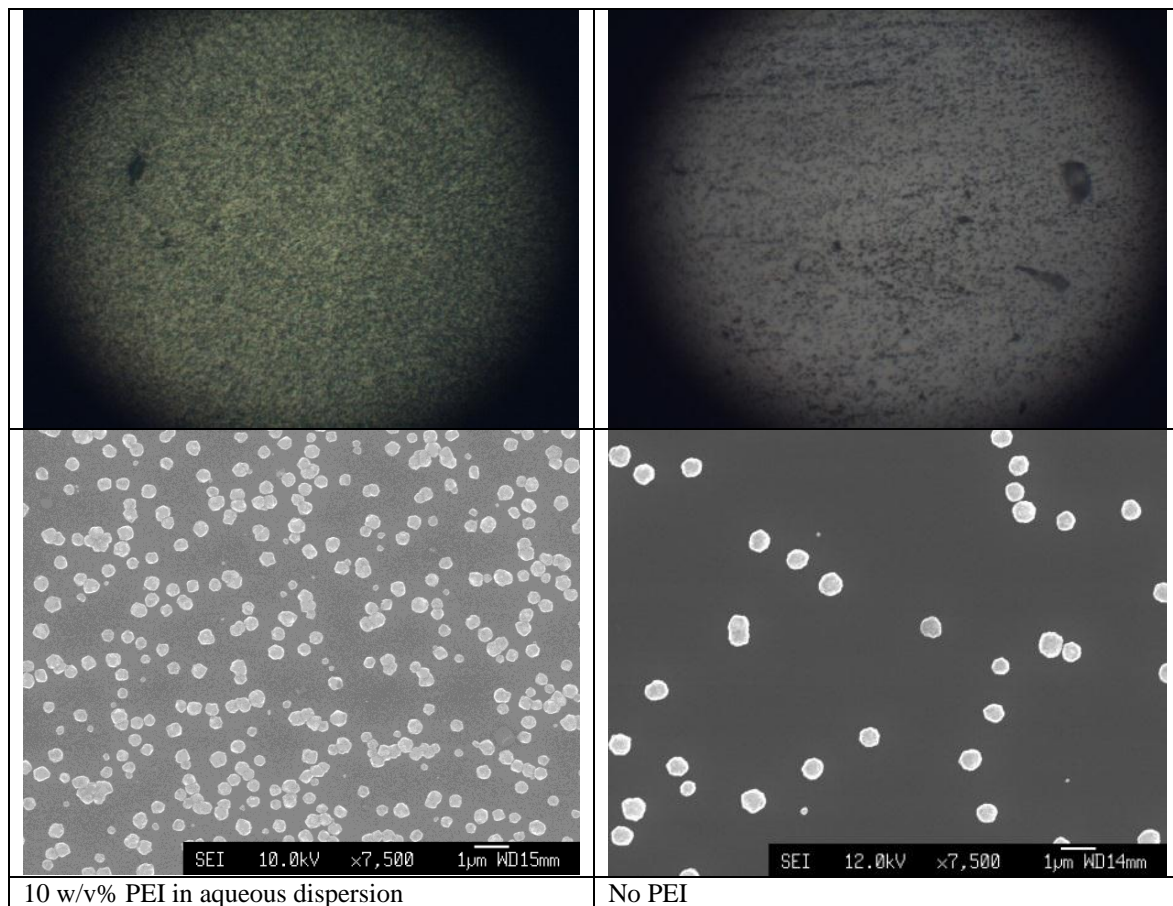


**Figure 15:** Comparison of self-assembly process when PEI is used (electrostatic interactions dominant) and when PEI is not used (gravitational settling dominant). Images above: Optical microscopy ( $\times 50$ ). Images below: SEM imaging ( $\times 7500$ ).

On comparison of the above images, it is clear that electrostatic interactions are the dominant influence for encouraging nanodiamond nucleation. When a clean silicon surface is immersed in a

polymer containing ND particles, without an initial cationic polymer immersion, the ND will not naturally settle onto the substrate surface in large numbers - as shown by the experiment conducted with no PEI. This indicates that gravitational forces alone are not sufficient in encouraging nanodiamond nucleation, and therefore optimising polymer-polymer interactions is critical in increasing nucleation density.

## 9.2.1 Increasing PEI immersion time

To optimise electrostatic interactions between sequential polymer immersions, it is important that each immersion results in a full coverage of the substrate.



**Figure 16:** A schematic diagram of the processes leading up to successful self-assembly of a ND nucleation layer. Not drawn to scale. Step 1: A clean, dry silicon substrate. Step 2: Silicon substrate is coating in a thin layer of cationic polymer. Step 3: Substrate is immersed in an anionic polymer containing nanodiamond particles and excess polymer is washed away. Step 4: Remaining polymer is removed in MWCVD plasma and nanodiamond nuclei are grown into a continuous diamond film.

The influence of increasing, or repeating, immersion times on the likelihood of forming an even coating of PEI was investigated. Repeated immersions were hypothesised to be beneficial, as they would remove PEI polymer chains which have not formed successful configurations for bonding. This would result in bare silicon areas being exposed to a second immersion of PEI, increasing the likelihood of a complete coverage. All samples were immersed in a 10 w/v % PEI ( $M_w = 1300$  Da).

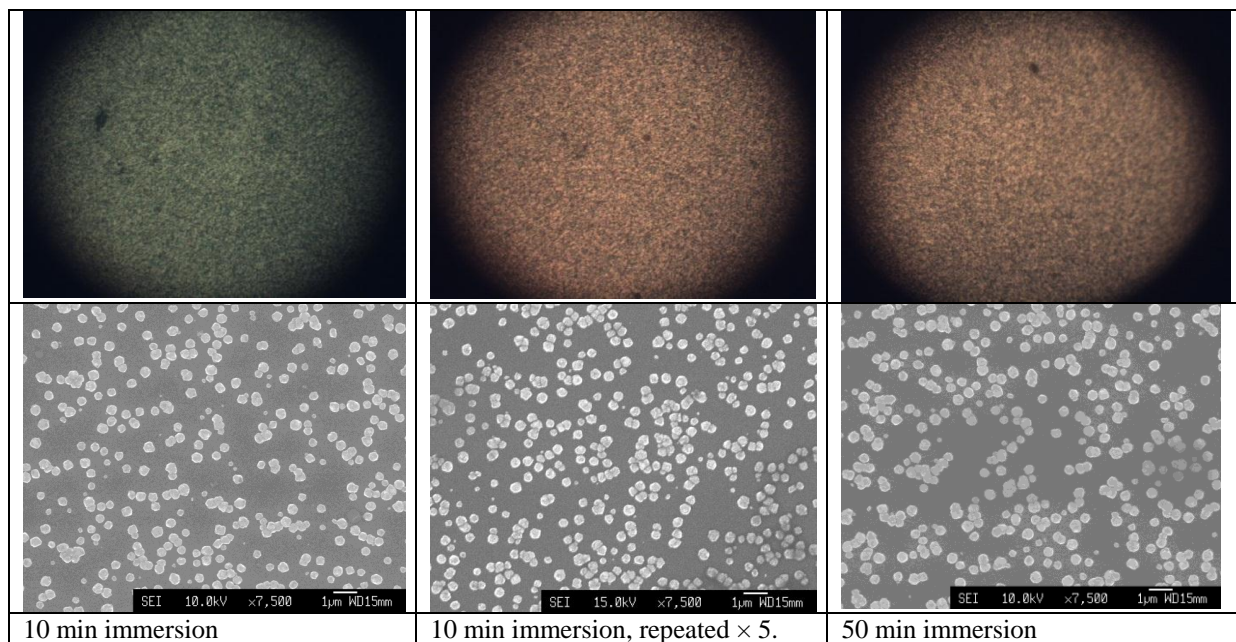


**Figure 17:** Comparison of PEI immersion times. Above: Optical microscopy ( $\times 50$ ). Below: SEM imaging ( $\times 7500$ ).

From the results, it was apparent that 10 min immersion in PEI is not limiting the extent of polymer attached to the substrate, and extending or repeating immersion times does not greatly improve nanodiamond density or uniformity. It is concluded that electrostatic interactions occurring between the silicon surface and PEI polymer are strong and fast to form, with the presence of excess polymer on the substrate surface being minimal.

## 9.2.2 Examining the molecular weight of PEI

The final variable examined in improving the effect of PEI on nucleation density, was its molecular weight. Molecular weight can affect the type and strength of crosslinking between the polymer chains. Previous research on the subject indicates that lower molecular weight improves uniformity and density by increasing the packing order of the polymer present on the surface. This leads to tighter crosslinking and a more even layer of polymer. (See **Section 5.1.2.**) Two PEI weights were compared, one with an average  $M_w$  of 800 Da and one with  $M_w = 1300$  Da. Both were made up to 10% wt. dispersions in DI water, with all other variables in the self-assembly process kept constant.

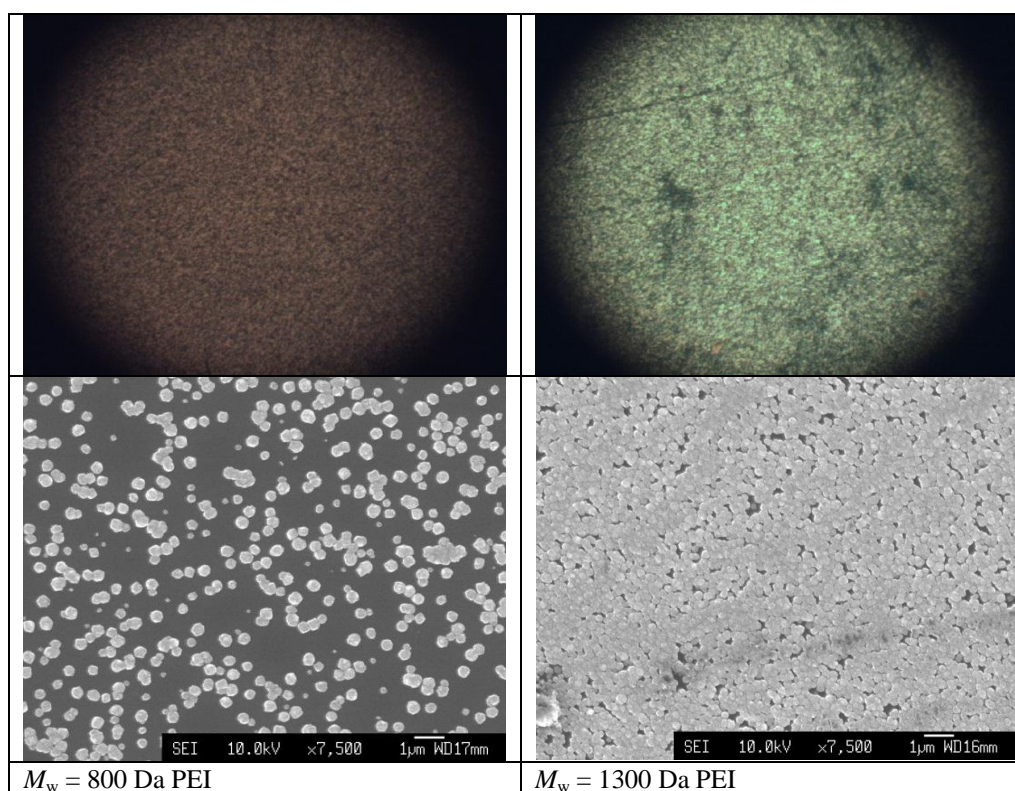


**Figure 18:** Comparison of the effects of PEI molecular weight on nanodiamond nucleation. Above: Optical microscopy ( $\times 50$ ). Below: SEM imaging ( $\times 7500$ ).

On comparison of the two samples imaged, the one with a higher  $M_w$  PEI clearly gives a higher nanoparticle density. Whilst a lower  $M_w$  has been shown in previous research to give a smoother polymer coating, this is apparently not true for this system. This may be due to larger molecular weight polymers having more degrees of freedom inherently and therefore more

configurations where they can successfully interact with both the silicon surface and the anionic polymer. A higher molecular weight will also produce a rougher polymer layer which will act to increase the surface area of PEI available for an anionic polymer to attach to.

It is concluded that whilst a lower molecular weight gives tighter crosslinking and more even coating of PEI, this is not conducive with increasing nanodiamond density or uniformity. On this basis, work was done on increasing the molecular weight of a different cationic polymer (poly (diallyldimethylammonium chloride), PDDA).

### 9.2.3 Comparing the effects of PDDA and PEI

PDDA was chosen as a possible alternative to PEI due to its use in previous research, it having a higher molecular weight (for the PDDA used in this work  $M_w = 100000$  Da whereas the highest PEI  $M_w$  used was 1300 Da) and similarity in structure – both have a H/C/N-containing backbone. Both PDDA and PEI were prepared as 10% wt. aqueous dispersions and Si substrates were immersed for 10 min. All other variables during the self-assembly process were kept constant.

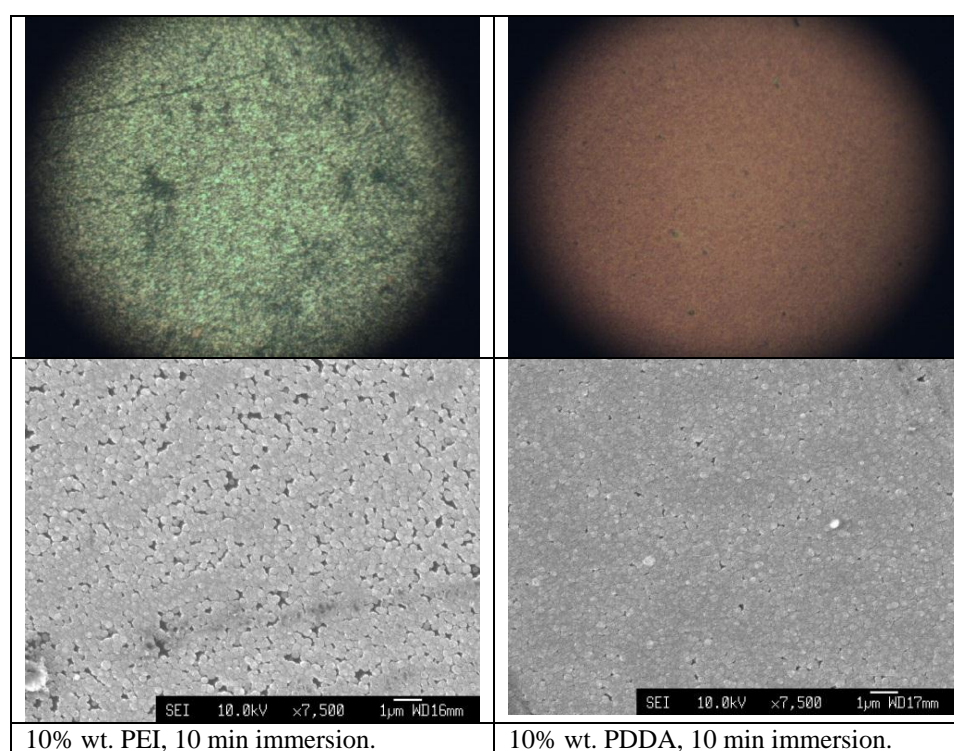


**Figure 19:** Comparison of PDDA and PEI polymers. Above: Optical microscopy ( $\times 50$ ). Below: SEM imaging ( $\times 7500$ ). For further images see **Appendix Section 11.1**.

From the images above (and those in **Appendix 11.1**), it is clear that PDDA gives improved nanodiamond density and uniformity. In part, this can be explained by the higher molecular weight of the PDDA polymer having more degrees of freedom in the chain, maximising the chance of successful interaction with the Si surface and the PSS-ND system, and thus increasing nanoparticle

density. It may also be explained by the relative zeta potentials of these solutions of PDDA (-9.06 mV) and PEI (-0.342 mV). PDDA has a larger disparity from PSS (1.908 mV) and so will form a stronger electrostatic interaction, thus resulting in higher nucleation density. A third explanation for the improvement of PDDA in comparison to PEI is the bulkiness of the PDDA polymer chain. PDDA contains a carbon ring which may act to increase polymer surface roughness at the PDDA-PSS interface, thus encouraging PSS to bond due to the increased surface area available. In reality the improvement in the nucleation density with PDDA may be a combination of all three reasons.

### 9.3 Washing after exposure to cationic polymer

After the silicon substrate has been immersed in PDDA, it is necessary to remove excess polymer. It is important that this step does not remove bonded polymer, as the monolayer of cationic PDDA on the Si surface will act as the attractive force which encourages the anionic polymer-nanodiamond to attach. However, the washing step must be vigorous enough that excess, non-bonded PDDA is not left on the surface prior to anionic-polymer immersion, as it may bond to the polymer chains in solution and not nucleate at the silicon surface.

Four different washing options were trialled and compared in order to determine the best washing method. One sample had no washing step after immersion in the cationic polymer; one was rinsed with deionised water; one rinsed in ethanol and one rinsed in methanol. These methods were chosen to determine if washing after immersion was necessary and if it was, which method would be best.

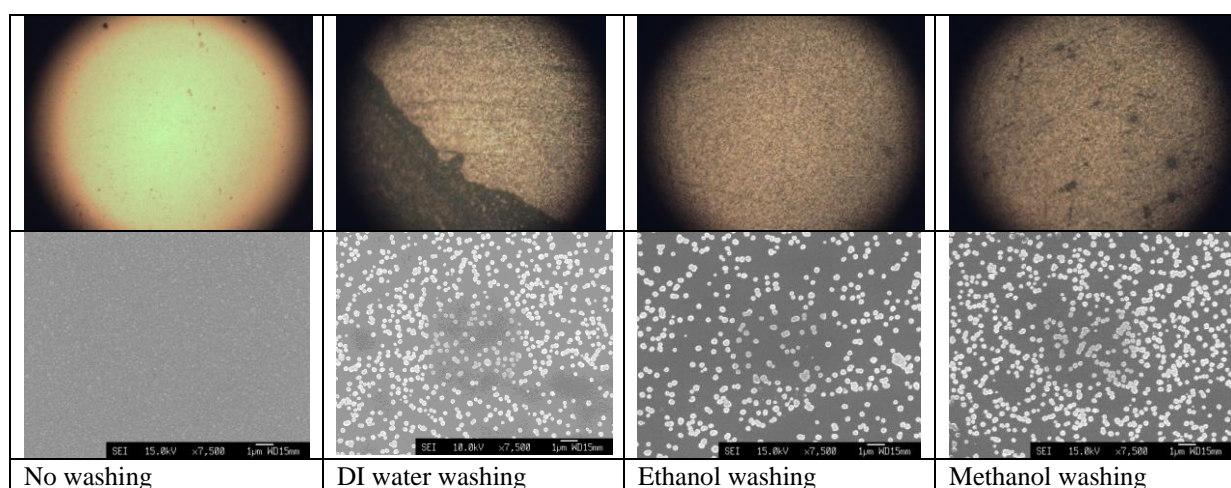


**Figure 20:** Comparison of various washing methods after silicon substrate immersion in a cationic polymer. Above: Optical microscopy images ( $\times 50$ ). Below: SEM images ( $\times 7\,500$ ).

Where washing did not occur, no ND particles were observed as having nucleated. This is due to them bonding to excess layers of polymer which are removed in later steps, resulting in a loss of all ND nucleated particles. Secondly, it was noted that washing with DI water results in a poor

nucleation uniformity. This may be due to water's Hydrogen bonds disrupting ionic bonding occurring between PDDA chains and silicon surface, resulting in polymer removal. The results clearly show a methanol or ethanol washing step is superior for producing a higher overall uniformity. However, as there is some evidence, under optical microscopy, of methanol producing surface damage (perhaps from removing bonded polymer) ethanol is recommended for washing.

After excess polymer has been washed away, it is necessary to dry the substrate to prevent an even drying resulting in tide-marks and decreased overall uniformity. Variables examined in improving the drying processes have been discussed in conjunction with drying post-anionic polymer immersion. (See **Section 9.6.**)

## 9.4 Optimising the anionic polymer in nanodiamond particle nucleation

Once a substrate has been coated with a single layer of the cationic polymer, either PEI or PDDA, it is necessary to immerse the coated substrate in an anionic polymer containing dispersed nanodiamond. In this investigation, PSS was used as the anionic polymer ( $M_w = 70000$  Da) and prepared from powder form into 10% wt. dispersion in water. The concentration of nanodiamond within this polymer solution, the pH, and the immersion time were varied to produce a system with maximum nanodiamond nucleation.

### 9.4.1 Immersion time in PSS

The length of time a silicon wafer is immersed in the dispersion of PSS, containing a fixed concentration of nanodiamond, was varied to test whether it had an influence on the nucleation density of nanodiamond particles. The time of immersion was increased in intervals up to 22 h to determine the maximum possible density. As well as looking at the exposure time, the immersion was repeated in order to examine the effects that substrate removal, washing, drying and re-immersion would have on end density. It was hypothesised that by removing excess PSS on the top of the substrate, this may allow more nanodiamond particles to nucleate during the second immersion.

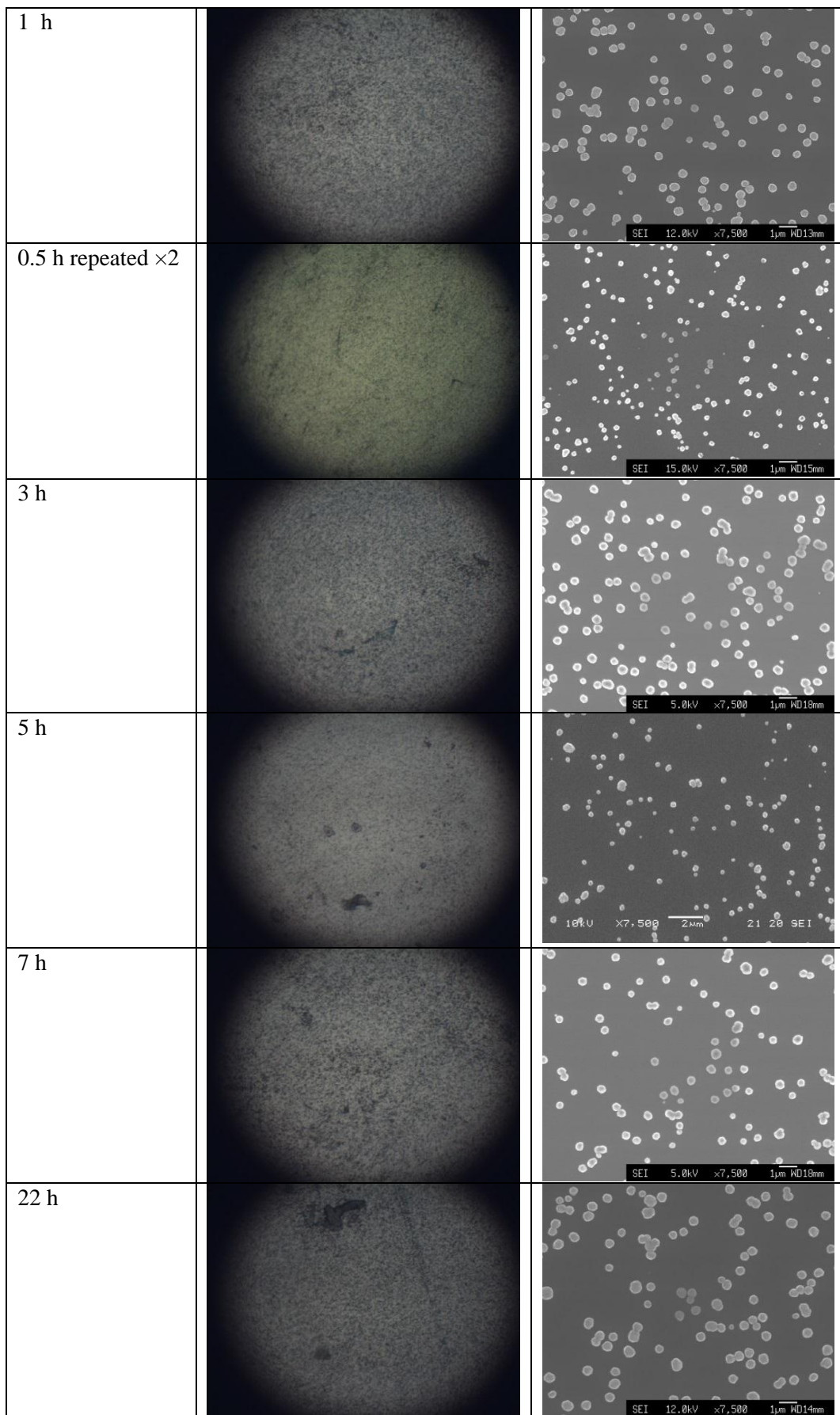
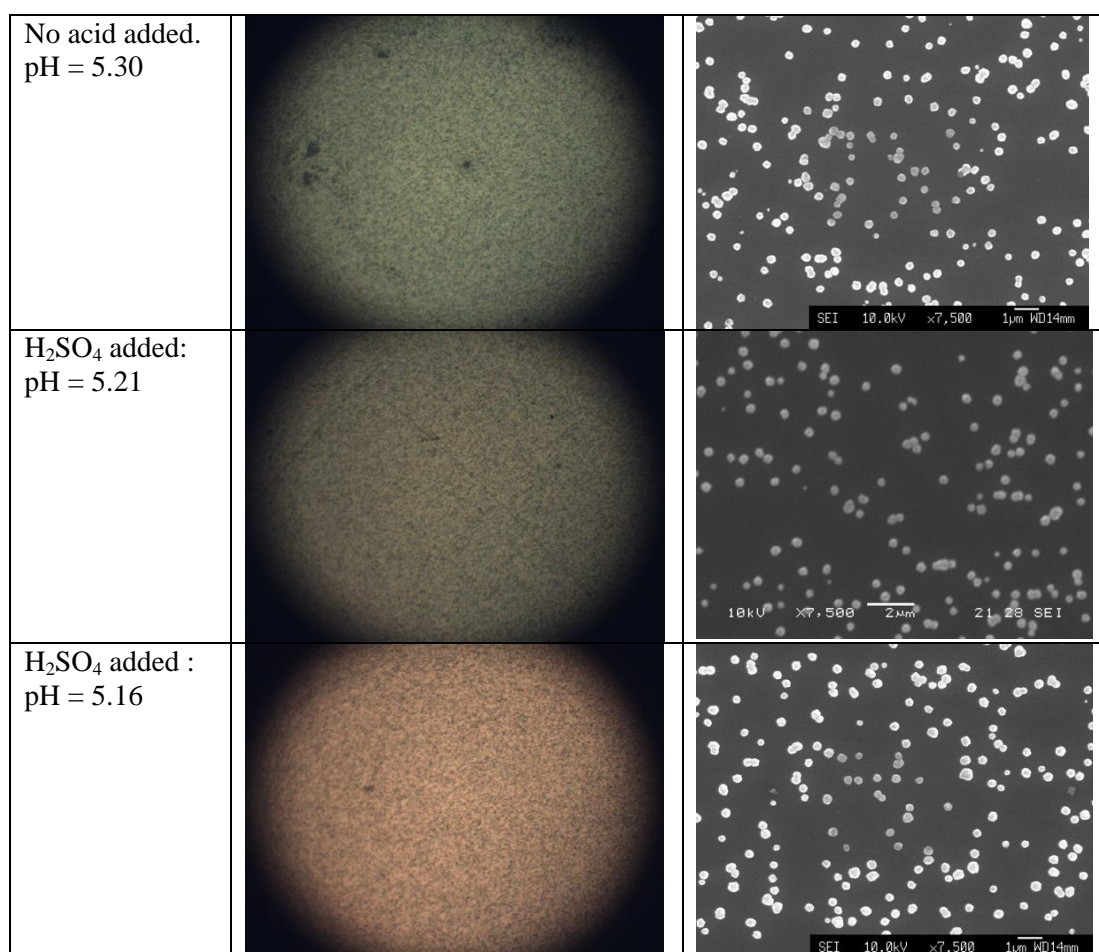


**Figure 21:** Comparison of PSS-ND immersion time for a silicon substrate coated with cationic polymer. Left: Optical microscopy images ( $\times 50$ ). Right: SEM images ( $\times 7500$ ).

No real change in the nanodiamond nucleation density was noted with either increasing or repeated immersion in PSS-ND dispersion. This reinforces earlier conclusions that electrostatic interactions occur very fast and do not require extended immersion times in order to be successful. Therefore, it was deemed that a 1 h immersion is sufficient for successful nanodiamond particle nucleation.

## 9.4.2 Effects of PSS pH on nanodiamond nucleation density.

Electrostatic attractions between the PDDA and PSS polymers are due to the exposed charges along their chains ( $N^+$  and  $SO_3^-$  respectively). As such, the ionic interactions may be affected by the concentration of  $H^+$  ions present in the solution (pH). A range of 10% wt. PSS samples were produced with the pH adjusted through adding drops of  $H_2SO_4$  and  $HNO_3$ . Two different acids were used to determine if the conjugate ions affected the extent of electrostatic attraction. Only decreases in pH were examined, due to the recommendation in previous literature of conducting self-assembly experiments at pH = 4-5.



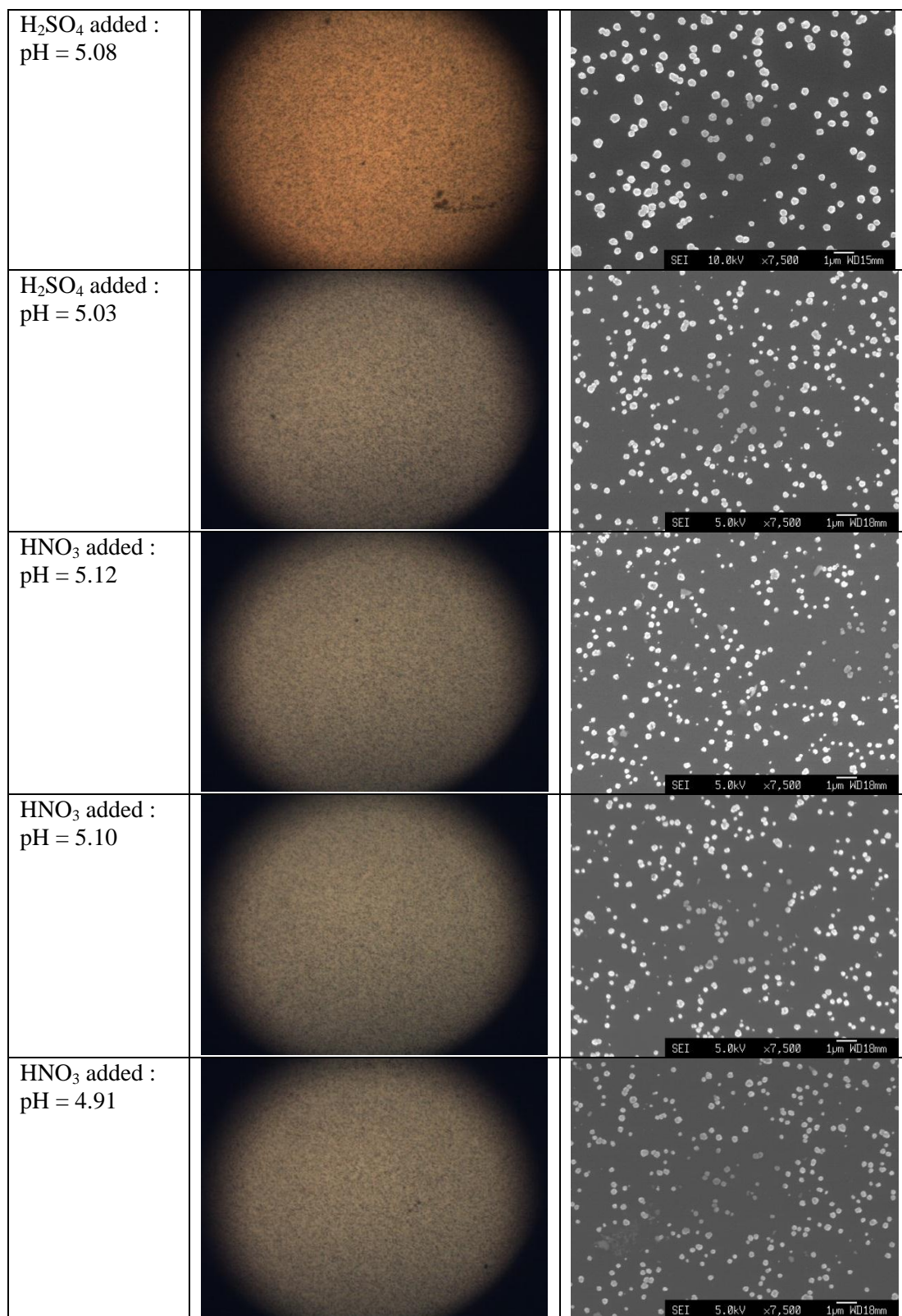


**Figure 22:** Comparison of the density and uniformity of self-assembled surfaces nucleated using 10% wt. PSS, 0.5% ND solutions at varying pH. Left: Optical Microscopy ( $\times 50$ ). Right: SEM imaging ( $\times 7500$ ).

No noticeable difference in nanodiamond particle density or uniformity was apparent when varying amounts of H<sub>2</sub>SO<sub>4</sub> and HNO<sub>3</sub> were added to the PSS-ND dispersion. However, it was noted that when acid was added to a PSS-ND solution, the zeta potential became less distinct with no clear

peak. This indicates that the PSS chains are forming different conformers and becoming less stable. From this data it was concluded that for improved stability of polymer mixtures acid should not be added.

For all solutions, the z-average of nanodiamond particles contained within the solution was also measured (see **Appendix 11.4** for data). No trend in z-average was noted and a mean average PSS-ND aggregate diameter of 509.05 nm ( $\sigma = 22.26$  nm) was calculated. The lack of a trend in the z-average indicates that the increased concentration of  $H^+$  ions is not encouraging agglomeration of nanodiamond particles.

### 9.4.3 Changing nanodiamond particle concentration within the PSS-ND dispersion

The concentration of nanodiamond dispersed in a 10 w/v % PSS solution was increased from 0.5 – 1.0% wt. Substrates nucleated in these solutions were grown for 5 min in a MWCVD reactor, keeping all other variables constant.

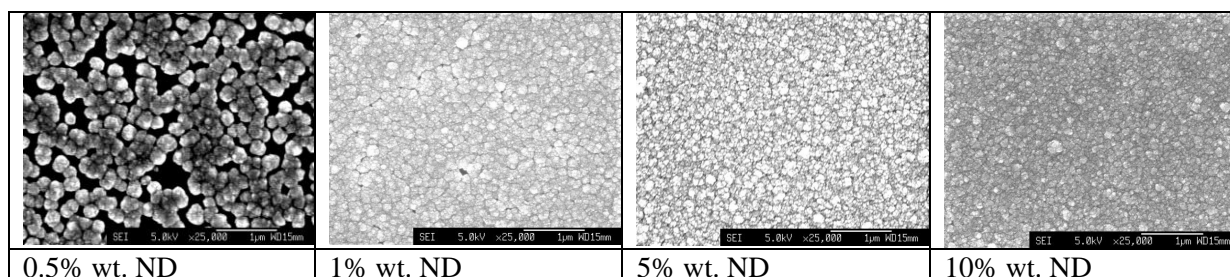


**Figure 23:** Concentration of nanodiamond particles within 10% wt. PSS solution varied to investigate effect on nucleation density. Images taken with SEM, magnification  $\times 25000$ . Further images in Appendix 11.5.

Changing the percentage of nanodiamond particulate within the PSS-ND dispersion had a large impact on the density of nucleated nanodiamonds. At 10% wt. ND a continuous film across the substrate was grown after 5 min deposition and indicating a high density of seeded nanodiamond particles. The 5% wt. ND sample also appears to be continuous at this magnification although areas of lower density can be seen at different magnification. Higher concentrations of nanodiamond particles were not investigated as 10% wt. ND produced a continuous film.

## 9.5 Investigations into washing methods after PSS-ND nucleation step

After the immersion in the PSS-ND dispersion, it is necessary that excess PSS-ND is thoroughly removed prior to MWCVD to produce a uniform diamond layer. Where the excess polymer was not

fully removed it was noted that the colour of CVD plasma changed and became more orange, and marks from the remaining polymer were noticeable on the substrate after the short deposition (see **Appendix 11.6**). Therefore, the solvent was chosen to maximise excess PSS removal without also removing PSS-ND bound to the Si surface. As the PSS was dispersed in DI water, all washing variations contained an initial DI water washing step for optimum polymer removal.

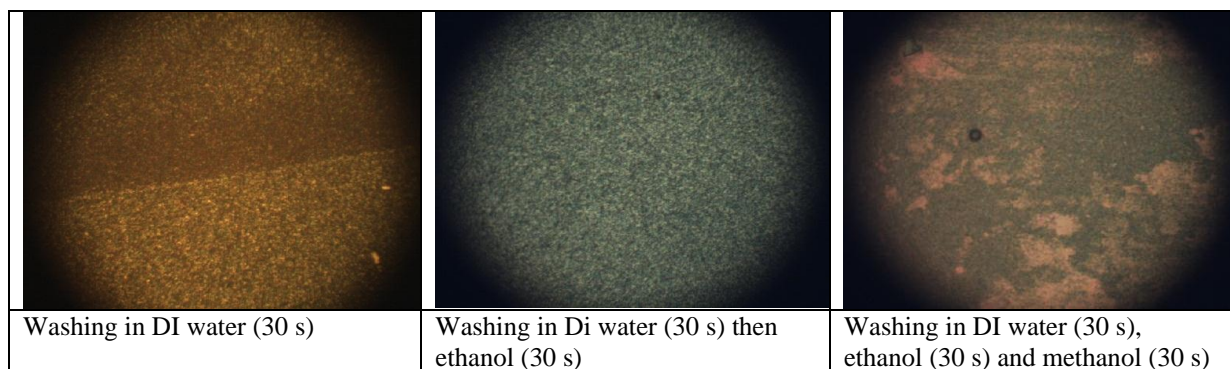


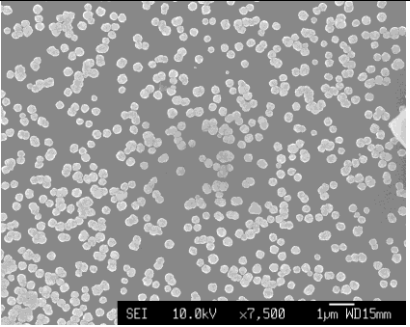
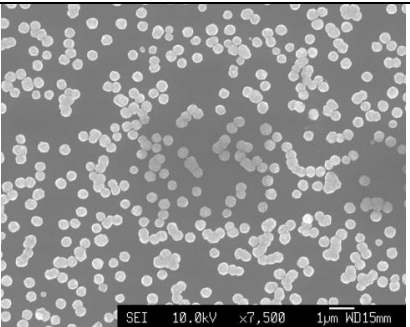
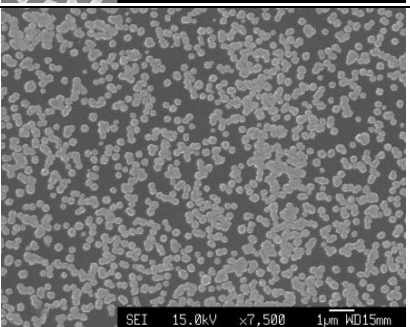
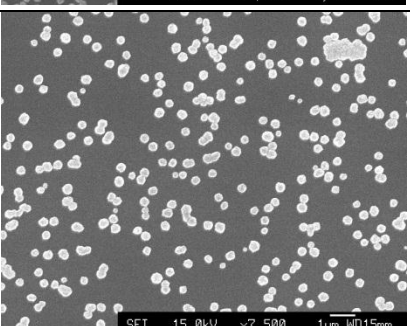
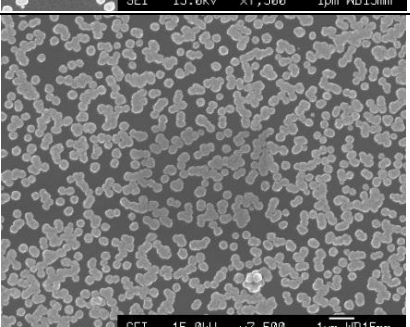
**Figure 24:** Comparison of differing washing methods after PSS immersion. Images taken using Optical microscopy ( $\times 50$ ). See **Appendix 11.7** for further images.

All three iterations gave a similar density of nanodiamond after deposition, indicating that the washing step does not significantly remove the seeded diamond, but instead removes solely the excess polymer. However, there is a wide variation in the uniformity of these samples observed with optical microscopy. In the case of DI water washing alone, the excess polymer appears to be only partially removed resulting in an uneven appearance when viewed at lower magnifications. When DI water washing is followed by ethanol washing, the sample shows both good uniformity and density. In the final sample, the washing method was extended using methanol. This has produced sections of the surface which have discoloured and show poor uniformity, indicating that this solvent removes too much of the nucleating layer.

The result of this comparison is that the self-assembled samples, after a 1 h immersion in ND-PSS dispersion, should be washed sequentially with DI water and ethanol.

## 9.6 Drying after both polymer immersions

The method of drying the substrates after each polymer immersions was looked at so that the best method could be chosen. It is important that drying methods do not affect the electrostatic interactions of either polymer by reacting with it and are not so vigorous as to remove attached particles or polymers. In this experiment pressurised  $N_2$  gas was compared with a pressurised air flow from an air compressor.

Drying method after PDDA	Drying method after PSS		
N <sub>2</sub> gas flow	Natural drying		
Natural drying	N <sub>2</sub> gas flow		
Natural drying	Air gas flow		
Air gas flow	Air gas flow		
N <sub>2</sub> gas flow	N <sub>2</sub> gas flow		

**Figure 25:** Comparison of differing methods for drying samples after immersion in cationic and anionic polymers. Left: Optical microscope images ( $\times 50$ ), right: SEM images ( $\times 7500$ ).

Two conclusions are apparent from the above data: firstly, wherever a natural drying step was used the uniformity of the resultant film decreased substantially. This is due to the solvents used to wash the substrate not drying evenly without the aid of a gas flow. Secondly, when a sample was dried with pressurised air, the density of the nucleated diamonds decreased. Air gas flow drying may introduce contaminants onto the surface of the substrate between polymer immersions. This would act to decrease electrostatic interactions, resulting in a decrease of nucleated nanodiamond particles. Therefore, for best uniformity and nucleation density the use of pressurised N<sub>2</sub> to dry samples after immersion in both PDDA and PSS is recommended.

## 9.7 Recommendation of a standard operating procedure

The above experimental results were collated to produce a standard operating procedure (SOP) for producing self-assembled ND nucleation layers on silicon samples with a high density of nanodiamond particles and good overall uniformity. This procedure is outlined below.

Using nitrile gloves and plastic tweezers to minimise damage, rinse a single Si substrate (1 cm<sup>2</sup>) with deionised water, acetone, ethanol and methanol sequentially, drying with N<sub>2</sub> between each rinse. Immerse the substrate in 10% wt. PDDA ( $M_w = 100000$  Da) aqueous polymer solution for 10 min. Shake off excess PDDA solution and wash in ethanol (40 s) before drying in N<sub>2</sub> flow (10 s). Immerse the PDDA-coated-substrate in a 10% wt. PSS ( $M_w = 70000$  Da) + 10% ND aqueous solution for 1 h. Finally, shake off excess PDDA, wash in DI water (30s), dry with N<sub>2</sub> (10s), wash in ethanol (30s) and dry in N<sub>2</sub> (10s) once more. The substrate should still be shiny and uniform in appearance at the end of this process. After the self-assembly nucleation process is completed, the nucleated substrate can be grown for 5 min in a MWCVD reactor with 500 cm<sup>3</sup> min<sup>-1</sup> H<sub>2</sub>, 35 cm<sup>3</sup> min<sup>-1</sup> CH<sub>4</sub>, 4 cm<sup>3</sup> min<sup>-1</sup> N<sub>2</sub>,  $P = 1$  kW and  $p = 110$  Torr to assess the process.

The repeatability of this SOP was confirmed using five separate silicon substrate. All five were shown to produce highly uniform continuous layers of nanodiamond particles (see **Appendix 11.8**).

### 9.7.1 Duration of deposition by MWCVD

A deposition time of 5 min is necessary in order to remove all traces of polymer and ensure a uniform finish. Where the above SOP has been conducted but deposition for only 3 min, a non-uniform film was produced, with swirls of polymer marks being noticeable under optical microscopy (see

**Appendix 11.9).** Therefore, in cases where a non-continuous film is required to assess the nucleation density, a decrease in methane concentration is recommended to slow the rate of deposition.

To achieve an estimation of the density of nucleated nanodiamond particles achieved by the SOP methodology, the quantity of CH<sub>4</sub> added to the MWCVD reactor was decreased from 35 to 15 cm<sup>3</sup> min<sup>-1</sup>. This acted to prevent the formation of a continuous film through decreasing the quantity of carbon radicals present in the reactor. The mean nucleation density using this method was calculated to be  $190 \times 10^{+7} \pm 5 \times 10^{+7}$  particles cm<sup>-2</sup>.

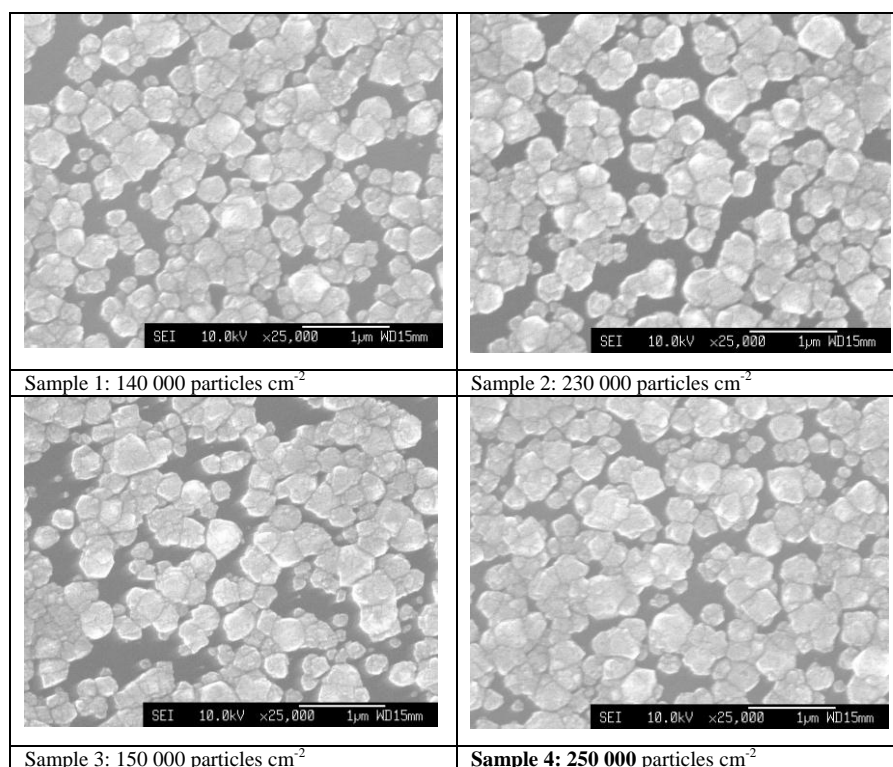


**Figure 26:** Mean density of nanodiamond particles produced using best-practice methodology

## 9.7.2 Diameter of diamond nanoparticles deposited after $t = 5$ min

The SOP method described above results in the formation of a continuous nanodiamond film after 5 min MWCVD deposition. This can make it impossible to estimate the nanoparticle diameter, as they have coalesced into a film. For this reason, diamond nanoparticle diameters have been measured using the above SOP but with a lower concentration of ND in the PSS-ND dispersion. This acts to decrease the density of nanodiamond particles seeded on the substrate, whilst maintaining the same diameter as it is determined by the length of deposition and the growth conditions. Using this method the mean diameter of diamond nanoparticles when using the self-assembly SOP was estimated as 301.9 nm after a deposition of  $t = 5$  min. ( $\sigma$ : 86.5 nm, range: 77 - 417.5 nm).

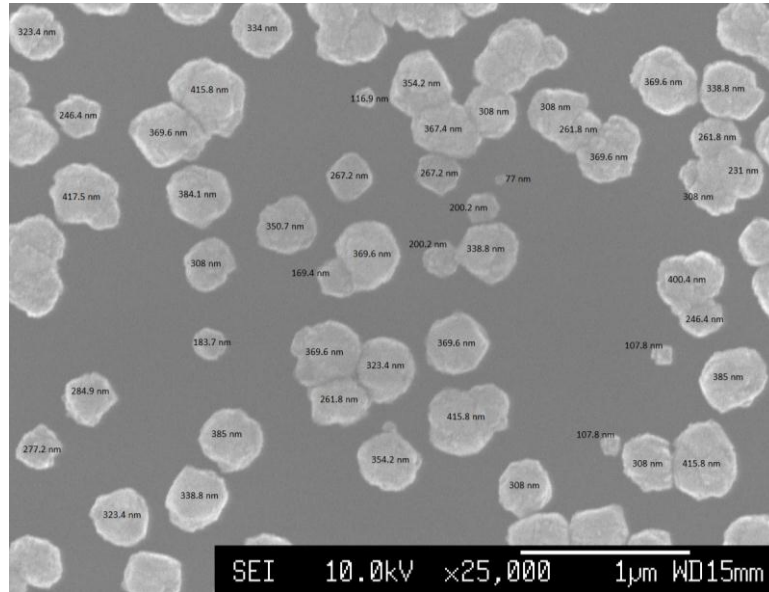


**Figure 27:** Measuring diameter of grown nanodiamond particles. Mean: 301.9 nm. Standard Deviation: 86.5 nm. Range: 77 – 417.5 nm

### 9.7.3 Thickness of continuous film deposited for $t = 5$ min

A high density of nucleated nanodiamond particles were produced on a silicon substrate using the above SOP method. This was then deposited on for 5 min by MWCVD in order to produce a continuous nanodiamond layer. To measure the thickness of the continuous film grown, the sample was cleaved using a laser machining system and the cross section imaged using SEM. The thickness of the continuous film was measured to be 300 nm.

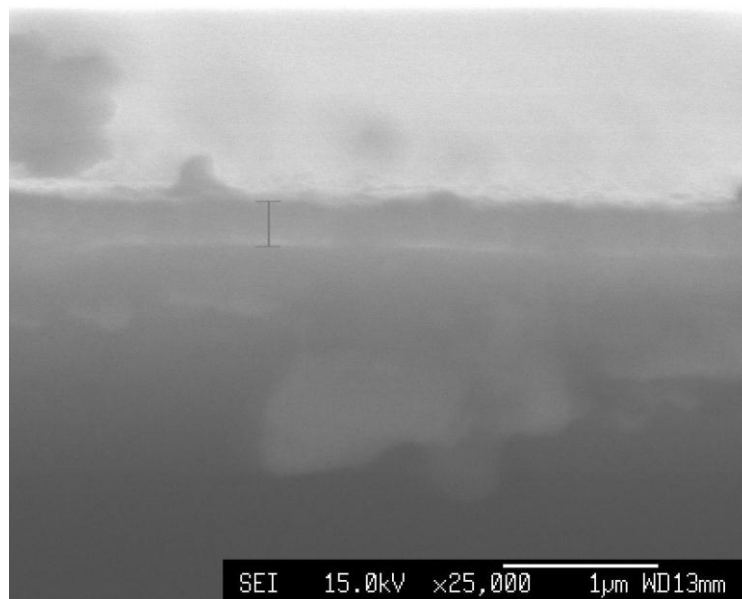


**Figure 28:** Thickness of continuous film grown using best practice methodology: 300 nm.

On comparison of film thickness to nanodiamond particle diameter (see **Section 9.7.2**), it was concluded that a monolayer has been successfully formed.

## 9.8 Alterations to the SOP when a resist coating is used for selected-area deposition

When producing refractive lenses from diamond, a silicon mould, etched with the kinoform or CRL design, is nucleated with nanodiamond particles. The top, un-etched surface of the silicon mould is protected with a resist during the self-assembly process and is removed prior to CVD. This selected-area deposition method ensures that only nanodiamond particles are present in the trenches of the silicon mould and are grown into a continuous nanodiamond film. Growth continues until a refractive lens structure is produced of the desired thickness. The diamond-coated mould structure is then removed from the MWCVD reactor and the silicon mould etched away. This leaves the nanocrystalline diamond layer in the shape of a refractive optical lens, ready to be tested on the DLS synchrotron x-ray source.

While the above SOP method was successful at nucleating 1 cm<sup>2</sup> silicon substrates, it was important to test it on substrates with a resist layer if it is to be used in the fabrication of refractive lenses. The resist used in these investigations was UV111 which is easily removed using acetone, ethanol or methanol. For that reason, all cleaning steps (including the initial silicon wash) were done using DI water alone. The resist was then removed after the self-assembly SOP was completed with a 10 s immersion in acetone in an ultrasonic bath before the MWCVD step.



## 10. Future work

In the future it is hoped that the methodology described above will be successful in fabricating high-density, nanodiamond, refractive lenses capable of focusing x-ray beams, where  $E > 15$  keV and where current optics are no longer viable, to sharp focal points with a short focal length. For this to occur, a better signal-to-noise ratio and narrower focal width must be achieved. This will be completed by producing lenses with fewer aberrations and shorter focal lengths. It is possible to create lenses with fewer surface aberrations by nucleating lens moulds with a higher density of nanodiamond particles, as described within this report. In the near future, this SOP is to be used to grow diamond kinoform lenses suitable for testing with x-ray beams.

Improvements of the kinoform design are currently being conducted, with the aim of producing Si moulds with deeper trenches. These will result in the fabrication of thicker nanocrystalline diamond structures being possible, and so allowing a greater x-ray aperture. This new diamond kinoform design, along with the selected-area deposition, self-assembly SOP developed in the course of this project, is to be tested by producing a new generation of lenses to be analysed at the DLS synchrotron B16 beamline.



## 11. Conclusion

Experiments were conducted to increase the density of nanodiamond particles nucleating a 1 cm<sup>2</sup> silicon substrate using an electrostatic self-assembly process. Electrostatic interactions were optimised by adjusting the experimental parameters to improve uniformity of attractive forces between the silicon surface, the cationic polymer coating, and nanodiamond particles present in an anionic polymer dispersion.

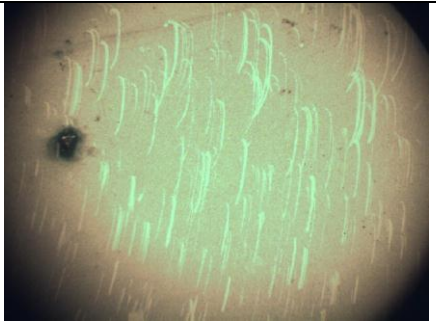
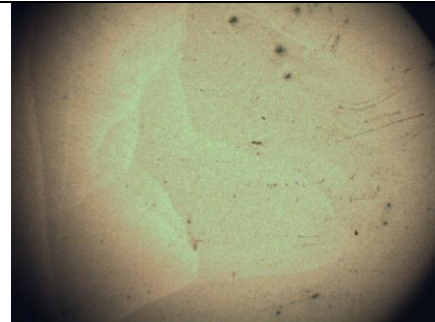
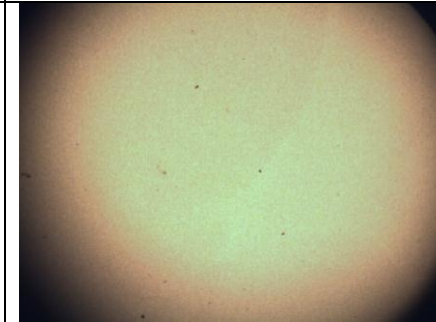
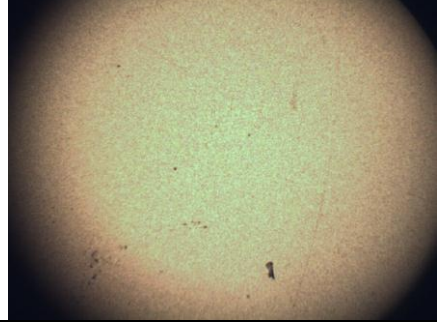
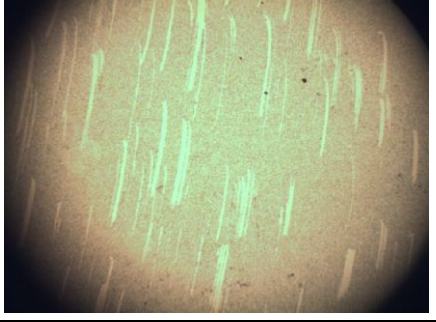
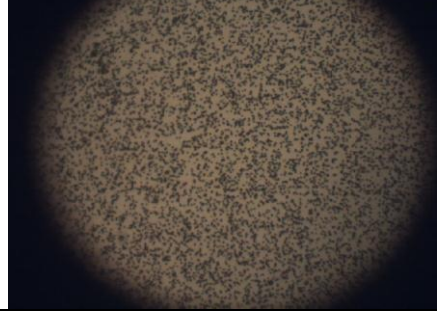
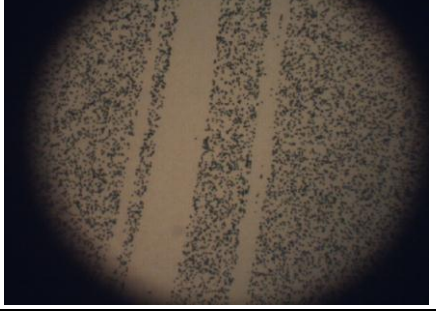
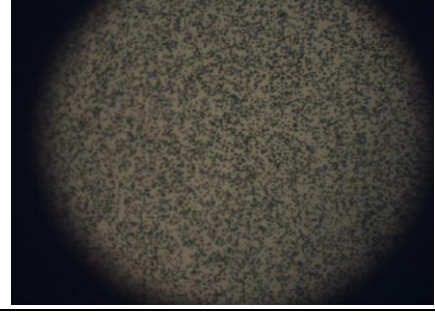
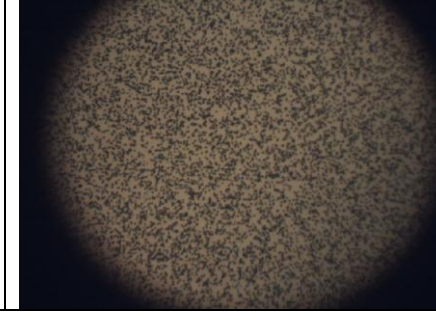
A best practice, repeatable SOP was developed and samples achieved a uniform density of  $190 \times 10^7 \pm 5 \times 10^7$  particles cm<sup>-2</sup> for short depositions where  $t < 5$  min and a continuous film thickness of 300 nm for  $t = 5$  min.

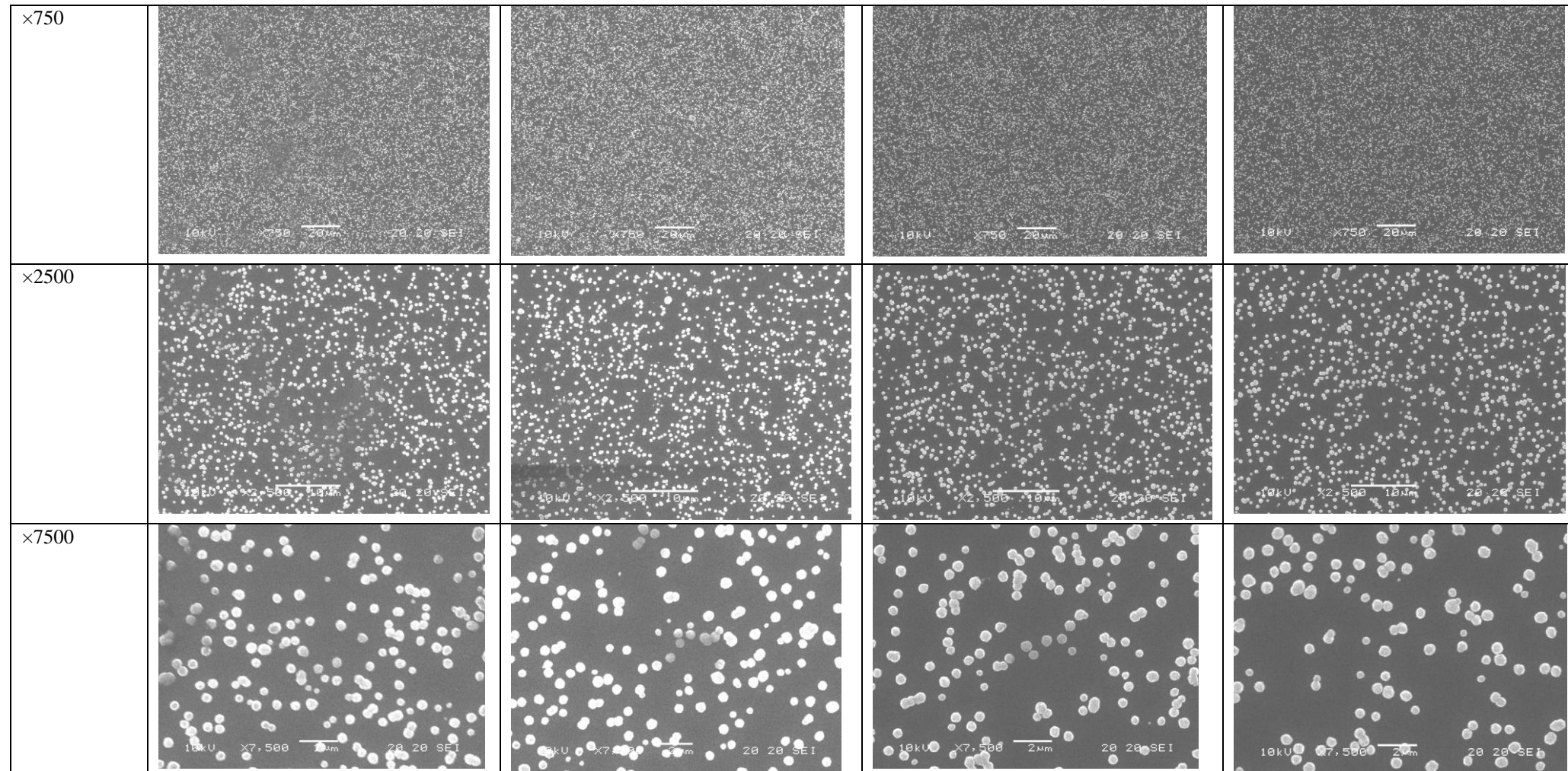
The method was further adapted for the selected-area nucleation of nanodiamond particles onto silicon substrates with a resist. In the future, this method will be used for producing refractive lenses using a silicon mould partially coated with a resist. Nanocrystalline diamond refractive lenses, such as kinoforms and compound refractive lenses will be used for focusing x-ray beams with decreasing focal spots, higher transmission and reduced aberrations.



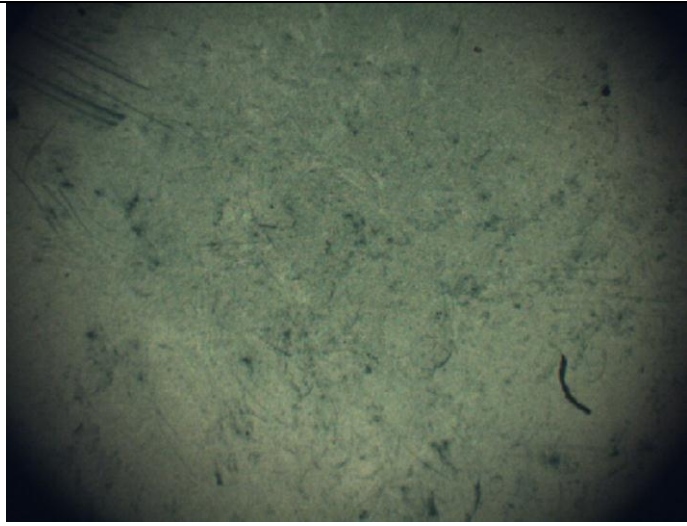
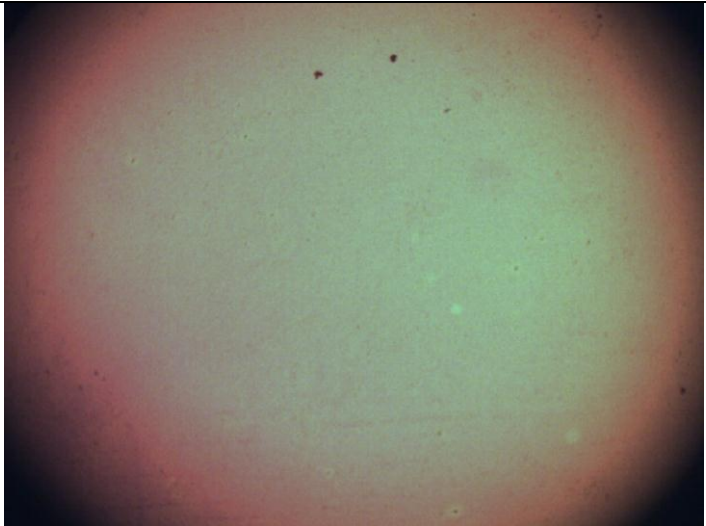
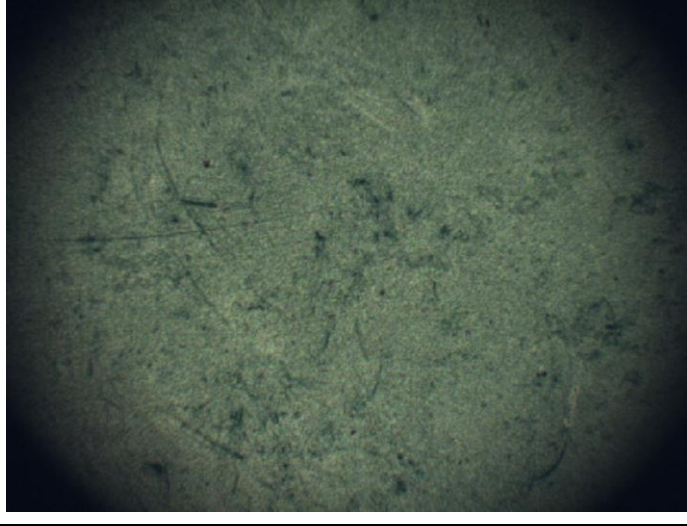
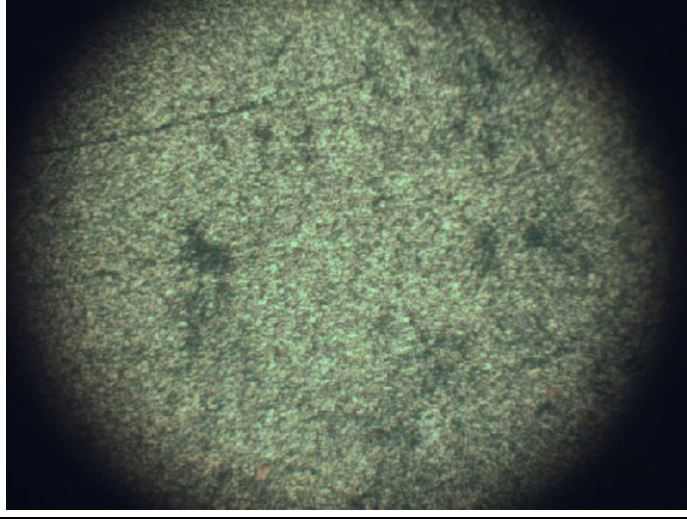
# 11. Appendices

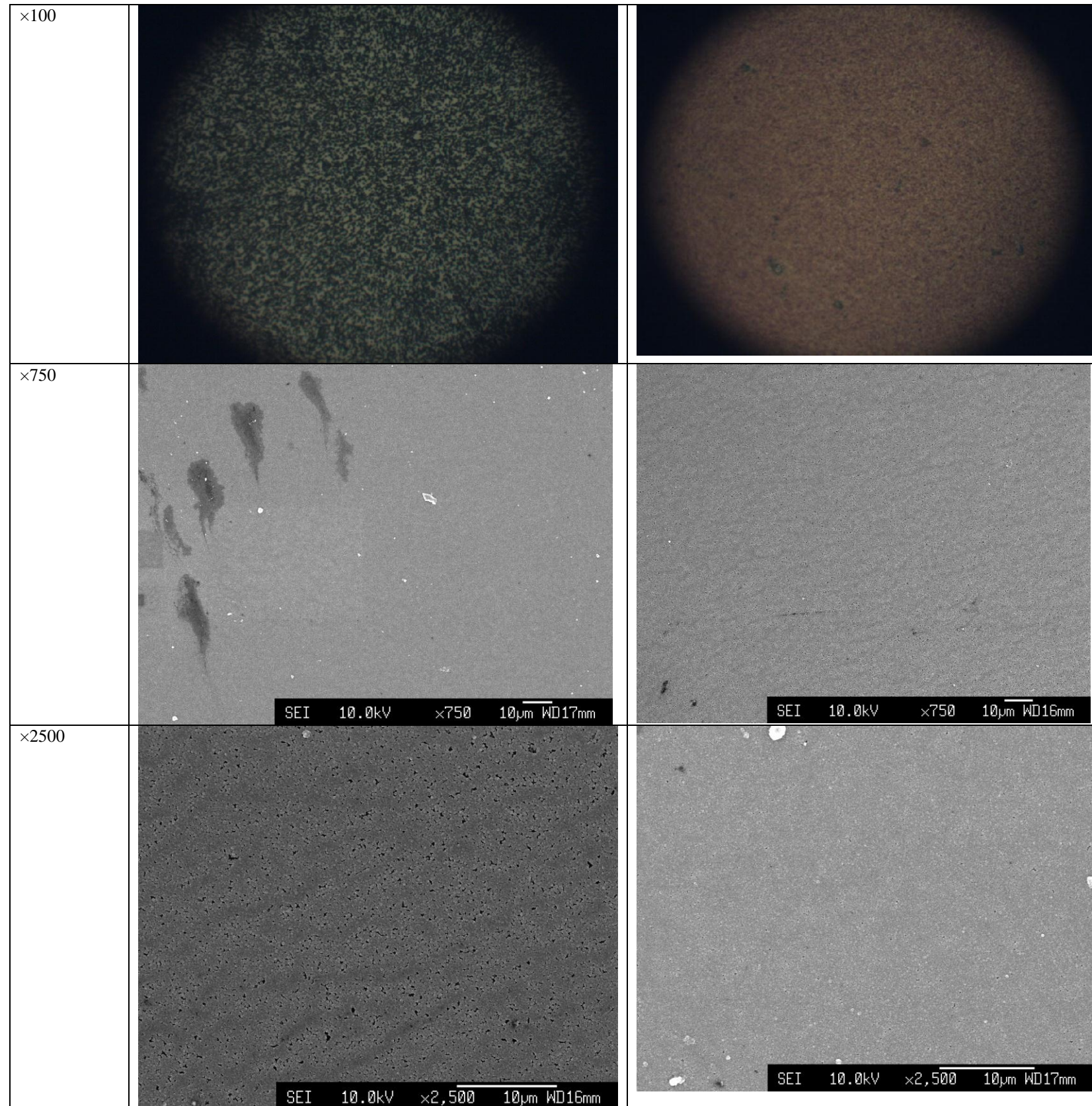
## 11.1 Cleaning Methods

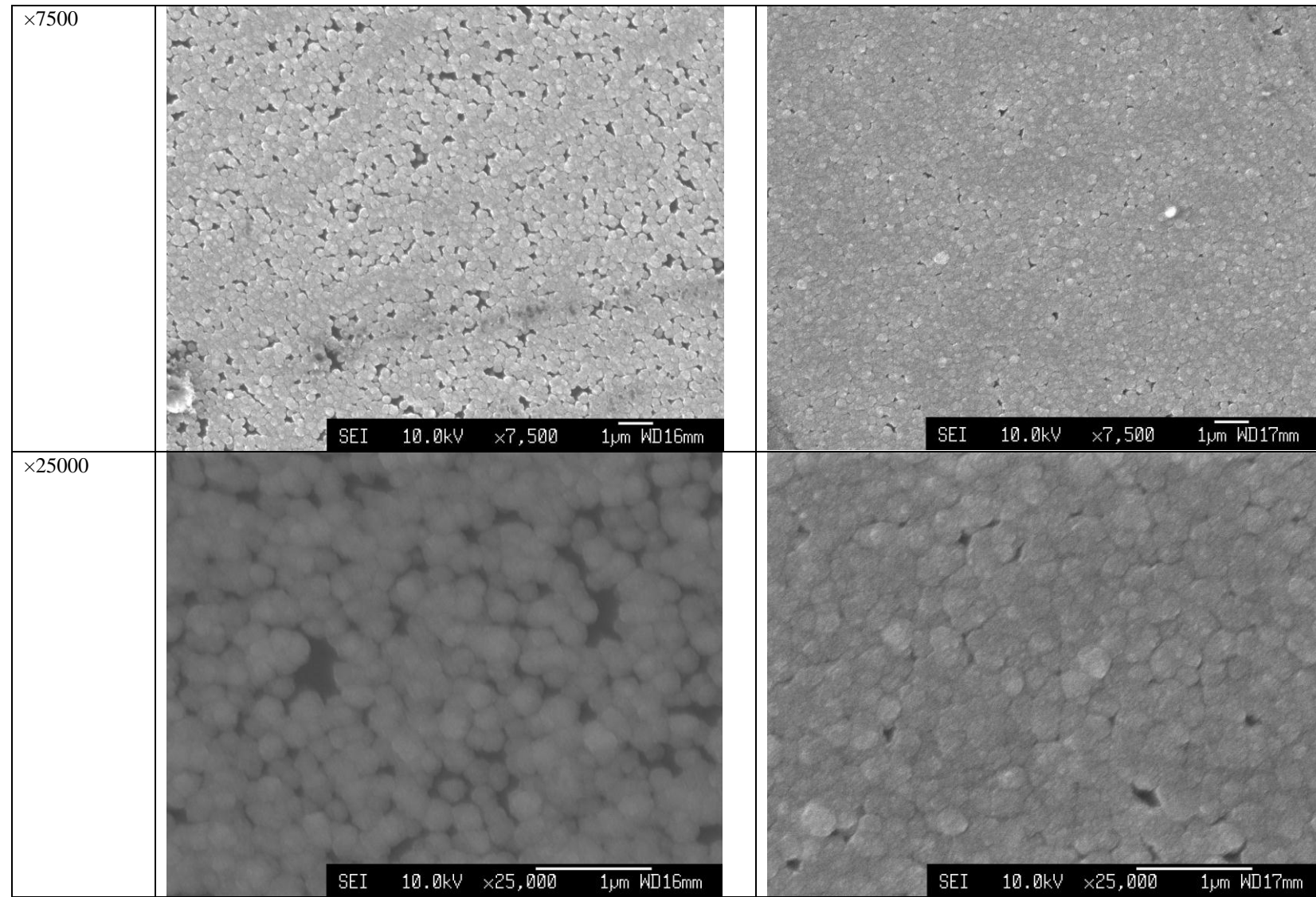
Magnification	Method 1	Method 2	Method 3	Method 4
×5				
×10				
×50				
×100				



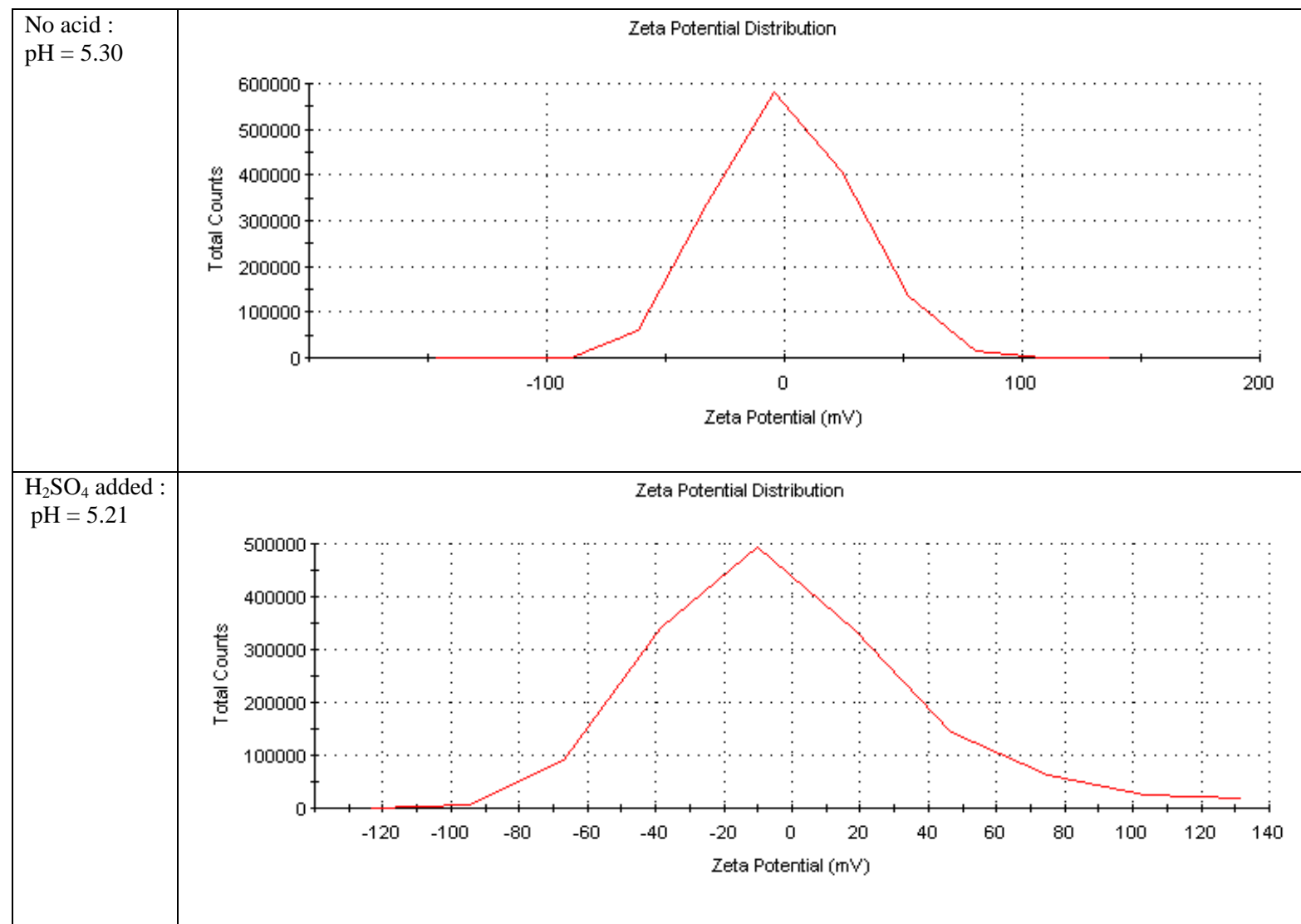
## 11.2 Comparison of PDDA and PEI cationic polymers

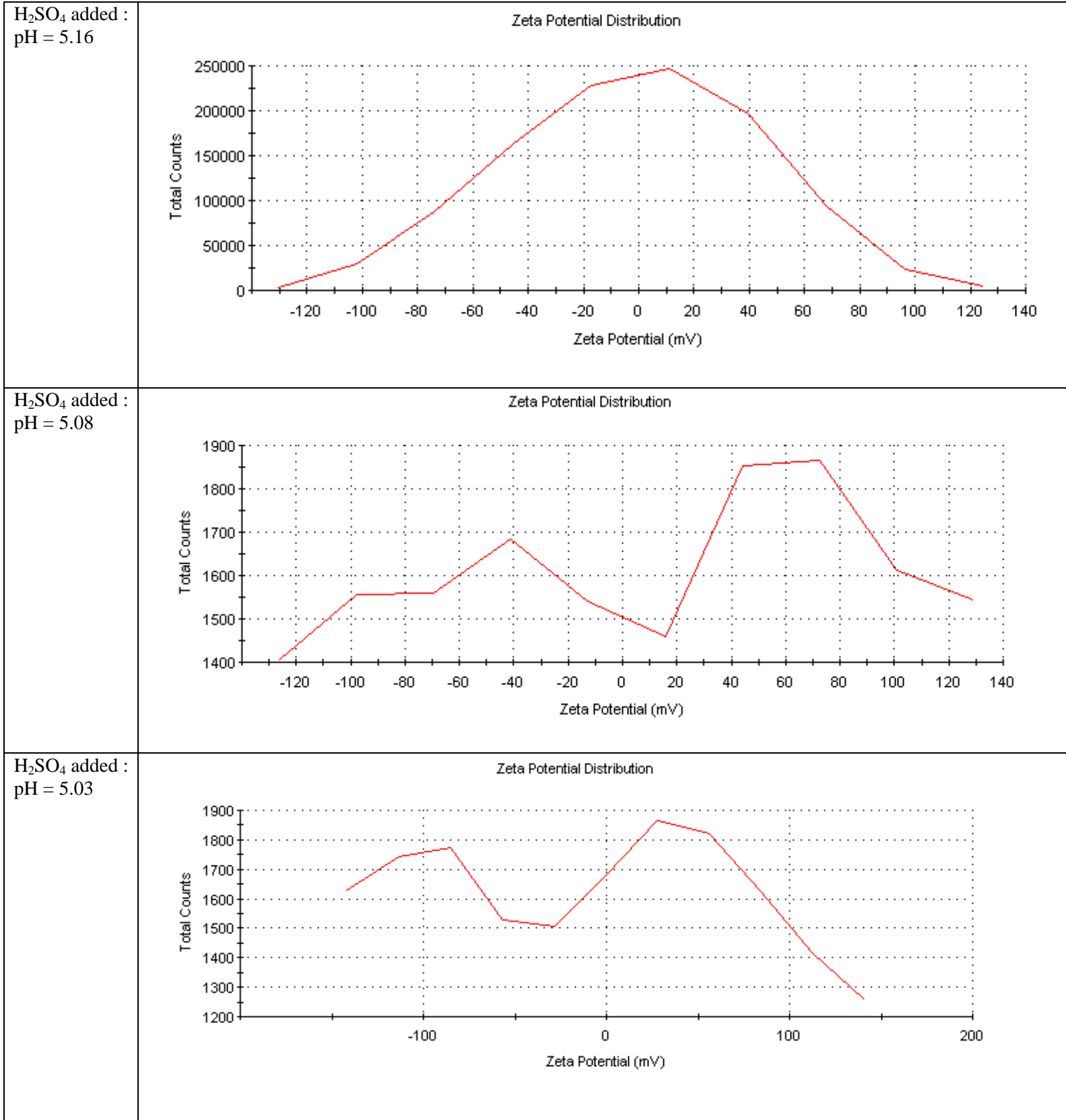
Magnification	10% wt. PEI immersion	10% wt. PDDA immersion
×5		
×10		
×50		

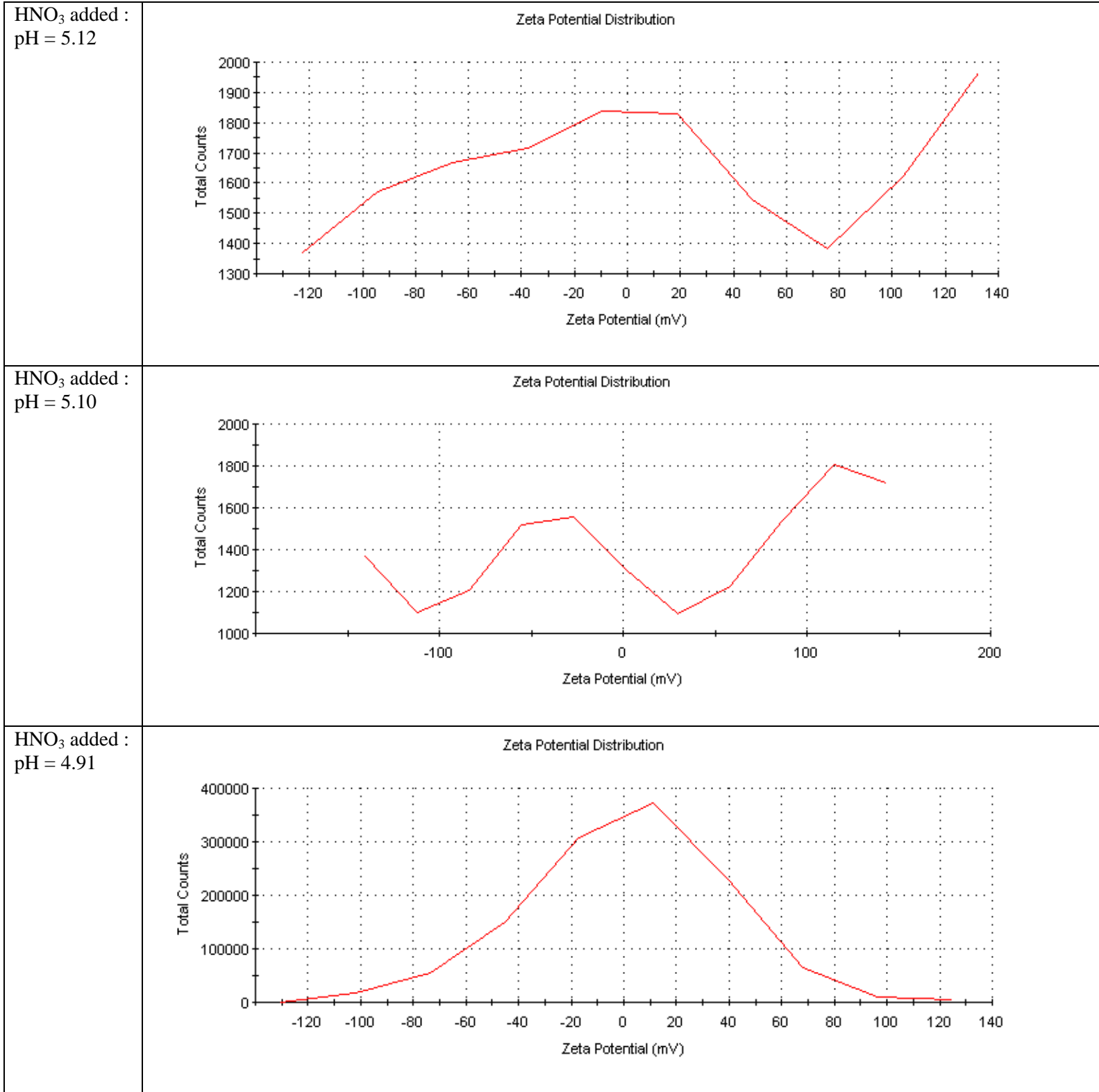




### 11.3 Effects of PSS pH: Zeta potential graphs



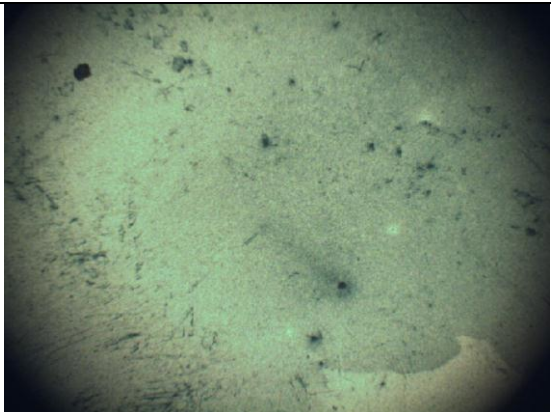
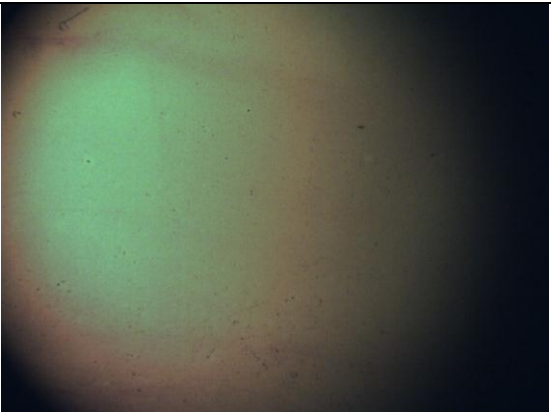
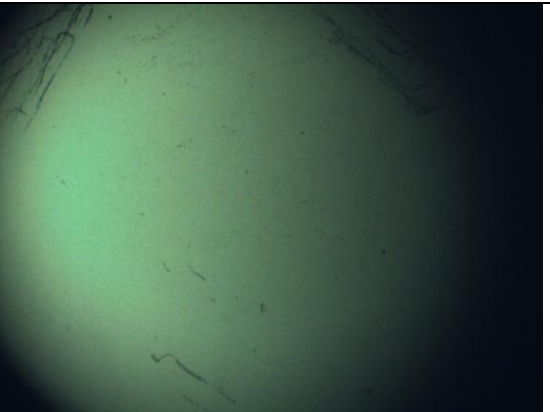
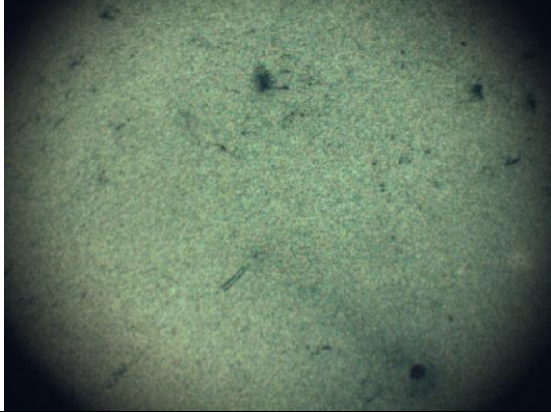
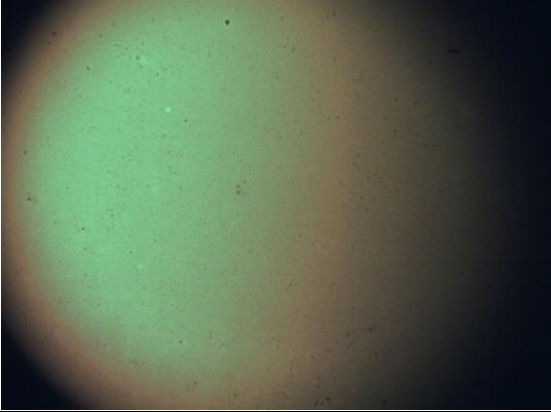
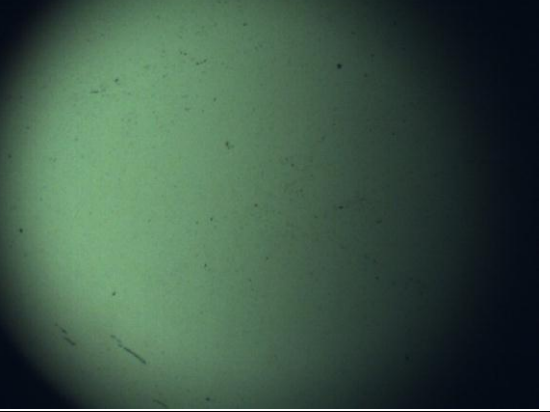


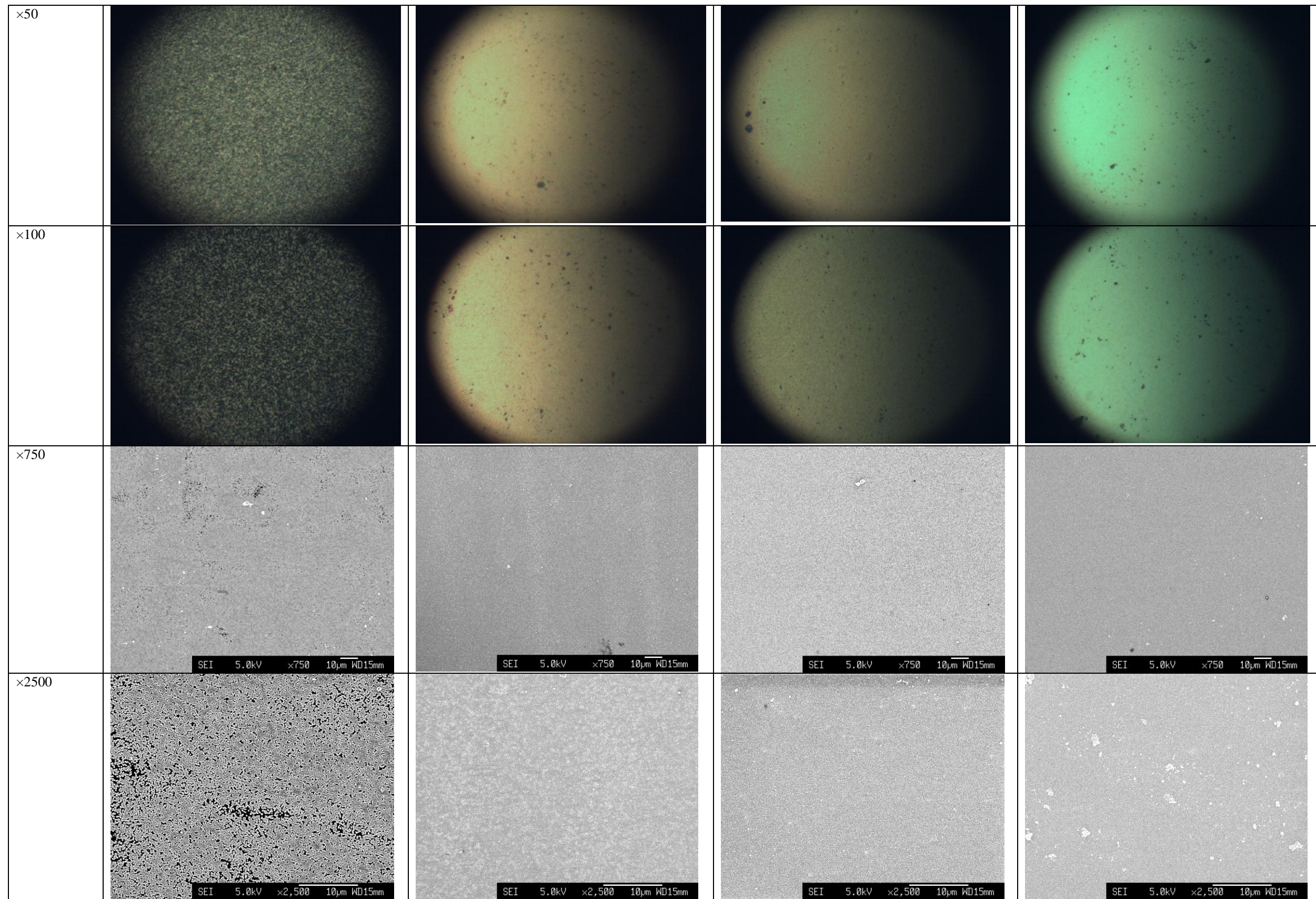


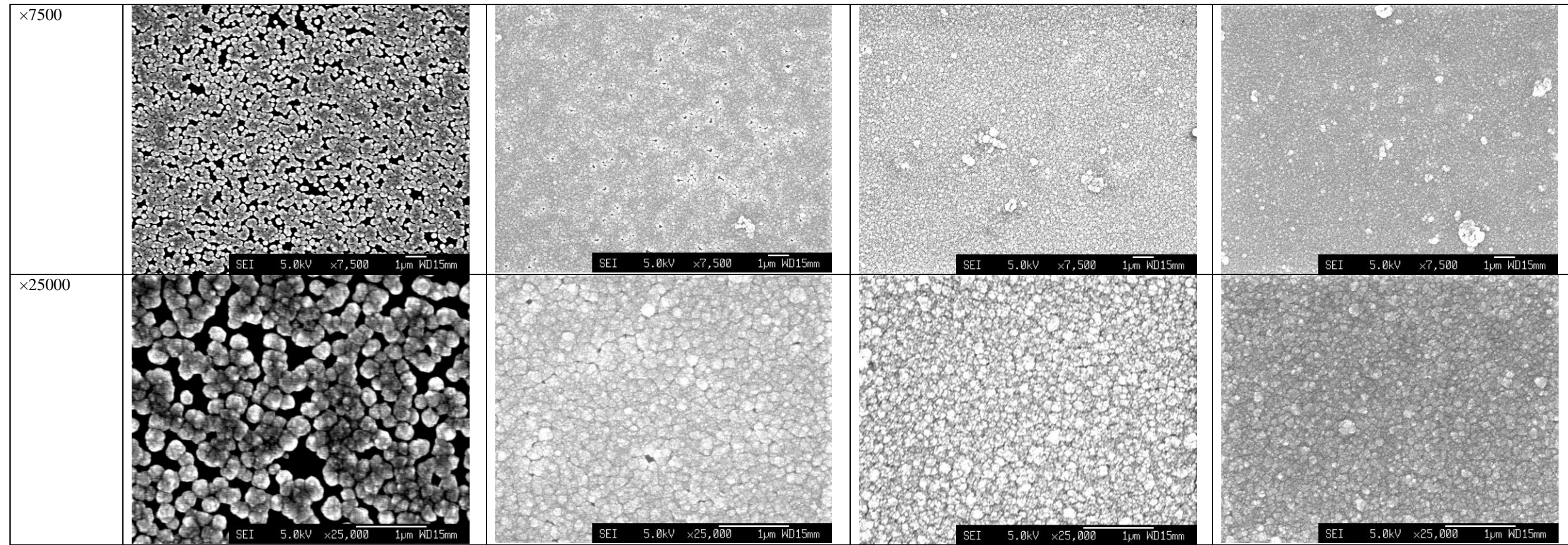
**11.4 Variations in z-average with changing pH**

pH of 10% wt. PSS, 0.5% ND in water	z-average (nm)
5.30	506.9
5.21	528.4
5.16	503.0
5.08	519.0
5.03	482.6
5.12	548.6
5.10	484.7
4.91	499.2

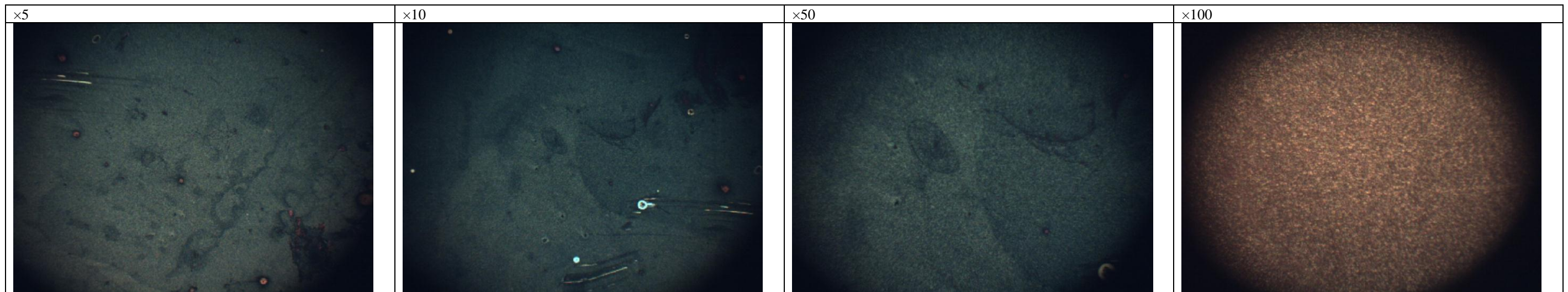
**11.5 Increasing concentration of nanodiamonds within 10% wt. PSS polymer solution**

Magnification	0.5% Nanodiamond	1% Nanodiamond	5% Nanodiamond	10% Nanodiamond
×5				
×10				

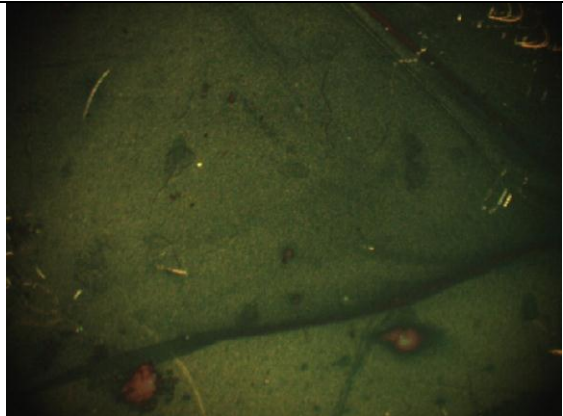
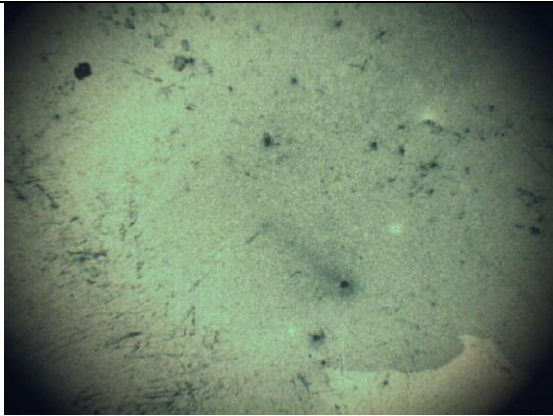
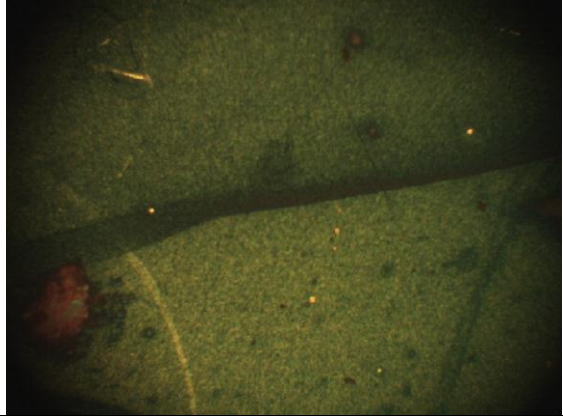
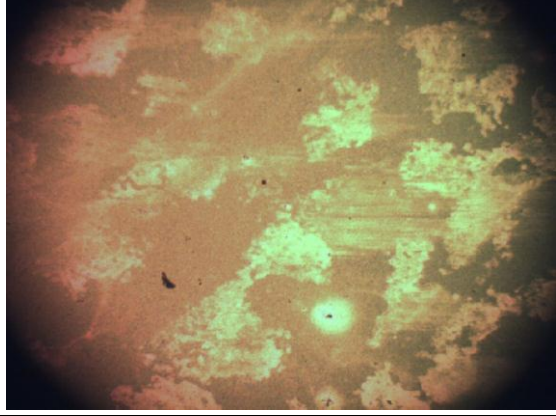
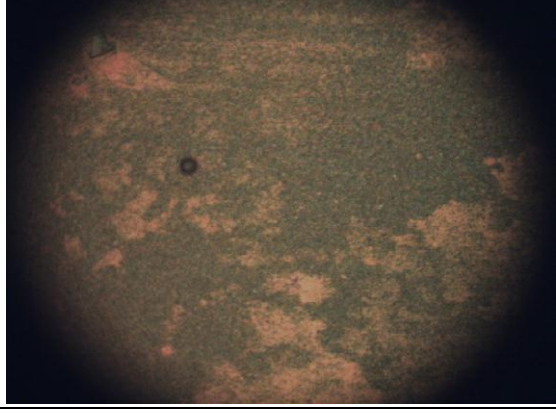


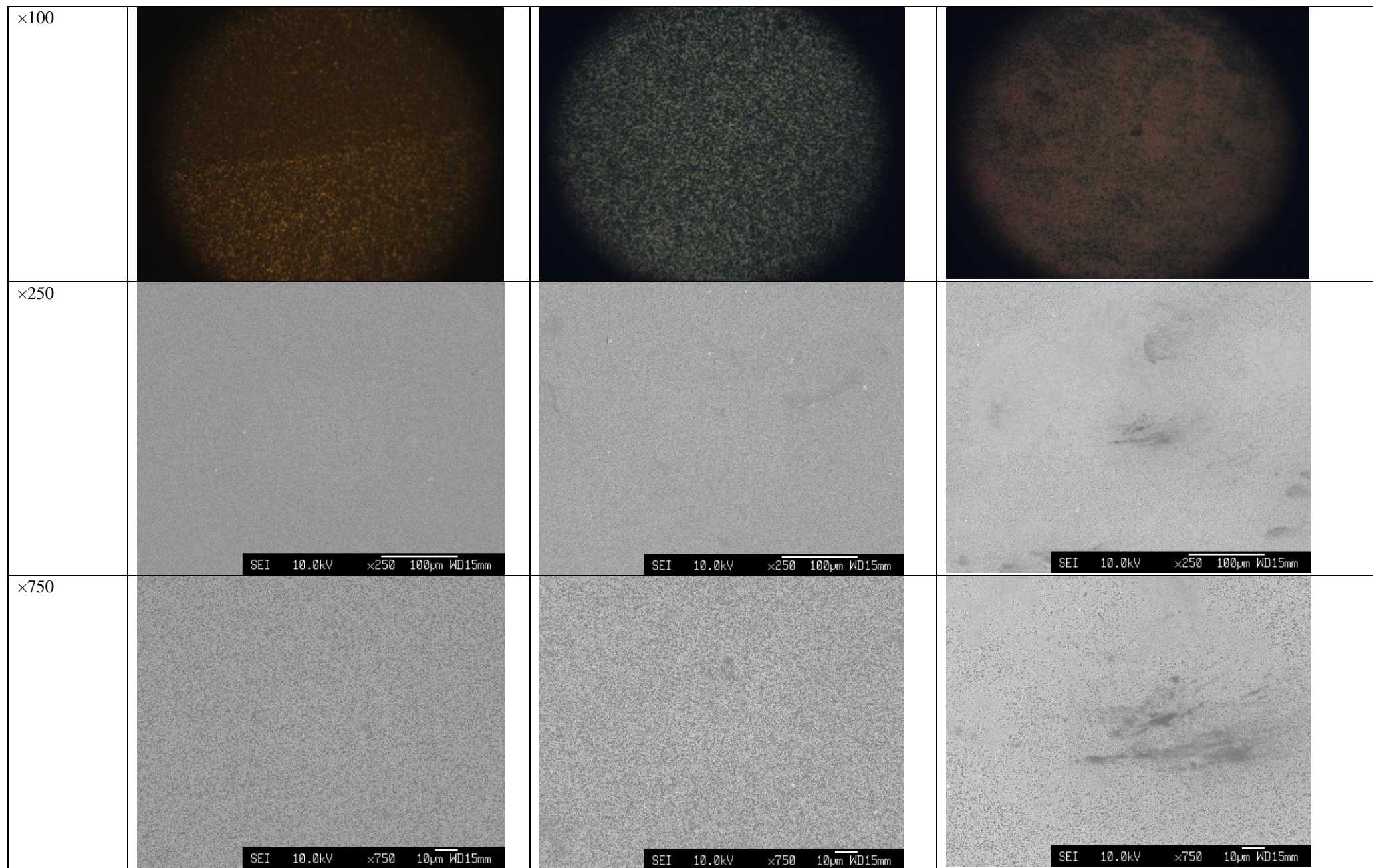


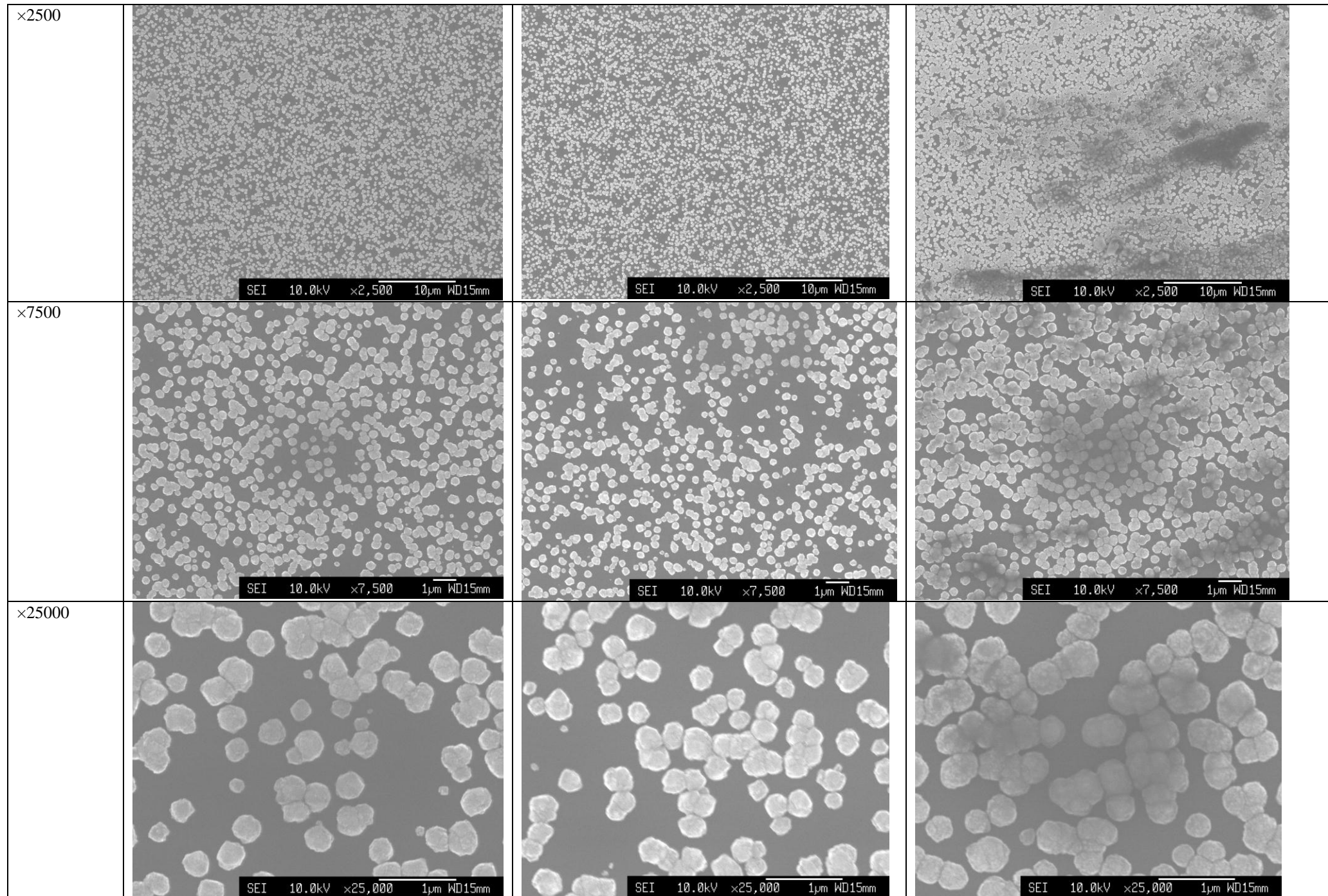
**11.6 Insufficient removal of PSS polymer, prior to growth**



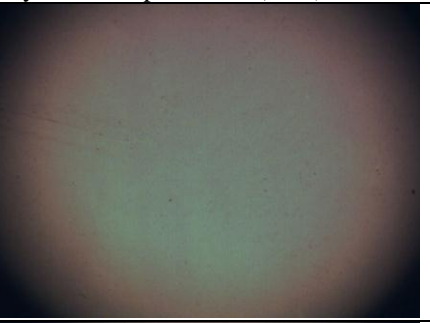
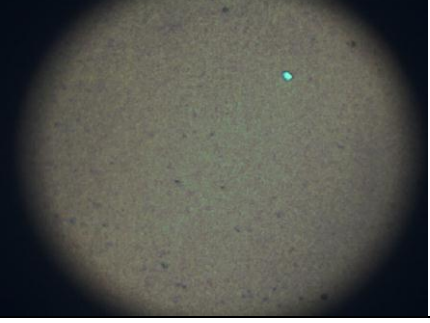
11.7 Investigations into washing methods.

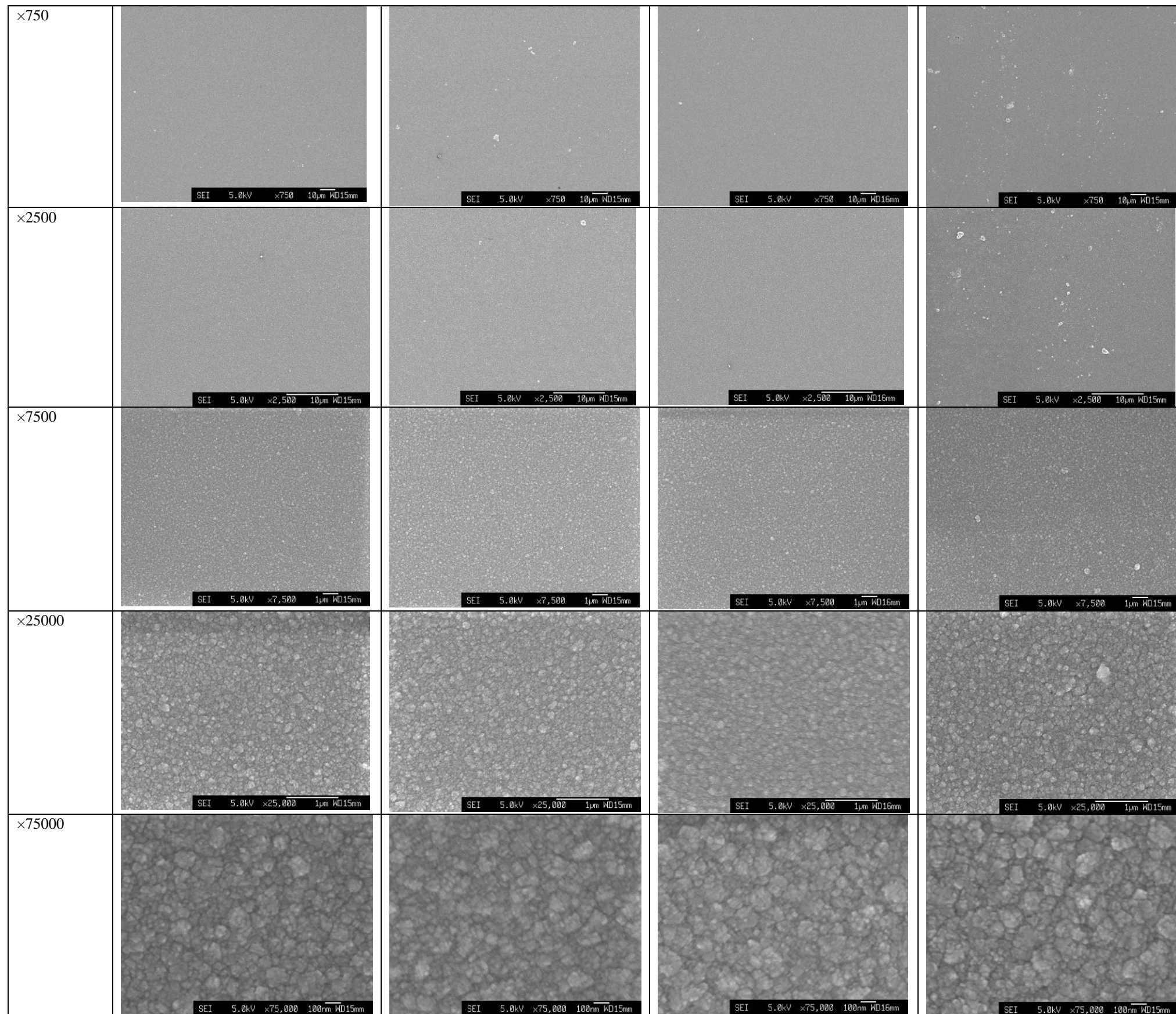
Magnification	DI water rinse (30 s)	DI water rinse (30 s) & Ethanol rinse (30 s)	DI water rinse (30 s), Ethanol rinse (30 s) & Methanol (30 s)
×5			
×10			
×50			



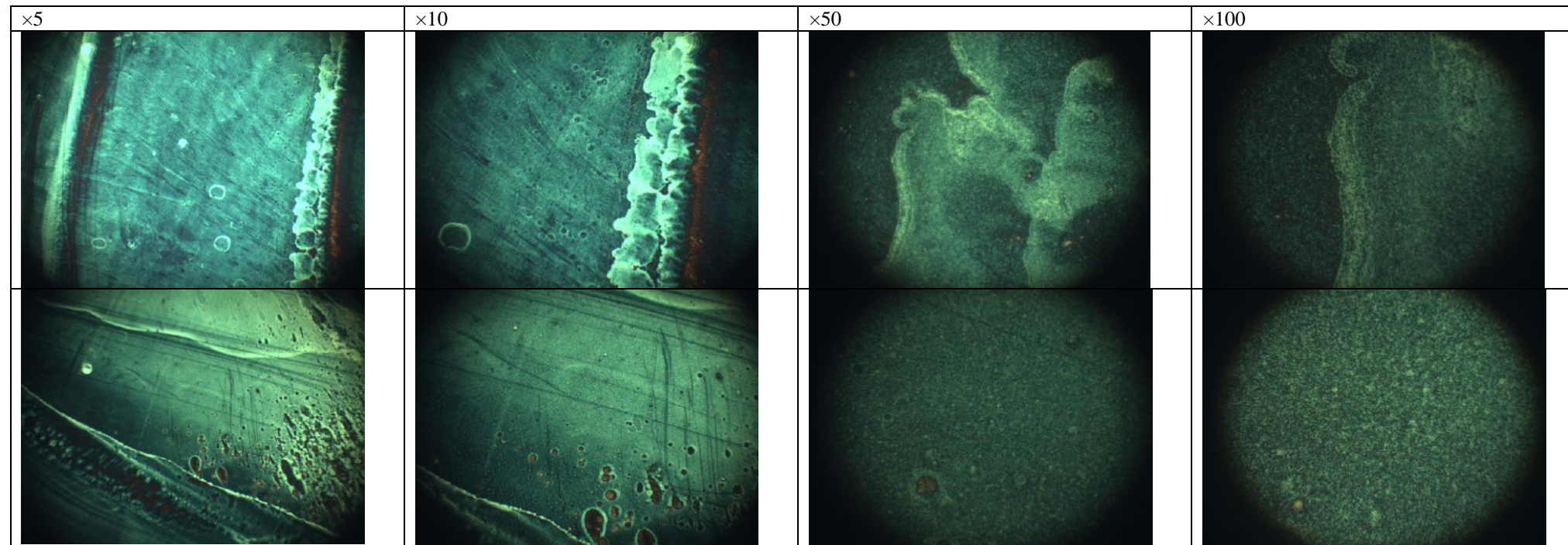


11.8 Recommendation of a standard operating procedure – showing repeatability of the process

Magnification	All samples have undergone exactly the same procedure (SOP)			
×5				
×10				
×50				
×100				



11.9 Insufficient growth within a MWCVD (3 min)



# References

- 
- <sup>1</sup> Hershey, W., *The Book of Diamonds*, Hearthsides Press (1940) 22.
  - <sup>2</sup> McCarthy, J.R., *Fire in the Earth: the story of the diamond*. Ch. 12: Diamond Superstition. Harper & Brothers (1942) 3.
  - <sup>3</sup> Bain & Company, Inc., *Diamond Industry Report*, Bain & Company, Inc. and Antwerp World Diamond Centre (2011).
  - <sup>4</sup> Stratford, J., *A Dictionary of Western Alchemy*. Theosophical Publishing House (2011) 4
  - <sup>5</sup> Holmberg, K., Matthews, A., *Coatings Tribology: Properties, Mechanisms, Techniques and Applications in Surface Engineering*, Elsevier (2009) 263.
  - <sup>6</sup> US Geological Survey, *Minerals Yearbook: Volume 1: Metals and Minerals: 2008*. Government Printing Office (2011) 21.
  - <sup>7</sup> Askeland, D.R., Fulay, P.P., Wright, W.J., *The Science and Engineering of Materials*, Cengage Learning (2010) 44.
  - <sup>8</sup> Keer, H.V., *Principles of the Solid State*, New Age International Publishers (1993) 122.
  - <sup>9</sup> Zaitsev, A.M., *Optical Properties of Diamond: A data handbook*, Springer (2001) ix.
  - <sup>10</sup> Tulansky, S., *The History and Use of Diamond*, Taylor & Francis (1962) 43.
  - <sup>11</sup> Davidson, J.L., *Diamond Materials VI*, The Electrochemical Society (2000) 226.
  - <sup>12</sup> Dismukes, J.P., Ravi, K.V., *Proceedings of the Third International Symposium on Diamond Materials*, The Electrochemical Society (1993) 881.
  - <sup>13</sup> Barnard, A.S., *The Diamond Formula: Diamond Synthesis – a Gemmological Perspective*, Butterworth-Heinemann (2000) 51.
  - <sup>14</sup> Nebel, C., Ristein, J., *Thin-Film Diamond II, Semiconductors and Semimetals Volume 77*, Academic Press (2004) 221.
  - <sup>15</sup> Holleman, A.F., Wiberg, E., Wiberg, N., *Inorganic Chemistry*, Academic Press (2001) 785.
  - <sup>16</sup> Hill, G., Holman, J., *Chemistry in Context*, Nelson Thornes (2000) 124.
  - <sup>17</sup> Bundy, F.P., *Journal of Geophysical Research*, **85** (1980) 6930.
  - <sup>18</sup> [http://www.cleanroom.byu.edu/EW\\_orientation.phtml](http://www.cleanroom.byu.edu/EW_orientation.phtml)
  - <sup>19</sup> Goindaraju, N., Das, D., Kosel, P.B., Singh, R.N., *ECS Transactions*, **33** (2010) 155.
  - <sup>20</sup> Shendervoa, O.A., Gruen, D.M., *Ultrananocrystalline Diamond: Synthesis, Properties and Applications*, William Andrew (2012) 77.
  - <sup>21</sup> Swain, G.M., *Thin-Film Diamond II*, Academic Press (2004) 133.
  - <sup>22</sup> Schroer, C.G., Kurapova, O., Patommel, J., Boye, P., Feldkamp, J., Lengeler, B., Burghammer, M., Riekel, C., Vincze, L., van der Hart, A., Kuchler, M., *App. Phys. Lett.* **87** (2005) 124103.
  - <sup>23</sup> Thibault, P., Elser, V., Jacobsen, C., Shapiro, D., Sayre, D., *Acata Crystallogr A* **62** (2006) 248.
  - <sup>24</sup> Newton, M.C., Leake, S. J., Harder, R., Robinson, I.K., *Nature Mater.* **9** (2009) 120.
  - <sup>25</sup> Song, C., et al. *Phys. Rev. Lett.* **100** (2008) 025504.
  - <sup>26</sup> Mancuso, A.P., Williams, G.J., *Nature Photonics* **6** (2012) 574.
  - <sup>27</sup> Lee, R.E., *Scanning electron microscopy and x-ray microanalysis* PTR Prentice Hall (1993) 124.
  - <sup>28</sup> Porterfield, W.W., *Inorganic Chemistry* Academic Press (2013) 10.
  - <sup>29</sup> Shima-Edelstein, R., Gouzman, I., Hoffman, A., *Carbon* **39** (2001) 337.
  - <sup>30</sup> Chakk, Y., Brener, R., Hoffman, A., *App. Phys. Lett.* **66** (1995) 2819.
  - <sup>31</sup> Reinke, P., Oelhafen, P., *J. Appl. Phys.* **84** (1998) 2612.
  - <sup>32</sup> Tang, Y., Aslam, D.M., *J. Vac. Sci. Technol. B* **23** (2005) 1088.
  - <sup>33</sup> Takarada, T., Takeza, H., Nakagawa, N., Kato, K., *Diamond Relat. Mater.* **2** (1993) 323.
  - <sup>34</sup> Arezzo, F., Zaceheti, N., Zhu, W., *J. Appl. Phys.* **75** (1994) 5375.
  - <sup>35</sup> Iijima, S., Aikawa, Y., Baba, K., *App. Phys. Lett.* **57** (1990) 2146.
  - <sup>36</sup> Chakk Y., Brener R., Hoffman, A.J., *Chem. Vap. Dep.* **4** (1995) 153.
  - <sup>37</sup> Maeda, H., Ikari, S., Okubo, T., Kusakabe, K., Morooka, S., *J. Mater. Sci.* **28** (1993) 129.
  - <sup>38</sup> Chakk, Y., Brener, R., Hoffman, A., *App. Phys. Lett.* **66** (1995) 2819.
  - <sup>39</sup> Ralchenko, V.G., *Diam. Rel. Mater.* **2** (1993) 904.
  - <sup>40</sup> Jin, S., *App. Phys. Lett.* **60** (1992) 957.
  - <sup>41</sup> Yang, G.S., Aslam, M., Kuo, K.P., Reinhard, D.K., Asmussen, J., *J. Vac. Sci. Technol. B* **13** (1995) 1030.

- <sup>42</sup> Malshe, A.P., Beera, R.A., Khanolkar, A.A., Brown, W.D., Naseem, H.A., *Diamond Relat. Mater.* **6** (1997) 430.
- <sup>43</sup> Jayasinghe, S.N., *Physica E: Low-dimensional Systems and Nanostructures* **33** (2006) 398.
- <sup>44</sup> Fenn, J.B., Mann, M., Meng, C.K., Wong, S.F., Whitehouse, C.M., *Science* **246** (1989) 64.
- <sup>45</sup> Hayati, I., Bailey, A.I., Tadros, Th.F., *Nature* **319** (1996) 41.
- <sup>46</sup> Fox, O.J.L, Holloway, J.O.P, Fuge, G.M., May, P.W., Ashfold, M.N.R, *Mater. Res. Soc. Symp. Proc.* **1203** (2010) 27.
- <sup>47</sup> Sumant, A.V., Gilbert, P.U.P.A., Grierson, D.S, Konicek, A.R., Abrecht, M., Butler, J.E., Feygelson, T., Rotter, S.S., Carpick, R.W., *Diamond Relat. Mater.* **16** (2007) 718.
- <sup>48</sup> Wang, W.L., Liao, K.J., Zhang, R.Q., *Mater. Lett.* **44** (2000) 336.
- <sup>49</sup> Wolter, S.D., Stoner, B.R., Glass, J.T., Ellis, P.L., Buhaenko, D.S., Jenkins, C.E., Southworth, P., *Appl. Phys. Lett.* **62** (1993) 1215.
- <sup>50</sup> Jiang, X., Klages, C.P., Zachai, R., Hartweg, M., Fusser, H.J., *Appl. Phys. Lett.*, **62** (1993) 3438.
- <sup>51</sup> Otano-Rivera, W., Pilione, L.J., Messier, R., *Appl. Phys. Lett.* **72** (1998) 2523.
- <sup>52</sup> Schreck, M., Roll, H., Stritzker, B., *Appl. Phys. Lett.* **74** (1999) 650.
- <sup>53</sup> Yugo, S., Kanai, T., Kimura, T., Muto, T., *Appl. Phys. Lett.* **58** (1991) 1036.
- <sup>54</sup> Jiang, X., Klages, C.P., Zachai, R., Hartweg, M., Fusser, H.J., *Appl. Phys. Lett.* **62** (1993) 3438.
- <sup>55</sup> May P.W., *Phil. Trans. Roy. Soc. London A* **358** (2000) 473.
- <sup>56</sup> Jiang, X., Klages, C.P., *Diamond Relat. Mater.* **2** (1993) 1112.
- <sup>57</sup> Kim, D.G., Seong, T.Y., Baik, Y.J., *J. Electrochem. Soc.* **145** (1998) 2095.
- <sup>58</sup> Floter, A., Guttler, H., Schulz, G., Steinbach, D., Lutz-Elsner, C., Zachai, R., *Diamond Relat. Mater.* **7** (1998) 283.
- <sup>59</sup> Gruen, D.M., Buckley-Golder, I., *MRS Bulletin* **23** (1998) 16.
- <sup>60</sup> Erdemir, A., Halter, M., Fensk., G.R., Csencsits, R., Krauss, A.R., Gruen, D.M., *Tribology Trans.* **40** (1997) 667.
- <sup>61</sup> Erdemir, A., Bindal, C., Fenske, G.R., Zuiker, C., Csencsits, R., Krauss, A.R., Gruen, D.M., *Diamond Films and Technology* **6** (1996) 31.
- <sup>62</sup> Azevedo, A.F., Baldan, M.R., Ferreira, N.G., *Int. J. Electrochem.* **2012** (2012) 508453.
- <sup>63</sup> Poghossian, A., Abouzar, M.H., Razavi, A., *Electrochimica Acta* **54** (2009) 5981.
- <sup>64</sup> Abouzar, M.H., Poghossian, A., Razavi, A., *Biosensors and Bioelectronics* **24** (2009) 1298.
- <sup>65</sup> Halley, J.D., Winkler., D.A., *Complexity* **14** (2007) 10.
- <sup>66</sup> Kushner, D.J., *Bacteriological Rev.* **33** (1969) 302.
- <sup>67</sup> Denkhov, N., Velev, O.D., Kralchevski, P., Ivanov, I., Yoshimura, H., Nagayama, K., *Langmuir* **8** (1992) 3183.
- <sup>68</sup> Lehn. J.-M., *Science* **295** (2002) 2400.
- <sup>69</sup> Hosokawa, K., Shimoyama, I., Miura, H., *Artificial Life* **4** (1994) 413.
- <sup>70</sup> Forster, P.M., Cheetham, A.K. *Ang. Chem. Int. Ed.* **41** (2002) 457.
- <sup>71</sup> Rechtsman M.C., Stillinger F.H., Torquato S., *Phys. Rev. E* **75** (2007) 031403.
- <sup>72</sup> Barnard, A.S., *J. Mater. Chem.* **18** (2008) 4038.
- <sup>73</sup> Chang, L.-Y., Osawa, E., Barnard, A.J., *Nanoscale* **3** (2011) 958.
- <sup>74</sup> Lee, S.-K., Kim, J.-H., Jeong, M.-G., Song, M.-J., Lim, D.-S., *Nanotech.* **21** (2010) 505302.
- <sup>75</sup> Hanaor, D.A.H., Michelazzi, M., Leonelli, C., Sorrell, C.C., *Journal of the European Ceramic Society* **32** (2012) 235.
- <sup>76</sup> Kim J.H., Lee, S.K., Kwon O.M., Hong, S.I., Lim, D.S., *Diamond Relat. Mater.* **18** (2009) 1218.
- <sup>77</sup> Williams, O.A., Douh ret, O., Daenen, M., Haenen, K., Osawa, E., Takahashi, M., *Chem. Phys. Lett.* **445** (2007) 255.
- <sup>78</sup> Huang, H.J., Dai, L.M., Wang, D.H., Tan, L.S., Osawa, E., *J. Mater. Chem.* **18** (2008) 1347.
- <sup>79</sup> Liu, Y.L., Sun, K.W., *Nanoscale Res. Lett.* **5** (2010) 1045.
- <sup>80</sup> <http://www.virginiasemi.com/pdf/siliconetchingandcleaning.pdf>
- <sup>81</sup> Tremsin, A.S., Siegmund, O.H.W, *Proc. SPIE.* **4139** (2000) 1.
- <sup>82</sup> Robinson, R. *Removing contaminants from Silicon wafers to facilitate EUV optical characterization*, Brigham Young University, 2003. [Volta.byu.edu/pubs/RossCleaning.doc](http://volta.byu.edu/pubs/RossCleaning.doc)
- <sup>83</sup> [http://www.jh-vac.com/image/pdf/Plasma%20Cleaning%20of%20Surfaces\\_en.pdf](http://www.jh-vac.com/image/pdf/Plasma%20Cleaning%20of%20Surfaces_en.pdf)
- <sup>84</sup> Kafader, U., Sirringhaus, H., von Kanel, H. *Appl. Surf. Sci.* **90** (1995) 297.
- <sup>85</sup> Kim, J., *Pure and Appl Chem.* **74** (2002) 2031.

- 
- <sup>86</sup> Sigma-Aldrich, Safety Data Sheet 409014 (2012).
- <sup>87</sup> Marcelo, G., Pilar Tarazona, M., Saiz, E., *Polymer*. **46** (2005) 2584.
- <sup>88</sup> Sigma-Aldrich, Safety Data Sheet, 482595 (2007).
- <sup>89</sup> Tsai, H.-Y., Wu, C.-W., Lin, Y.-M., Chang, H.-C., *J. Ceramic Proc. Res.* **13** (2012) 82.
- <sup>90</sup> Kotov, N.A., *Nanostructured Mater.*, **12** (1999) 789.
- <sup>91</sup> Sigma-Aldrich, Safety Data Sheet, 434574 (2010).
- <sup>92</sup> Sukhorukov, G.B., Mohwald, H., Decher, G., Lvov, Y.M., *Thin Solid Films* **285** (1996) 220.
- <sup>93</sup> Correa-Duarte, M.A., Giersig, M., Kotov, N.A., Liz-Marzan, L.M., *Langmuir* **14** (1998) 6430.
- <sup>94</sup> Berret, J.F., Herve, P., Morvan, M., Yokota, K., Destarac, M., Oberdisse, J., Grillo, I., Scheweins, R., Electrostatic Self-assembly : A New Route Towards Nanostructures. *Soft Matter Brochure* (2005) <http://arxiv.org/abs/cond-mat/0501083v1>
- <sup>95</sup> Berret, J.F., Vigolo, B., Eng, R., Herve, P., *Macromolecules* **37** (2004) 4922.
- <sup>96</sup> McNaught, A.D., Wilkinson, A., *Green Book, 2<sup>nd</sup> ed.* **68** (1996) 60.
- <sup>97</sup> Malvern Instruments, Zetasizer Nano series technical note 5.
- <sup>98</sup> Besra, L., Liu, M., *Prog Mater Sci*, **52** (2007) 1.
- <sup>99</sup> Zarbov, M., Brandon, D., Cohen, N., Shemsesh, L., *J. Mater. Sci.* **41** (2006) 8115.
- <sup>100</sup> Wazed Ali, S., Rajendran, S., Joshi, M., *Polymers & Polymer Composites* **18** (2010) 237.
- <sup>101</sup> Shiratori, S.S., Rubner, M.F., *Macromolecules* **33** (2000) 4213.
- <sup>102</sup> Hees, J., Kriele, A., Williams, O.A., *Chem. Phys. Lett.* **509** (2011) 12.
- <sup>103</sup> Altankov, G., Richau, K., Groth, Th., *Werkstofftech* **34** (2003) 1120.
- <sup>104</sup> Hattori, T., *Ultraclean Surface Processing of Silicon Wafers: Secrets of VLSI Manufacturing*, Springer-Verlag Berlin Heidelberg (1998) 133.
- <sup>105</sup> Horiba Scientific, *Zeta Potential of Electrolytes*. <http://www.horiba.com/scientific/products/particle-characterization/applications/polyelectrolytes>
- <sup>106</sup> Dougherty, G.M., Rose, K.A., Tok, J.B.-H., Pannu, S.S., Chuang, F.Y.S., Sha, M.Y., Chakarova, G., Penn, S.G., The Zeta Potential of Surface-Functionalized Metallic Nanorod Particles in Aqueous Solution. (2007) <https://e-reports-ext.llnl.gov/pdf/347379.pdf>
- <sup>107</sup> Hahner, G., Woll, Ch., Buck, M., Grunze, M., *Langmuir* **9** (1993) 1955.
- <sup>108</sup> Campos, R.A., Trava-Airoldi, V.J., Bagnato, O.R., Moro, J.R., Corat, E.H., *Vacuum* **89** (2013) 21.
- <sup>109</sup> Suzuki T., Mitsui, T., Fujino, T., Kato, M., Satake, Y., Saito, H., Kobayashi, S., *Key Engin. Mater.*, **389-390** (2009) 72.
- <sup>110</sup> Bongrain, A., Scorsone, E., Rousseau, L., Lissorgues, G., Gesset, C., Saada, S., Bergonzo, P., *J. Micromech. Microeng.* **19** (2009) 074015.
- <sup>111</sup> Enlund, J., Isberg, J., Karlsson, M., Nikolajeff, F., Olsson, J., Twitchen, D.J., *Carbon* **43** (2005) 1839.
- <sup>112</sup> Uetsuka, H., Yamada, T., Shikata, S., *Diam. Relat. Mater.* **17** (2008) 728.
- <sup>113</sup> Zhang, J., Zimmer, J.W., Howe, R.T., *Diam. Relat. Mater.* **17** (2008) 23.
- <sup>114</sup> Masood, A., Aslam, M., Tamor, M.A., Potter, T.J., *J. Electrochem. Soc.* **138** (1991) L67.
- <sup>115</sup> Ha, S.C., Kanga, D.H., Kim, K.B., Min, S.H., Kim, I.H., Lee, J.D., *Thin Solid Films* **341** (1999) 216.
- <sup>116</sup> Field, J.E., *The Properties of Diamonds, Academic Press, Ltd.*, London (1979).
- <sup>117</sup> Zhuang, H., Song, B., Staedler, T., Jiang X., *Langmuir* **27** (2011) 11981.
- <sup>118</sup> Sigma Aldrich, Safety Data Sheet, 408719
- <sup>119</sup> Sigma Aldrich, Safety Data Sheet, 522376
- <sup>120</sup> Sigma Aldrich, Safety Data Sheet, 243051
- <sup>121</sup> Fox, O.J.L., PhD Thesis, University of Bristol (2011).